"AN ANALYTICAL APPROACH TO THE DESIGN OF PILLARS IN COAL

Part 3: Coal Testing and Size Effects"

FINAL REPORT, PHASE 3

BY
K. Barron

Work on this project was carried out under the auspices of the Canada Centre for Mineral and Energy Technology, Energy, Mines and Resources, Canada

D.S.S. File # 24ST-23440-3-9234

D.S.S. Contract Serial # OST83-00401

Canmet Scientific Authority: Dr. M. Das

June 1985

148 pp

SUMMARY

In part 1 of this report an analytical model was developed to predict coal pillar strengths. In part 2 this model was tested against data from the literature and was found to be applicable provided that a judicous choice was made for the coal properties input into the model. It was recommended that a comprehensive coal testing program be carried out to determine the input coal properties for one coal and also to investigate the size effects on coal strength properties under triaxial conditions, the existence of the brittle/ductile transition zone and the validity of a number of assumption made in the model. This part 3 report gives to results of this testing program.

The coal selected proved to be extremely variable and consequently the conclusions of the work can only be considered is being tentative. There is evidence however to show that a general expression:

$$\sigma_3 = P_{3T} \left\{ \frac{\sigma_1^{C} - \left(k \sqrt{\frac{H}{W}}\right)}{P_{1T}^{C} - \left(k \sqrt{\frac{W}{H}}\right)} \right\}^{C}$$

where $$C = C_R + (C_R - C_1) \sqrt{\frac{H_1}{W_1}} \cdot \sqrt{\frac{W}{H}}$$

can be used to describe the size effects on the peak and residual strength of coal under triaxial conditions. Tentative limits of $1.25 < \sqrt{\frac{W}{H}} < 1.4$ have been set on the applicability of this expression.

The implications of this expression are important as they indicate that the implicit assumption made by others in the past that uniaxial size effects can be directly applied to triaxial conditions is wrong. It appears that

(i) As the confining pressure increases, the variation of specimen strength with size decreases until the brittle - ductile transition point is reached. There are no size effects beyond this point.

(ii) As the size increases the peak specimen strength becomes asymptotic to the residual strength.

(iii) The residual strength is independent of size.

It was also shown that the brittle-ductile transition point is difficult to determine since it is defined by the intersection of two non-linear curves bending in the same direction. The equations developed in the part I report should be re-defined taking into account the non-linearity of both these curves.

The assumption in the model that the angle of friction of broken coal is a constant is not exactly true, it diminishes with the increasing confining pressure. However, a linear approximation is possibly acceptable. Nonetheless, the model equations should also be modified to allow for non-linearity of this function. The uniaxial compressive strength of broken coal is a very important parameter in the model and is exceptionally hard to determine accurately. Possibly the best way to determine it is from the back analysis of coal plate tests in which the coal fractures rather than yields. This requires further investigation.

Overall the test results were disappointing since, due to the variability of the selected coal, firm conclusions cannot be made. Nonetheless a number of directions for further work and testing are indicated. However these should not be carried out until the pillar model equations have been re-developed taking into account the non-linearity of sliding friction of coal surfaces and the non linearity of the angle of friction of broken coal.

CONTENTS

		PAGE
1.	INTRODUCTION	1
1.1	Phase 1 summary	2
1.2	Phase 2 summary	3
1.3	Unanswered questions	4
2.	OBJECTIVES, APPROACH AND TEST PLANS	8
2.1	Objectives	8
2.2	Proposed approach	9
2.3	Detailed test program plans	10
2.3.1	Group A - Uniaxial tests in solid coal specimens	10
2.3.2	Group B - Triaxial tests on solid coal specimens	12
2.3.3	Group C - Triaxial tests on re-compacted broken coal	14
2.3.4	Group D - Shear box tests on cut coal specimens	16
2.3.5	Group E - Uniaxial model pillars	16
3.	UNIAXIAL TESTS ON SOLID COAL SPECIMENS - GROUP A RESULTS AND ANALYSIS	18
3.1	Equipment and procedures	18
3.2	Group A1: Uniaxial cube test results	20
3.2.1	Deviations from the program plan	20
3.2.2	Results	20
3.2.3	Strength versus modulus correlation	20
3.2.4	Mean normalised cube strength, σ_{cn}, versus minimum cube dimension (W)	23
3.3	Group A2: Uniaxial tests on rectangular prisms (square base)	26
3.3.1	Deviations from the program plan	26
3.3.2	Results	26
3.3.3	Prism strength/shape effects	27
3.3.4	Correlation of prism strength with modulus	28
3.4	Group A3: Uniaxial tests on circular prisms	37
3.4.1	Deviation from the program plan	37
3.4.2	Results	37
3.4.3	Prism strength/shape effects	37
3.4.4	Correlation of all data with modulus	39
3.5	Summary and conclusions	42
4.	TRIAXIAL TESTS ON COAL SPECIMENS - GROUP B RESULTS AND CONCLUSIONS	45
4.1	Deviations from the program plan	45
4.2	Group B2 Results	46
4.2.1	Results	46
4.2.2	Strength correlation with modulus	46
4.2.3	σ_1/σ_3 relationship at failure	50
4.3	Group B3 Results	53
4.3.1	Results	53
4.4	Group B4 Results	53
4.4.1	Results	53
4.4.2	σ_1/σ_3 relationship at failure	53
4.5	Comparison of Group B2 and B4 Results	58
4.5.1	Peak Strengths	58

		PAGE
4.5.2	Residual Strengths	58
4.5.3	Transition Point	58
4.6	Some theoretical aspects of size effects	63
4.7	Comparison of Results with the Theoretical Considerations	65
4.7.1	Group B2 and B4 Results	65
4.7.2	Comparison of the General Expression with Group B2, B3 and B4 Results	66
4.8	Limits of Application of the General Expression	70
4.9	Tentative Conclusions	73
5.	TRIAXIAL TESTS ON RE-COMPACTED BROKEN COAL	76
5.1	Equipment and procedures	76
5.2	Deviation from the Program Plan	76
5.3	Results	76
5.4	Comparison of the Results with the Residual Strengths for the Solid Coal Specimens	83
5.5	Broken Coal Properties	83
5.6	Coefficient of Sliding Friction of Coal on Coal	86
5.7	Transition Point relationship to μ_B	88
5.8	Tentative Conclusions	89
6.	GROUP D - SHEAR BOX TESTS - CUT COAL SPECIMENS	90
6.1	Equipment and Procedures	90
6.2	Results	90
6.3	Comparison with Broken Coal and Residual Strength Properties	101
6.4	Tentative Conclusions	102
7.	UNIAXIAL MODEL PILLARS (H/W < 1) - GROUP E	103
7.1	Deviation from the Program Plan	103
7.2	Results	103
7.3	Comparison with Uniaxial Prism Results	103
7.4	Comparison with the Prism Strength Formulae derived from the Pillar Model	103
7.5	Tentative Conclusions	108
8.	CONCLUSIONS AND RECOMMENDATIONS	111
8.1	With Respect to Uniaxial Prism Tests	111
8.2	With Respect to Triaxial Tests on Solid Coal Specimens	111
8.3	With Respect to Triaxial Tests on Broken Coal Specimens	113
8.4	With Respect to Shear Box Tests	114
8.5	With Respect to Model Pillars (Plates)	114
8.6	Recommendations	115
9.	REFERENCES	117
10.	ACKNOWLEDGEMENTS	118

Figures

		PAGE
Figure 1:	Size effects on Mohr envelopes	5
Figure 2:	Stress/strain curves for triaxial tests - varying confining pressure	13
Figure 3:	Stress/deformation curves for slip tests on broken coal specimens	13
Figure 4:	Possible estimate of transition point by differences between peak and residual stresses	13
Figure 5:	600,000 lb capacity MTS testing machine and control unit	19
Figure 6:	Uniaxial cube test - 3" cube #5	21
Figure 7:	E versus q_c correlation - 1" cubes	22
Figure 8:	E versus q_c correlation - 2, 3 and 4 inch cubes	24
Figure 9:	Mean normalised cube strength versus cube size	25
Figure 10:	Uniaxial rectangular prisms - $\frac{\bar{q}_{pN}}{q_c}$ versus (W/H)	30
Figure 11:	Uniaxial rectangular prisms - $\bar{q}_{pN}$ vs $\left(\frac{W}{H}\right)$	31
Figure 12:	Uniaxial rectangular prisms - $\bar{q}_{pN}$ vs $\left(\frac{W}{H}\right)^{\alpha}$	32
Figure 13:	Uniaxial rectangular prisms - $\bar{q}_{pN}$ vs $\left(\sqrt{\frac{W}{H}}\right)$	33
Figure 14:	Uniaxial rectangular prisms - $\bar{q}_p\left(\frac{H}{W}\right)$ versus E	35
Figure 15:	$\bar{q}_{pN}$ versus $\sqrt{\frac{W}{H}}$, for cylindrical, rectangular and all prisms	38
Figure 16:	$\bar{q}_{pN}\frac{H}{\sqrt{W}}$ versus E, for all prisms	40
Figure 17:	$\frac{\bar{q}_p}{E}$ versus $\left(\sqrt{\frac{W}{H}}\right)$ - all data	43
Figure 18:	Typical load-deformation curve for triaxial tests on solid coal	47
Figure 19:	Correlation of principal stress difference at failure with modulus	49
Figure 20:	σ_1 vs σ_3 - Group B2 - peak and residual strengths	52
Figure 21:	σ_1 vs σ_3 - Group B3 - peak and residual strengths	55
Figure 22:	σ_1 vs σ_3 - Group B4 - peak and residual strengths	57
Figure 23:	σ_1 vs σ_3 - Relationships - peak data - Groups B2 and B4	59
Figure 24:	σ_1 vs σ_3 - Relationships - residual data - Groups B2 and B4	60

PAGE

Figure 25: σ_1 vs σ_3 - all residual data 61

Figure 26: σ_1 vs σ_3 - peak data for groups B2 and B4 plus all residual data 62

Figure 27: Comparison of Group B2 and B3 peak strength data with the general expression 68

Figure 28: Comparison of Group B4 peak strength data with the general expression. 69

Figure 29: Comparison of all residual strength data with the general expression. 71

Figure 30: Effect of Size on the Peak and Residual Strengths of the test coal. 72

Figure 31: WHYKHAM FARRANCE loading frame for uniaxial tests on re-compacted coal specimens. 77

Figure 32: Typical load-deformation curve for re-compacted coal tests. 79

Figure 33: σ_1 vs σ_3 all re-compacted peak strengths. 82

Figure 34: Comparison of re-compacted strengths with solid coal residual strengths. 84

Figure 35: σ_1 vs σ_3 for recompacted coal specimens, assuming a linear relationship. 85

Figure 36: σ_1 vs σ_3 for residual strengths, assuming a linear relationship. 87

Figure 37: Shear test apparatus 91

Figure 38: Shear test #1 92

Figure 39: Shear test #2 93

Figure 40: Shear test #3 94

Figure 41: Shear test #4 95

Figure 42: Shear test #5 96

Figure 43: Shear test #6 97

Figure 44: Shear test #7 98

Figure 45: Shear test #8 99

Figure 46: Shear test - all data. 100

Figure 47: "Plate" specimens after testing 104

Figure 48: Uniaxial test on a coal plate 105

TABLES

		PAGE
Table 1:	Mean normalised strengths for uniaxially loaded rectangular prisms	29
Table 2:	Mean strengths for uniaxially loaded rectangular prisms - correlation with modulus	34
Table 3:	Mean strengths for all uniaxially loaded prisms - correlation with modulus	41
Table 4:	Group B2 - Mean peak and residual strength data	48
Table 5:	Men peak and residual strengths - Group B2	51
Table 6:	Mean peak and residual strengths - Group B3	54
Table 7:	Mean peak and residual strengths - Group B4	56
Table 8:	Comparison of planned and actual number of tests - recompacted coal samples.	78
Table 9:	Re-compacted coal specimens - triaxial data	80
Table 10:	Linear τ σ correlation for shear box tests	101
Table 11:	Summary of plate specimen results	106
Table 12:	Comparison of plates with prisms	106
Table 13:	Comparison with formulae - $P_B = 100$, $P_{IT} = 12{,}700$	106
Table 14:	Comparison with formulae - $P_B = 390$, $P_{IT} = 12{,}700$	106
Table 15:	Comparison with formulae - $P_B = 390$, $P_{IT} = 8{,}000$	109

APPENDICES

		PAGE
Appendix A1:	Uniaxial cube strength tests - group A1	119
Appendix A2:	Uniaxial tests on rectangular prisms with a square base - Group A2	121
Appendix A3:	Uniaxial tests on circular prisms - Group A3	124
Appendix B1:	Triaxial tests on solid coal (Dia. 2 1/8") - Group B2	126
Appendix B2:	Triaxial tests on solid coal (3 inch dia.) - Group B3	128
Appendix B3:	Triaxial tests on solid coal (2 1/8" dia., 2 3/8" high) Group B4	129
Appendix C1:	Triaxial tests - recompacted broken coal (35,000 psi, H = 2.375, D=0.84)	130
Appendix C2:	Triaxial tests - recompacted broken coal (25,000 psi, H = 2.375, D = 0.84)	132
Appendix C3:	Triaxial tests - recompacted broken coal (35,000 psi, H = 4.2, D = 2.12)	134
Appendix C4:	Triaxial tests - recompacted broken coal (25,000 psi, H = 4.2, D = 2.12)	136
Appendix D:	Shear box test results	137
Appendix E:	Uniaxial tests on coal plates (H/W < inch)	138

1. INTRODUCTION

The ability to design pillars for underground coal mining operations is of prime importance in room and pillar mining during both the development and extraction phases, and in longwall mining to control entries between panels, etc. Pillar failure during mining represents a major potential safety hazard and is generally avoided in practice by overdesigning the pillar using large safety factors, however, this may result in reduced extraction ratios and in loss of reserves. It is also essential to be able to design stable barrier pillars between mining panels, not only for structural stability but also to prevent ventilation leakage between mined out areas which could cause spontaneous combustion and mines fires.

Although much past rock mechanics research has been devoted to assessing pillar loads and pillar strengths, no one approach to pillar design has been completely satisfactory, and pillar design still owes much to trial and error procedures during actual mining operations. A satisfactory analytical design method for determining stable pillar dimensions, whilst not eliminating the necessity for design adjustments made on the basis of site experience, would contribute significantly to safety and underground strata control.

With these overall objectives in mind CMRC proposed a two part contract research study to D.S.S. (CANMET) in 1980. This contract was awarded and completed in March 1983. The objectives of this contract were as follows:-

The objectives of this contract were as follows:-

Phase 1: To develop an analytical approach to define coal pillar stability and lead to the evaluation of optimum pillar dimensions.

Phase 2: To evaluate the applicability of this analytical approach to pillar design by testing it using experimental data extracted from the extensive literature on the subject.

The results of these two earlier phases of work are summarised below:

1.1 Phase 1 summary (1)

In Phase 1, as planned, the Centre developed a new computer based approach to the analysis of the stability of pillars in coal mines. In this analytical approach the mean vertical stress acting on the pillar is calculated using either tributary area theory or Coates' modified pillar loading hypothesis; the initial vertical elastic stress distribution across the pillar is then approximated. The pillar is split into narrow vertical slices and the stresses acting on each slice, starting at the pillar edge, are calculated and compared to the failure criteria. If the slice fails, the residual stress capacity of the slice is determined and the difference between this stress and the initial stress is shed onto the remaining, as yet unfailed, slices. Successive analysis of each slice in turn allows the depth of the failed zone, the vertical stress distribution in the failed zone and the elastic core of the pillar, and the confining stress build up in the failed zone to be calculated.

The failure criteria used in this analysis are based on Mohr theory as defined by a parabolic (or a general curvilinear) Mohr envelope. At low confining stresses brittle fracture occurs; at high confining stresses a pseudo-ductile failure mechanism is invoked which allows a slice to yield. The brittle/pseudo-ductile transition point is defined as the point on the Mohr envelope where the shear resistance to sliding exceeds the shear resistance to fracture. Consequently the failed zone may comprise only a fracture zone or a fracture zone plus a yield zone; likewise the pillar may fail by brittle fracture or by yielding.

Pillar strength has been defined as the mean pillar stress required to just extend the failed zone to the centre of the pillar. This strength can be determined by either the above slice by slice analysis or from deterministic equations which have been evolved by integrating over the pillar width.

A wide range of hypothetical analyses were performed which revealed a number of important conclusions:-

(i) There is a minimum pillar stress below which fracture cannot initiate in the pillar; hence there is a minimum pillar strength.

(ii) In specific circumstances, once fracture initiates at the pillar edge the failed zone must propogate immediately to the centre of the pillar. This unstable situation has been called "catastrophic failure" and could be regarded as a model of a "pillar burst". The critical pillar dimensions to avoid such catastrophic failure can be calculated.

(iii) In more normal circumstances, there is a failed zone at the periphery of the pillar with a central elastic core. As the pillar loading increases the failed zone gradually extends into the pillar until it reaches the centre when the pillar is deemed to have failed. This failure is called "ultimate failure"; the critical pillar dimensions to avoid ultimate failure can be calculated, as can the residual load capacity of the failed pillar.

From these phase 1 results it would appear that this analytical model does give a qualitative approximation of the observed behaviour of coal pillars. This leads naturally into Phase 2 of this contract in which the object is to "verify" the model by using it to predict the results of a number of experimental case histories reported in the literature.

1.2 Phase 2 summary (2)

This study phase considered experimental data on coal pillars obtained from the literature and attempted to use the model to predict these experimental results.

It was shown that the analytical model gave a good fit to the results of all, except one, of the fourteen case histories considered from the literature provided that a judicous choice was made for the values of the input parameters for the solid and broken coal properties. Unfortunately the case histories did not give sufficient data to adequately define these required input properties, hence "typical" estimated values had to be used for some of these properties. In these circumstances therefore, although the model may give a good "prediction" of the field data, some doubt must remain as to the validity of the model because of this use of "typical" estimated rather than actual properties.

Very strong indirect evidence was obtained to indicate that the proposed

brittle/pseudo-ductile failure theory developed in the Phase 1 report is applicable both to coal specimens and to coal pillars within the stress ranges normally encountered in coal mines. The evidence is, however, indirect and it was recommended that a "Phase 3" study be carried out; this would comprise a comprehensive specimen testing program aimed at giving direct proof of the validity of this failure theory. In addition such a testing program would give answers to some outstanding questions on size effects on various parameters.

Thus the results of Phase 2 of this study were inconclusive; the model developed still appears to be qualitatively sound and will give a good quantitative prediction of field results if the input properties are judiciously chosen. Verification of these input paramters is however lacking and thus some doubt must remain with respect to the model applicability and validity. A number of questions still remain to be answered before this model may be accepted or rejected; these questions are discussed below.

1.3 Unanswered Questions

The main questions remaining to be answered all relate to the determination and use of the coal properties in the model:-

(i) Size/shape effects on coal strength; are they applicable to triaxial conditions? The basic coal strength parameter used by most workers is the uniaxial 1 inch cube strength. Coal strength is very dependent on the specimen size and shape and much work is reported in the literature establishing accepted coal strength/size/shape relationships for uniaxially loaded specimens. The value for the uniaxial strength used in the model is that given by these relationships for a cube of size equal to the pillar height.

However, the model takes into account the triaxial loading conditions generated in the pillar. The question therefore arises as to whether the size/shape effects established for uniaxial conditions can be assumed to apply under triaxial conditions? This is illustrated in Figure 1 where the Mohr circles (1) and (2) are the uniaxial strength of a large and a small specimen respectively. If the uniaxial size effects apply to triaxial conditions without

CMRC

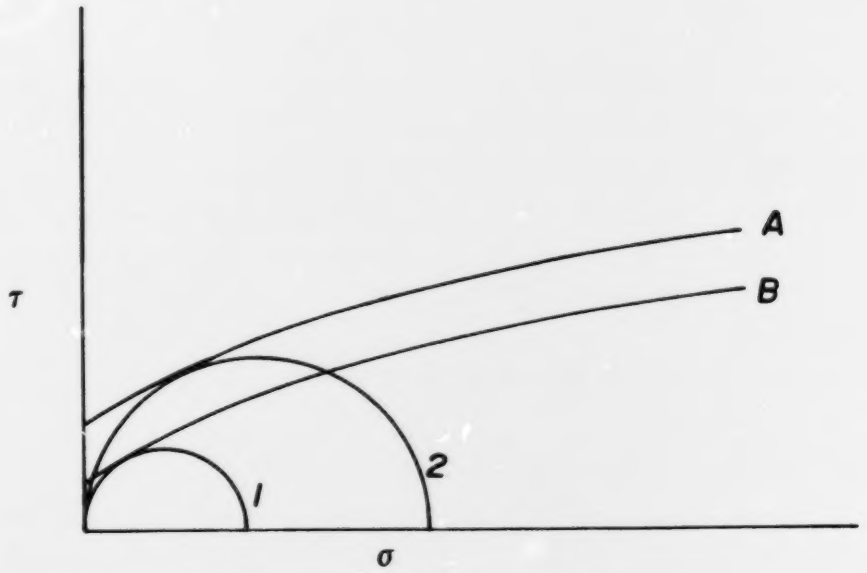

a.

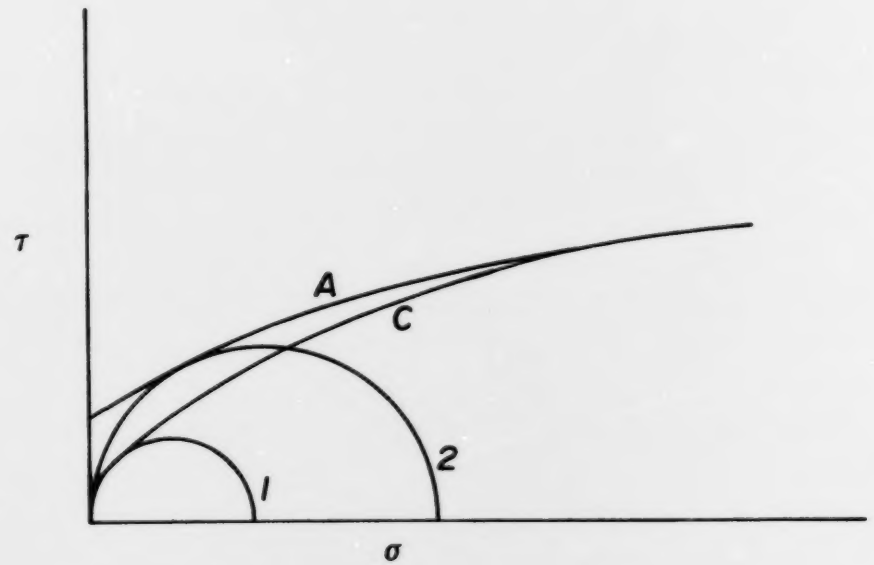

b.

SIZE EFFECTS ON MOHR ENVELOPES

DWN. BY : KJC	DATE : 24/06/88
SCALE: NTS	FIGURE : 1

modification then this will result in parallel Mohr envelopes as illustrated in curves A and B of Figure 1A. However, a good case could be made to suggest that, once pseudo-ductile yielding commences then the strengths may be size independent. In such a case the Mohr envelopes would converge, as illustrated in Figure 1B. There are no previous studies that address this question, but it must be answered if full benefit is to be obtained from this model capability. It is essential to use the correct size adjusted Mohr envelope in inputing the coal parameters in the model.

(ii) Frictional properties of coal The model also requires the input of two other coal parameters namely μ_B the sliding coefficient of friction on a fractured coal surface and ϕ_B the angle of internal friction of broken coal. An argument could be made that $\mu_B = \tan \phi_B$ but there is insufficient evidence in the literature to confirm or deny this. An investigation should therefore be carried out to determine these two parameters and to determine whether or not μ_B is related in any way to ϕ_B.

In addition, it is assumed in the model that the coefficient of sliding friction, μ_B, is a constant independent of the applied normal stress. Whilst this is a reasonable first approximation there is evidence in the literature that μ_B varies with normal stress (see Phase 1 report, Page 68). This could easily be investigated during experiments aimed at determining μ_B and ϕ_B.

(iii) Brittle/pseudo-ductile transition point The failure criterion developed in Phase 1 of the study and used in the model defines a brittle/pseudo-ductile transition point on the Mohr envelope as being that point on the Mohr envelope where the shear resistance to sliding exceeds the shear resistance to fracture. This failure criterion has been used successfully to predict hard rock behaviour at exceptionally high confining pressures; it has not previously been applied to coal or at such relatively low confining pressures. At least one reputable reviewer has questioned the application of this failure criterion to coal at the relatively low stress levels experienced in coal pillars. Some significant evidence backing the use of this failure criterion has been obtained from the case histories; however this evidence is indirect and, in view of the fundamental nature of this query to the whole conceptional approach, it is believed that a test program should be specifically designed

and carried out to prove or disprove the application of this failure criterion to coal.

(iv) Standard tests to determine the coal property parameters As seen above the model requires the input of coal property parameters that have not usually been measured in past studies. Hence there is a need to develop standardized test procedures to determine these parameters and, if possible, to develop a single simple laboratory test from which all these parameters might be obtained.

A proposal was therefore submitted to D.S.S. aimed at carrying out a detailed laboratory coal testing program to seek the answers to the questions posed above. This proposal was accepted and the contract awarded in March 1984. Section2 of this report gives the broad contract objectives and the detailed test program as planned.

2. OBJECTIVES, APPROACH AND TEST PLANS

2.1 Objectives

The broad study objectives as defined in the contract were as follows:-

To develop and prove the applicability of an analytical technique for assessing coal pillar stability and designing optimum pillar dimensions as developed under DSS Contract 1SQ80-00161 through a comprehensive laboratory testing program on coal samples. More specifically they can be stated as follows:

1. To determine if the coal strength/size/shape relationships established for uniaxially loaded specimens are applicable to triaxial conditions or if they require modification for triaxial conditions.

2. To measure the frictional properties of fractured surfaces and broken coal (μ_B and tan ϕ_B respectively) and to determine what, if any, relationship exists between these parameters.

3. To determine the solid coal Mohr envelope and the shear resistance to sliding on a fractured surface in order to prove or disprove the postulated existence of the brittle/pseudo-ductile transition point and thus validate or disprove the application of this failure criterion to coal.

4. To develop standardized tests to obtain the coal properties required by the model and to attempt to develop a single test from which all this data might be obtained.

5. To apply the tests results in the analytical technique for verification purpose and for conclusion.

2.2 Proposed Approach

A detailed laboratory testing program is outlined in the next section which was aimed at achieving the objectives outlined above. All of these tests were to be carried out on one coal with the axis of the major principal stress perpendicular to the bedding planes. The tests were restricted to one coal only since it is believed that it is essential to verify these concepts by a meticulous and comprehensive program on a single coal; clearly if the concepts are verified for one coal then they are potentially applicable to other coals. The testing of specimens perpendicular to the bedding planes will eliminate complications that might arise by specimen anisotropy.

The planned tests were grouped into 5 categories:-

Group A: These tests were aimed at establishing the uniaxial strength/size/shape relationships for this coal.

Group B: These tests were aimed at investigating the applicability of the uniaxial size/shape relationships to triaxial conditions, and at determining the frictional characteristics on fractured surfaces.

Group C: These tests on recompacted coal were aimed at investigating and determining the internal frictional angle and the cohesion of the broken coal.

Group D: These tests were aimed at verifying the frictional characteristics of fractured surfaces obtained from the triaxial tests by an alternative shear box test method.

Group E: The uniaxial tests on specimens with large width/height ratios are in fact "model pillar" tests. Hence using the results of the above tests together with the analytical model it may be possible to predict these test results and thereby confirm or deny the concepts developed. If successful, then clearly this test could be potentially used as a "single test" to determine all the parameters required by the model.

2.3 Detailed test program plans

2.3.1 Group A - Uniaxial Tests on Solid Coal Specimens. (all tests carried out perpendicular to the bedding planes).

Objective: To define the effects of size and shape on the uniaxial strength of the test coal.

Group A.1: Cube Strength/Size Effect

1. Prepare 3* specimens each of cubes of edge dimensions 1", 2", 3", and 6"** respectively ----- 12 specimens.
2. Measure and weigh specimens - determine coal density.
3. Load cubes to failure, measure applied load and deformation between plattens.

   Plot - Stress - Strain curves -- determine modulus.
4. Correlate uniaxial crushing strength, σ_c with edge dimension D inches in.

* Note: For all tests in all groups the number of specimens tested may vary depending on survival rate from depredations of specimen preparation.

** Note: For all tests in all groups specimen size, and height/width ratios, will vary to some extent; thus all sizes given in these program plans are nominal sizes. In addition some changes were made in planned core diameters to conform to standard drill sizes.

Group A.2: Rectangular prisms (square base), H/W $\geq$ 1. - shape effects

1. Range of H/W ratios to be considered --- (1, 1½, 2)
2. Range of W, 1", 2", and 3"
3. Prepare 3 specimens of each following sizes

   (1x1); (2x2); (3x3) - already done in Group A above

(1½x1); (3x2); (4½x3)
(2x1); (4x2); (6x3) 18 additional specimens

4. Measure and weigh all specimens - determine density.
5. Load prisms to failure, measure applied load and deformation between plattens
   Plot stress/Strain curves -- determine modulus.
6. Correlate uniaxial prism crushing strength, σ_p, with height and width.
7. Derive general expression for rectangular specimen strengths relating all results cube strengths.

Group A.3: Circular prisms (circular section), (H/W $\geq$ 1)

1. Range of H/W ratios to be considered --- (1, 1½, 2)
2. Range of W - 1", 2", and 3"
3. Prepare 3 specimens of each of the following sizes
   (1x1); (2x2); (3x3)
   (1½x1); (3x2); (4½x3)
   (2x1); (4x2); (6x3) 27 specimens
4. Measure and weigh all specimens - determine density.
5. Load prisms to failure, measure applied load and deformation between plattens.
   Plot stress/Strain curves -- determine modulus.
6. Correlate uniaxial circular prism crushing strength, σ_{pc}, width/height and width.
7. Derive correction factors, if any, for translating circular section results to be equivalent to rectangular section results.
8. Derive general expression for circular and rectangular strengths in terms of cube strength for coal. Plot all results from groups A1, A2, and A3 in this form to demonstrate applicability of general expression.

2.3.2 Group B - Triaxial Tests on Solid Coal Specimens. (all tests carried out perpendicular to the bedding planes)

Objectives:

(i) To evaluate the applicability of uniaxial size/shape effects to triaxial conditions.

(ii) To determine Mohr envelope for peak stress for solid coal.

(iii) To determine Mohr envelope for residual stress for solid coal.

(iv) To determine Mohr envelope for sliding on fractured coal specimens.

Group B.1: Triaxial tests on circular prisms, H/W = 2, W = 1"

1. Prepare 3 specimens for testing at each of 6 confining pressures.
2. Use 6 confining pressures ranging from 0 psi to maximum of apparatus capacity. Note: uniaxial (0 psi) tests already completed with Group A3. Hence require 15 specimens.
3. Measure and weigh all specimens -- determine density.
4. Test procedure - for each specimen.
   (i) Apply confining pressure - load to failure at constant confining pressure measuring the load and specimen deformation. Continue load after peak stress at failure until arrive at "residual stress" for specimen. - Plot stress/Strain curve as as illustrated in Figure 2. Determine modulus.
   (ii) If possible, after residual stress established, unload specimen and conduct "slip tests" at incremental confining pressure steps - as illustrated in Figure 3.
5. Analysis
   (i) Plot Mohr envelope of peak stresses - derive equation of Mohr envelope in Balmers form. Is this envelope curvilinear?
   (ii) Plot Mohr envelope of residual stress - derive equation of Mohr envelope in Balmers form. Is this envelope curvilinear?
   (iii) Do the two envelopes intersect at some point. Determine the stresses at the point of intersection.

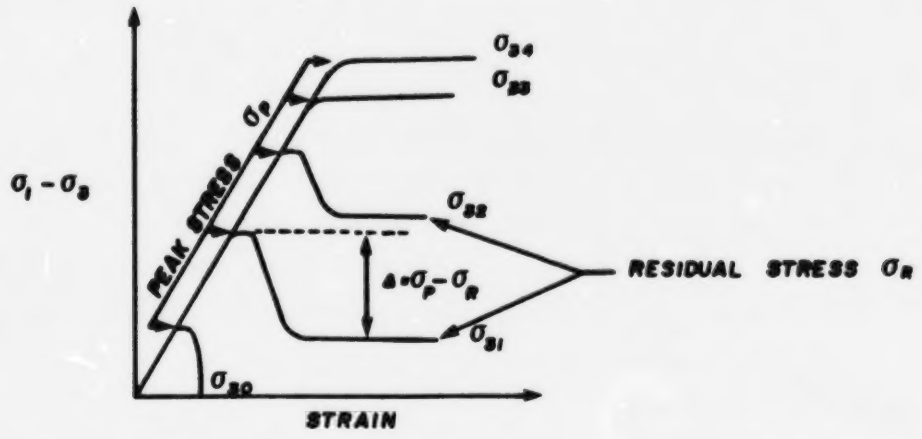

FIGURE 2 : STRESS / STRAIN CURVES FOR TRIAXIAL TESTS – VARYING CONFINING PRESSURE

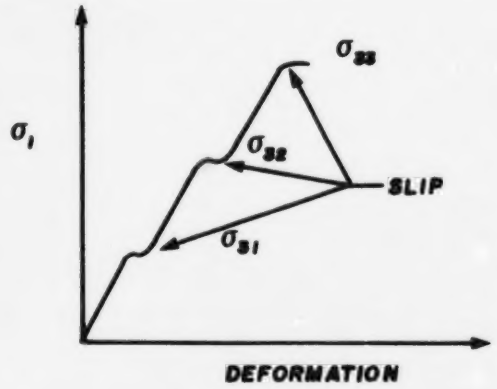

FIGURE 3 : STRESS/DEFORMATION CURVES FOR SLIP TESTS ON BROKEN SPECIMENS

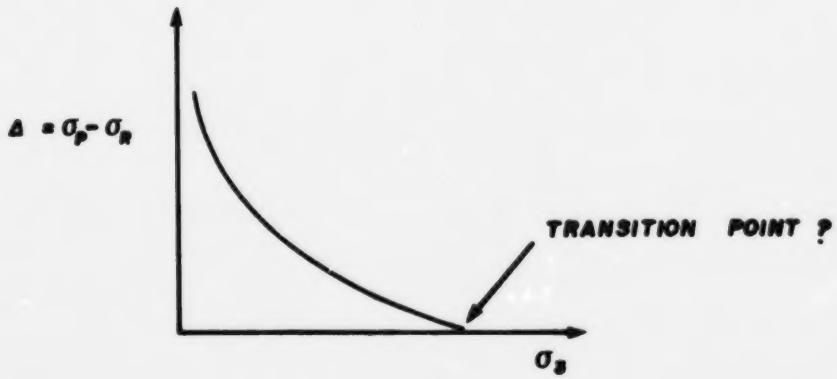

FIGURE 4 : POSSIBLE ESTIMATE OF TRANSITION POINT BY DIFFERENCES BETWEEN PEAK AND RESIDUAL STRESSES.

(iv) Plot the difference between the peak and residual stresses for each specimen against confining pressure, as shown in Figure 4. At what stress does this differential reach zero? Do these stresses coincide with the point of intersection of the Mohr envelopes?

(v) Plot Mohr envelope for the "slip test" results; derive equation of Mohr envelope in Balmers form. Does this envelope coincide with that for the residual stress envelope?

(vi) What is the "cohesion" given by the residual stress envelope and by the slip test envelope? Are they the same?

Group B2: Triaxial Tests on Circular Prisms, H/W = 2, W = 2"

Prepare specimens and repeat tests as in Group B1 for these 2" diameter specimens. -- 15 specimens
Repeat analysis given in Group B1

Additional analysis required:

(i) Do size effects determined from uniaxial tests apply to the triaxial tests?

(ii) Is the intersection point of Mohr envelope for peak & residual stress affected by size?

(iii) Are the residual envelope and the "slip test envelope" affected by size?

(iv) Is the cohesion given by the residual and slip test envelopes affected by size?

2.3.3 Group C: Triaxial Tests on Recompacted Broken Coal

Objectives

(i) To determine Mohr envelope for broken coal; does this change with degree of re-compaction (density)?

(ii) To determine if there is a "residual" stress for recompacted broken coal

(iii) To determine variation of cohesion of broken coal with degree of compaction

Group C1: Triaxial tests on recompacted broken coal (H/W = 2, W = 1")

(i) Crush and sieve coal to a particle size < 0.1".

(ii) Prepare 2" high by 1" diameter specimens by recompacting the coal by loading in steel cylinders. Prepare 18 specimens at each of 3 different re-compaction loads. - groups C1.1; C1.2; and C1.3; ----- 54 specimens

(iii) Measure and weigh all specimens - determine density

For each sub-group, C1.1, C1.2, C1.3 carry out following tests

(i) Triaxial tests at 6 different confining pressures from 0 psi to maximum capacity of apparatus.

(ii) Apply confining pressure - load to failure at constant confining pressures measuring the load and specimen deformation. Continue to load after peak stress has been reached and determine whether there is a "residual stress" for the specimen. Plot stress/ strain curves and determine modulus.

(iii) If possible, after "residual stress" established, unload specimen and conduct "slip tests" at incremental confining pressure steps.

Analysis

(i) Determine Mohr envelope for each of re-compacted broken coal groups, deriving equation in Balmers form. Is Mohr envelope curvilinear?

(ii) Determine Mohr envelopes for residual stresses and slip tests and compare with envelope above, at the three re-compaction densities.

(iii) Attempt to correlate Mohr envelope constants for broken coal results and solid coal results by relating to density variation.

(iv) Examine variation in "cohesion" with density.

(v) Examine variation of modulus with density.

Group C2: Triaxial tests on re-compacted broken coal (H/W = 2, W = 2")

(i) Prepare specimens as with group C1 but this time prepare 2" diameter specimens. - 54 specimens

(ii) Repeat Group C1 tests for sub groups, C2.1; C2.2; C2.3

(iii) Examine results to see if there is a size effect for recompacted broken coal.

2.3.4 Group D: Shear Box Tests - Cut Coal Specimens

Objective:

(i) To determine envelope for slip on cut surfaces by shear box tests.
(ii) To compare this envelope with Mohr envelope for "residual stress" and "slip tests" for solid and recompacted broken coal.

Test Procedure

(i) Prepare test specimens of size to fit shear box.
(ii) Run each specimen at 6 normal stresses from 0.1 x maximum normal stress capacity to 1 x maximum stress capacity of shear box. Repeat for 6 specimens.
(iii) Apply first normal load, increase shear load until slip occurs, apply second normal load, etc.

Analysis

Plot τ, σ, envelope and compare to residual stress and slip test envelope from solid and re-compacted broken coal.

2.3.5 Group E: Uniaxial Model Pillars ($H/W \leq 1$)

Objectives:

(i) To test specimens with low H/W ratios and compare with analytical model predictions.
(ii) To determine, if possible, stresses at brittle/pseudo ductile transition point.
(iii) To determine if maximum brittle fracture zone depth remains constant with varying width for constant height.
(iv) To determine if maximum brittle fracture zone depth varies with height for constant width, in accordance with analytical model.

Specimens Use, if possible 3 H/W ratios of 1/3, 1/6, 1/10

(i) Prepare following specimens (a) 1" high W = 3", 6", and 10"
(b) 1½" high W = 4½, 9", and 15"
(c) 2" high W = 4, 12, and 20"

3 specimens of each ---- 27 specimens

(ii) Test procedures

1. Load specimen uniaxially and measure specimen deformation between plattens.
2. Each specimen loaded until failure occurs, either by sudden failure or by "yield" as indicated by the stress - strain curve. Attempt to distinguish between catastrophic and non catastrophic failure.
3. After failure, examine specimen. If possible, measure depth of brittle fracture zone.

(iii) Analysis

1. For each set of same height. Determine depth of fracture zone -is this constant?
2. For each set at same height, by difference between the yield loads, determine the vertical stress at yield.
3. Examine vertical stress at yield for the 3 sets and determine the size effect relationship.
4. Use results from previous groups to predict stress distribution, fracture zone and strength of specimen, using analytical model.

As is frequently the case, the above detailed program plans were not able to be carried out exactly as planned for a variety of technical reasons. For each set of results presented in the ensuing sections, the deviations from this planned program are reported.

3. UNIAXIAL TESTS ON SOLID COAL SPECIMENS - GROUP A RESULTS AND ANALYSIS

3.1 Equipment and Procedures

All tests on the solid coal specimens (both uniaxial and triaxial) and on the triaxial tests on the re-compacted coal specimens were carried out in an MTS servo-controlled testing machine of 600,000 lbs capacity in compression (Figure 5). Four load capacity ranges of 60,000 lbs, 120,000 lbs, 240,000 lbs and 600,000 lbs can be pre-selected and were chosen, as appropriate, based on the behaviour of the first specimen in each group. The load was recorded directly in the Y axis of an X-Y recorder.

The specimen deformation was measured by averaging the output of two L.V.D.T.'s placed on either side of the specimen and measuring between the plattens. Consequently the deformation measured includes a small component of deformation attributable to deformation of the system in addition to that due to the specimen. This deformation was recorded on the X axis of the X-Y recorder.

The peak load, and residual loads where appropriate, were also recorded directly from the peak voltage output obtained from the control system memory. This enabled a good cross check to be made between the loads as recorded by the calibration of the X-Y recorder and the direct output from the load cell. Stresses were calculated from the recorded load and the measured specimen dimensions.

Strains were calculated using the specimen length and assuming that all deformation occurred within this specimen length. The Young's modulus, E, was calculated from the slope of the linear portion of the load-deformation recording prior to failure, using the specimen dimensions to translate this slope to the modulus.

After initial experimentation, the deformation rate was set to a constant rate of 1.1×10^{-4} inches/sec.

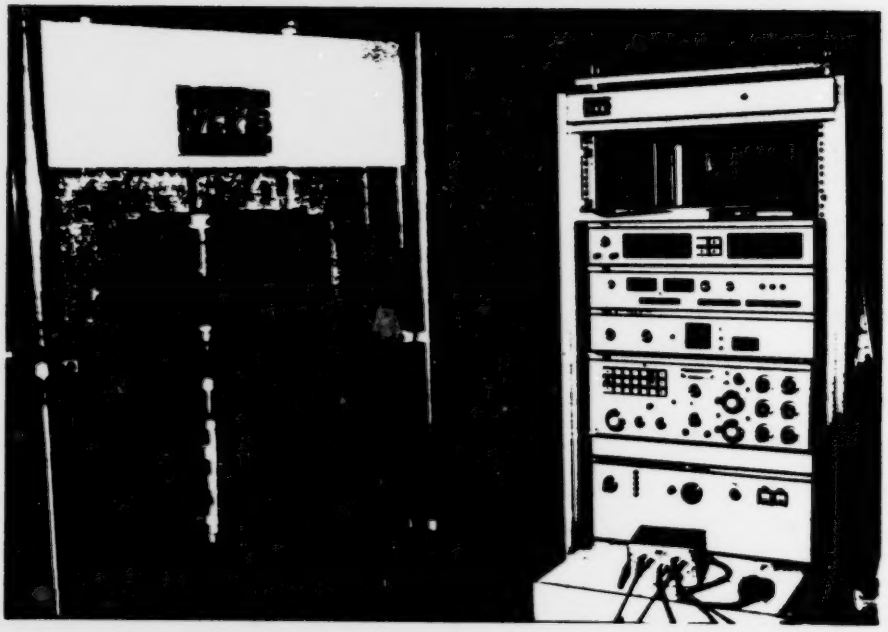

FIGURE 5: 600,000 lb capacity MTS testing machine and control unit

3.2 Group A1: Uniaxial cube test results

3.2.1 Deviations from the program plan

The results from these cube tests on coal showed a wide scatter; consequently a total of 33 cubes were tested at five different sizes rather than the planned number of 12 over 4 different sizes. The 1 inch cubes showed a particularly wide variation and 17 tests were carried out at this size.

3.2.2 Results

Figure 6 shows a typical load/deformation recording for one of the uniaxial cube strength tests. Appendix A1 tabulates the results of these 33 tests.

3.2.3 Strength versus modulus correlation

Examination of the strengths indicated an exceedingly wide variation at any one cube size; this was particularly noticeable for the 1 inch cube size where, perhaps, specimen preparation may have damaged the cubes. However it was noted that these variations were reflected in the modulus variations. Consequently a linear correlation between cube strength and modulus was attempted for each cube size, with the following results:-

(i) Batch 1 of the 1 inch cube size gave a reasonably good linear correlation between modulus and strength (Figure 7) given by:-

$$\sigma_c = 260 + 0.0257\ E \quad r = 0.97$$

(ii) Batch 2 of the 1 inch cube size gave a rather poor correlation given by (Figure 7).

$$\sigma_c = 917 + 0.00744\ E \quad r = 0.56$$

(iii) Combining both data sets, for all the 1 inch cubes, yielded

$$\sigma_c = 533 + 0.0166\ E \quad r = 0.71$$

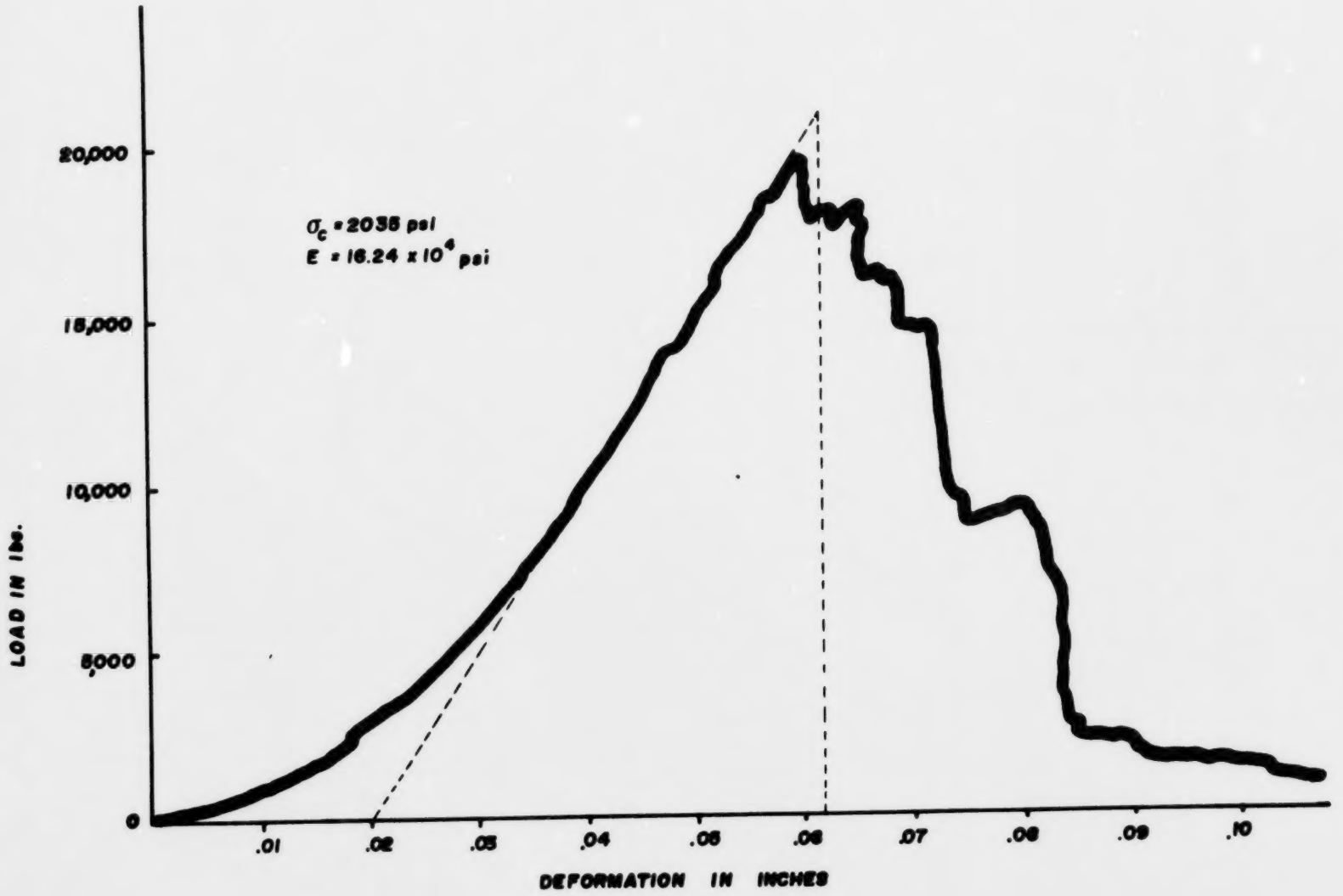

UNIAIAL CUBE TEST - 3" cube #5

FIGURE 6

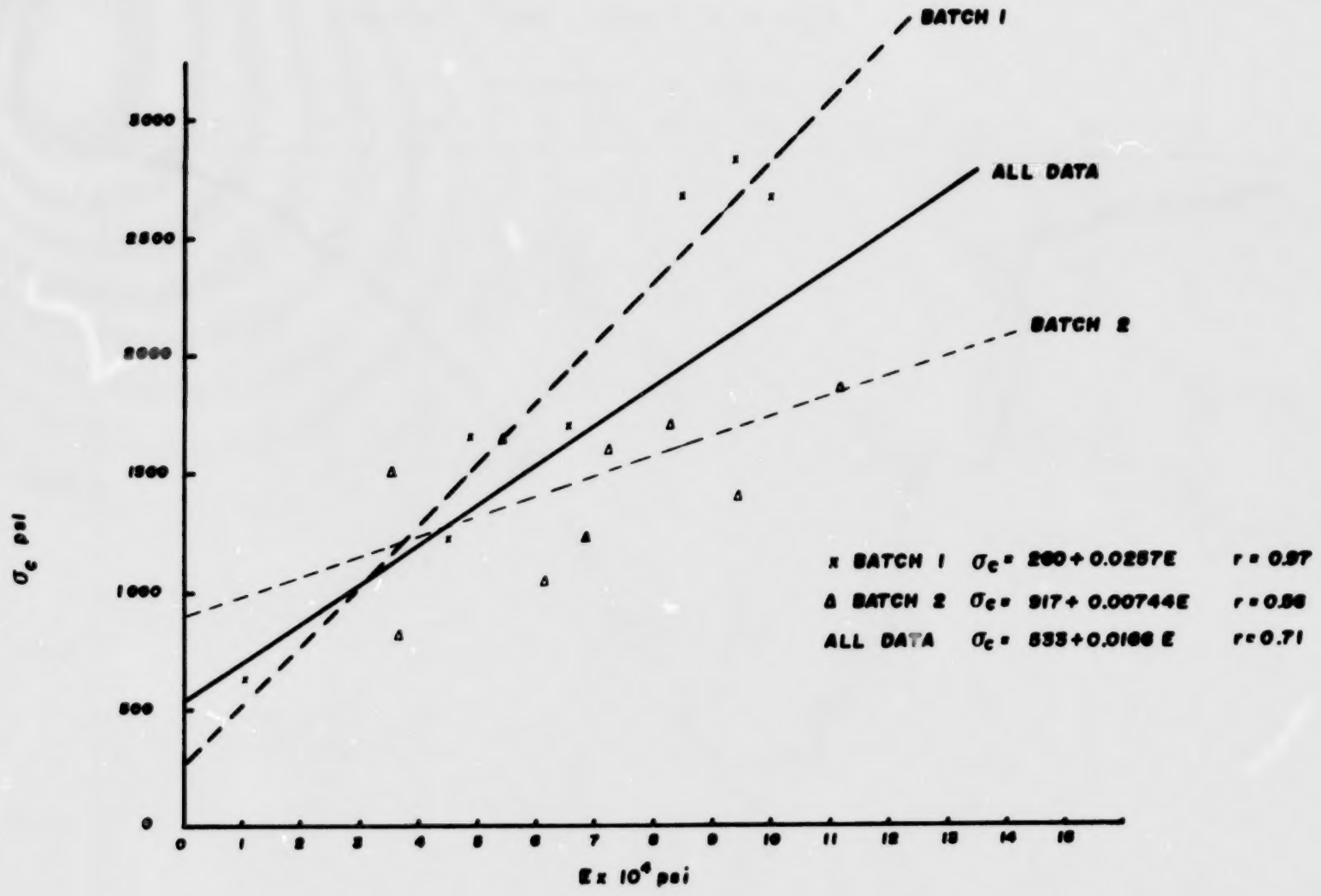

E vs σ_c CONDITION – 1" cubes

FIGURE 7

KJC 86

(iv) Modulus versus cube strength correlations for the 2, 3 and 4 inch cubes (Figure 8) yield

2 inch cubes	$\sigma_c = -344 + 0.0157\ E$	$r = 0.97$
3 inch cubes	$\sigma_c = 20.6 + 0.0121\ E$	$r = 0.87$
4 inch cubes	$\sigma_c = 375 + 0.0775\ E$	$r = 0.97$

With the exception of the second batch of 1 inch cubes, the correlation coefficients are quite good and it may be concluded that the cube strength, for any given cube size, is directly proportional to the cube modulus.

Hence, before considering the relationship between strength and cube size, all the strength data was normalised to the same modulus. (A modulus of 20×10^4 psi was arbitarily choosen, it being the approximate mean modulus for all tests including the triaxial tests).

The normalised cube strength, $\sigma_{cn} = \dfrac{\sigma_c}{E} \times 20 \times 10^4$

Even after normalising the strength data to a constant modulus, the 1 inch cubes still showed a very wide variation of strengths. It was therefore decided to consider only the mean normalised strengths for each cube size when investigating the correlation with cube dimensions; by this means it was hoped to minimize the influence of the large number (17) of 1 inch cubes when compared to the other sizes.

3.2.4 Mean normalised cube strength σ_{cn} versus minimum cube dimensions (W).

Figure 9 shows the mean normalised cube strength data ($\pm$ 1 standard deviation) plotted against the cube size. The minimum lateral cube dimension was taken as the cube size. A correlation was performed in the power curve form and yielded.

$\sigma_{cn} = 5033\ W^{-0.61}$ $\qquad r = 0.94$

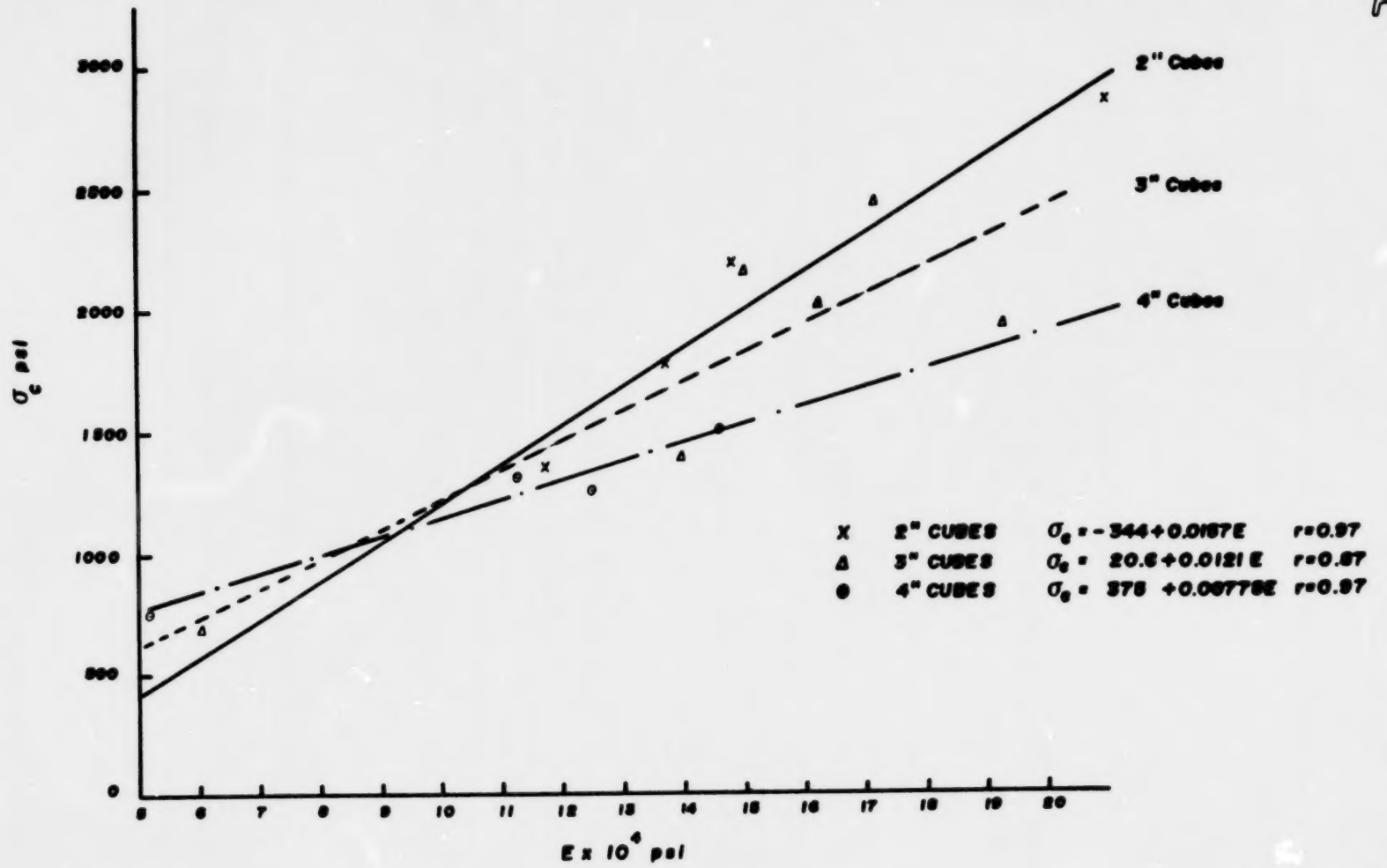

E vs σ_c CONDITION – 2,3,4 inch cubes

FIGURE 8

KJC 1968

CMRC

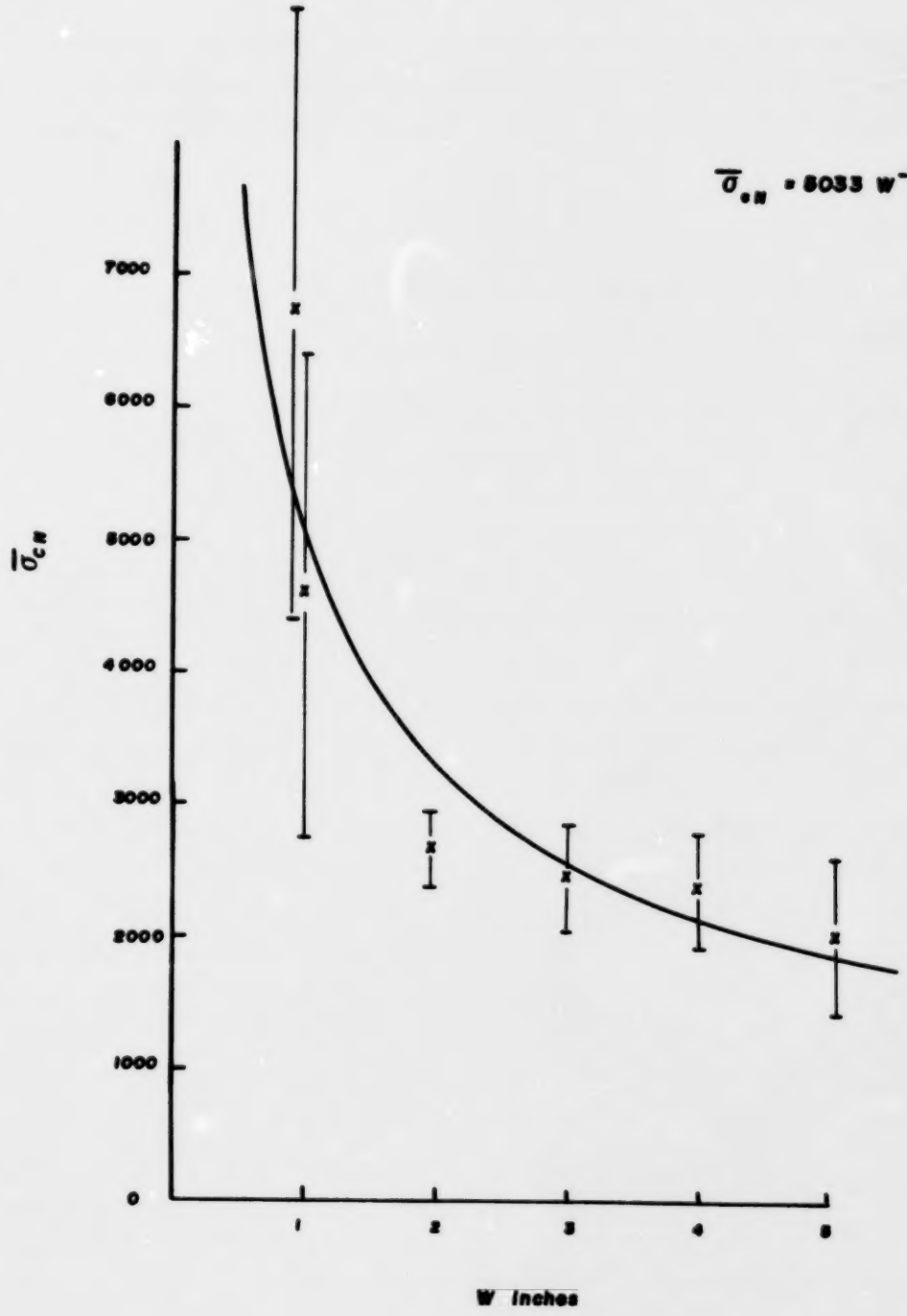

MEAN NORMALISED CUBE STRENGTH VERSUS CUBE SIZE

FIGURE 9

KJC 85

This is a surprisingly good correlation considering the variability of this coal. It also compares fairly well with the generally accepted relationship from past experiments on coal (see review in Appendix B, report Pt. 2 (2)) which gives

$$\sigma_c = k\ W^{-\frac{1}{2}}$$

This will be discussed further after consideration of the data from the rectangular and the circular prisms.

3.3 Group A2: Uniaxial tests in rectangular prisms (square base)

3.3.1 Deviations from the program plan

It should be noted that the cubes discussed in the previous section are also included in this data set (cubes being a special case of a rectangular prism).

In addition to the cubes, the following table compares the number of tests planned with the number actually performed.

H inches	W inch	H/W	planned #	actual #
1½	1	1.5	3	4
3	2	1.5	3	4
4½	3	1.5	3	3
2	3	1.5	3	2
4	2	2.0	3	5
6	3	2.0	3	0
			18	18

No 6 inch by 3 inch square prisms could be successfully prepared.

3.3.2 Results

Appendix A2 tabulates the results of these 51 tests (including cube data). All strength data was normalised to a constant modulus, E = 20 x 10^4 psi, as was done

in section 3.2 for the cube data. Analysis of size/shape effects was carried out using the mean normalised prism strength, $\bar{\sigma}_{pn}$.

3.3.3 Prism strength/shape effects

It was shown in the literature review of past uniaxial prism testing on coal (Part 2 report, Appendix B (2)) that there are three basic forms that have been used in the past to express these strength/shape effects. These three forms are as follows:

(a) The linear form

$$\frac{\sigma_p}{\sigma_c} = a + b \left(\frac{W}{H}\right)$$

where σ_c is the cube strength of a cube of width W.

The parameters a and b generally accepted from past work are given by

$$\frac{\sigma_p}{\sigma_c} = 0.778 + 0.222 \left(\frac{W}{H}\right)$$

(b) The power form

$$\sigma_p = k \frac{W}{H}$$

(Salamon and Munro's relationship (3) $\sigma_p = k \left(\frac{W^{0.46}}{H^{0.66}}\right)$ can be regarded as a variation of this power form)

(c) The "general" form

$$\sigma_p = k \frac{\overline{W}}{H}$$

This form was first proposed by Steart (4), used by Holland and Gadey (5) and shown by the author (2) to give a reasonable fit to all past data and, because it deals with prisms and cubes in a single expression, is thought by the author to be the preferrable form. Certainly it eliminates the need to be concerned about the differences between tests where W is varied and H held constant or vice-versa.

It was therefore decided to examine the test results for correlation in each of

these forms. Table 1 lists the relevant-data and gives the resulting equations and correlation coefficients.

When the linear form is examined (Figure 10) the expression obtained is:

$$\frac{\bar{\sigma}_{pN}}{\sigma_c} = 0.244 + 0.778 \quad (\frac{W}{H})$$

with a correlation coefficient r = 0.76.

This equation does follow the general trend of the results although the correlation coefficient is not particularly good. However it should be noted that the parameters a and b obtained are virtually reversed compared to the generally accepted values given above.

When the data is examined in the $\frac{\overline{W}}{H}$ form or in the general power form $(\frac{W}{H})^{\alpha}$ (Figures 11 and 12), the correlation coefficients are less than 0.25 and no correlation can be assumed to exist.

Examination of the data is the $\frac{\overline{W}}{H}$ from (Figure 13) yields

Linear correlation with $\frac{W}{H}$

$$\sigma_{pN} = 237 + 5595 \frac{W}{H}$$

with a correlation of coefficient r = 0.87

Clearly this latter form gives by far the best fit to the experimental data for this coal.

3.3.4 Correlation of prism strength with modulus

In deriving the above relationships the mean strength data was normalised to a constant modulus, assuming that the result shown to apply for the cube data also applied to the non-cubic prisms. This should be checked by eliminating the size/shape effects and correlating the mean strength, $\bar{\sigma}_p$ (un-normalised), with the measured modulus E. This was done by plotting $\sigma_p \left(\frac{H}{W}\right)$ versus E. Table 2 lists the relevant data and Figure 14 shows the resulting graph.

TABLE 1:

MEAN NORMALISED STRENGTHS FOR UNIAXIALLY LOADED RECTANGULAR PRISMS

σ_{pN}	σ_{cN}*	$\frac{\sigma_{pN}}{\sigma_c}$	W	H	$\frac{W}{H}$	$\sqrt{\frac{W}{H}}$	$\sqrt{\frac{W}{H}}$
psi	psi		inches	inches			
6688	5378	1.24	0.897	0.959	0.935	0.967	0.987
4577	5030	0.91	1.001	1.015	0.986	0.993	0.986
2666	3337	0.80	1.961	1.984	0.988	0.994	0.706
2443	2572	0.95	3.005	2.982	1.007	1.004	0.581
2354	2149	1.10	4.036	4.040	0.999	0.995	0.497
2011	1863	1.08	5.098	5.049	1.010	1.005	0.447
3589	5257	0.68	0.931	1.440	0.646	0.804	0.670
3087	3393	0.91	1.909	2.990	0.638	0.799	0.462
2002	2579	0.78	2.993	4.524	0.661	0.813	0.382
2146	3330	0.64	1.968	4.026	0.489	0.699	0.348
2530	5130	0.49	0.969	1.998	0.486	0.696	0.493

* Assuming $\sigma_{cN} = 5033\ W^{-0.61}$ (from cube strength relationship derived in section 3.2).

(a) Linear correlation with $(\frac{W}{H})$ gives

$$\frac{\bar{\sigma}_{pN}}{\sigma_{cN}} = 0.244 + 0.778\ (\frac{W}{H}) \qquad r = 0.76$$

(b) Linear correlation with $(\frac{W}{H})^{1/2}$

$$\bar{\sigma}_{pN} = 654 + 2753 \sqrt{\frac{W}{H}} \qquad r = 0.25$$

(c) Linear correlation with $(\frac{W}{H})^{\alpha}$

$$\bar{\sigma}_{pN} = 3108\ (\frac{W}{H})^{0.30} \qquad r = 0.23$$

(d) Linear correlation with $\sqrt{(\frac{W}{H})}$

$$\bar{\sigma}_{pN} = -237 + 5595 \sqrt{\frac{W}{H}} \qquad r = 0.87$$

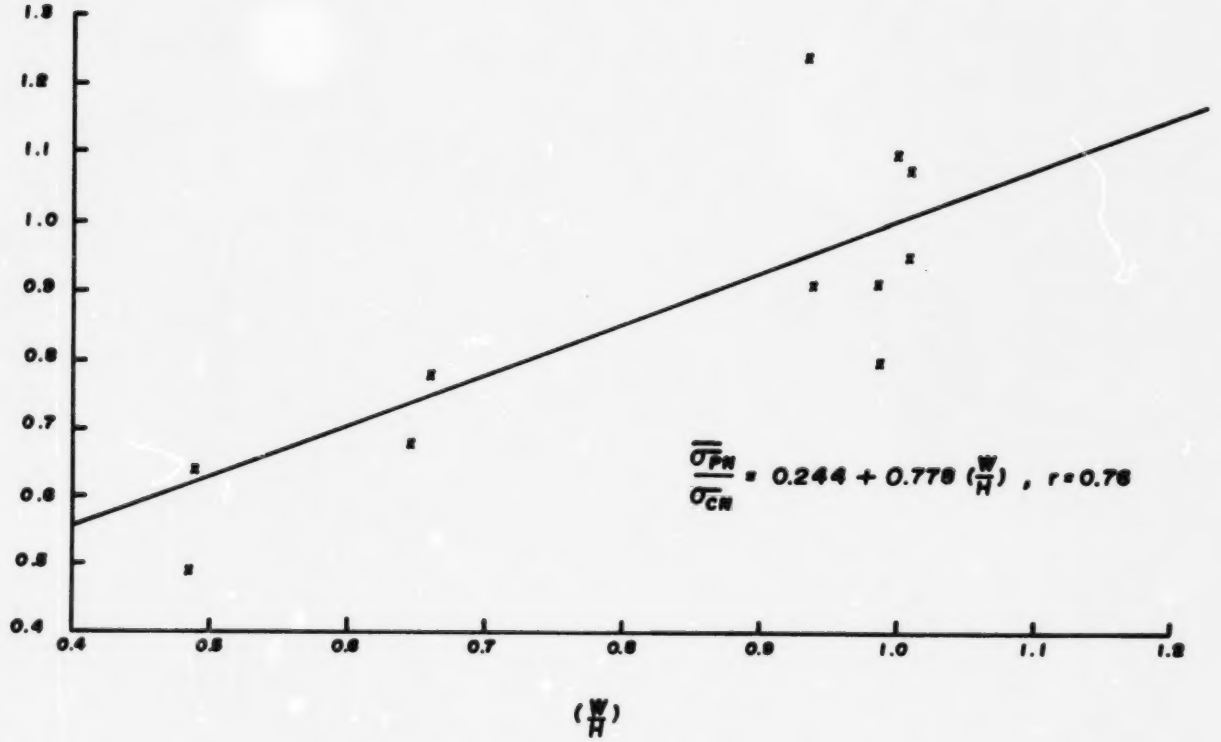

UNIAXIAL RECTANGULAR PRISMS - $\frac{\overline{\sigma_{PN}}}{\sigma_{CN}}$ vs $(\frac{W}{H})$

FIGURE 10

KJC 68

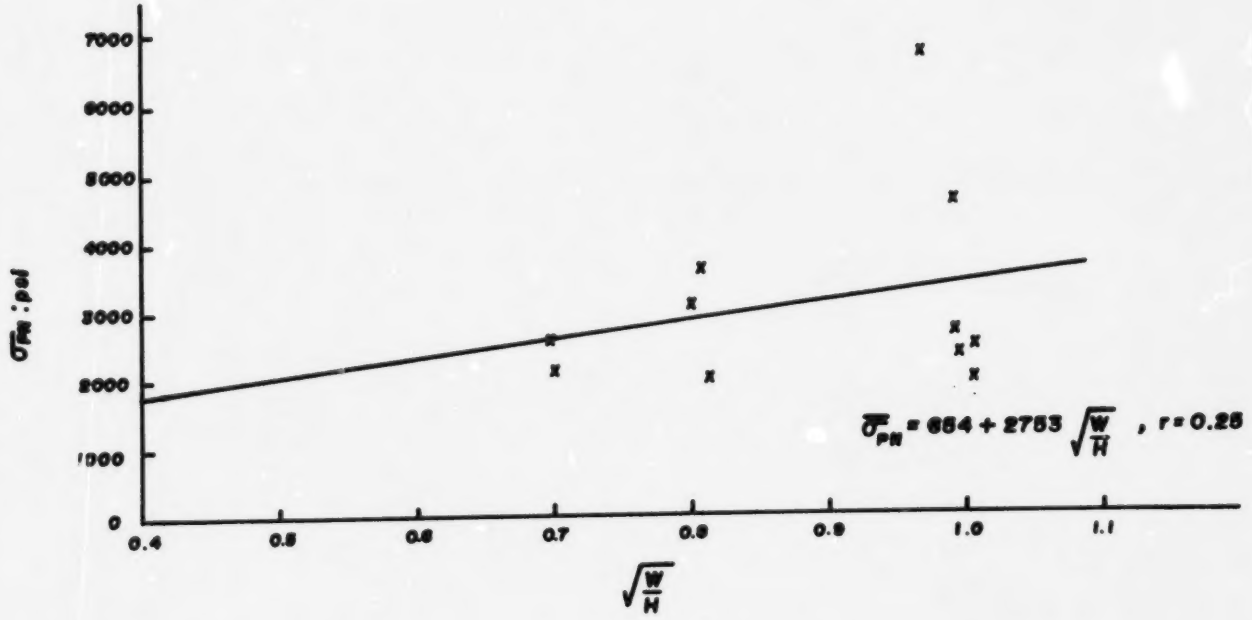

UNIAIAL RECTANGULAR PRISMS — $\overline{\sigma_{PH}}$ vs $\sqrt{\frac{W}{H}}$

FIGURE 11

KJC 86

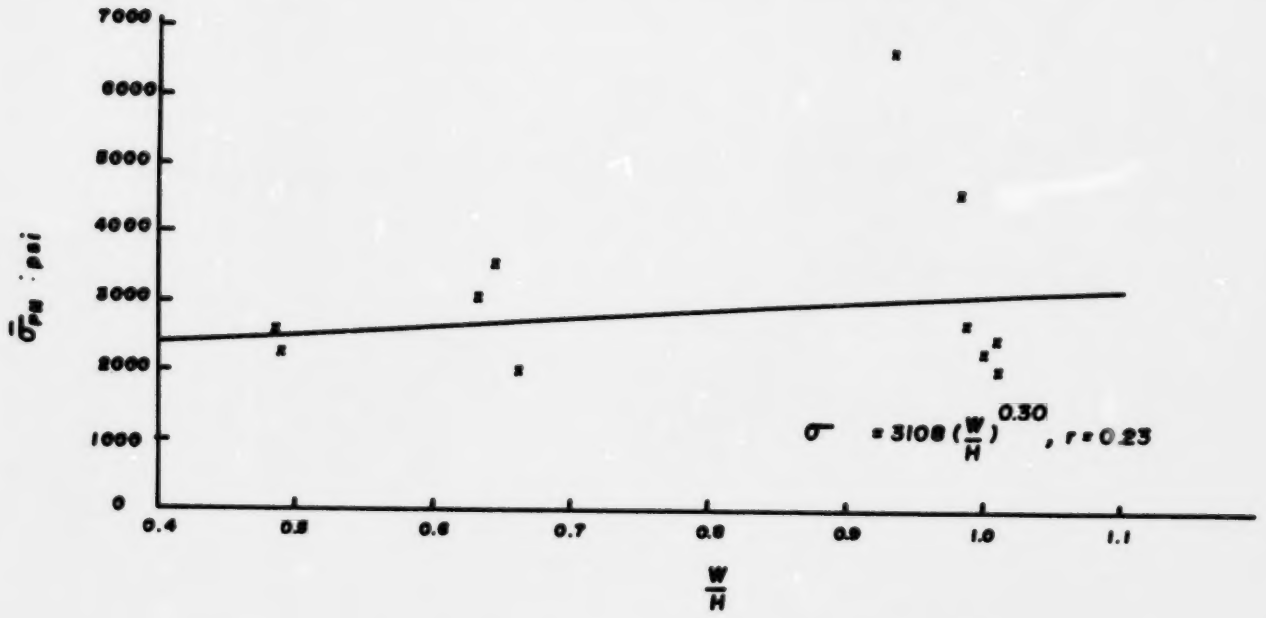

UNIAXIAL RECTANGULAR PRISMS – $\overline{\sigma_{PN}}$ vs $(\frac{W}{H})^{\alpha}$

FIGURE 12

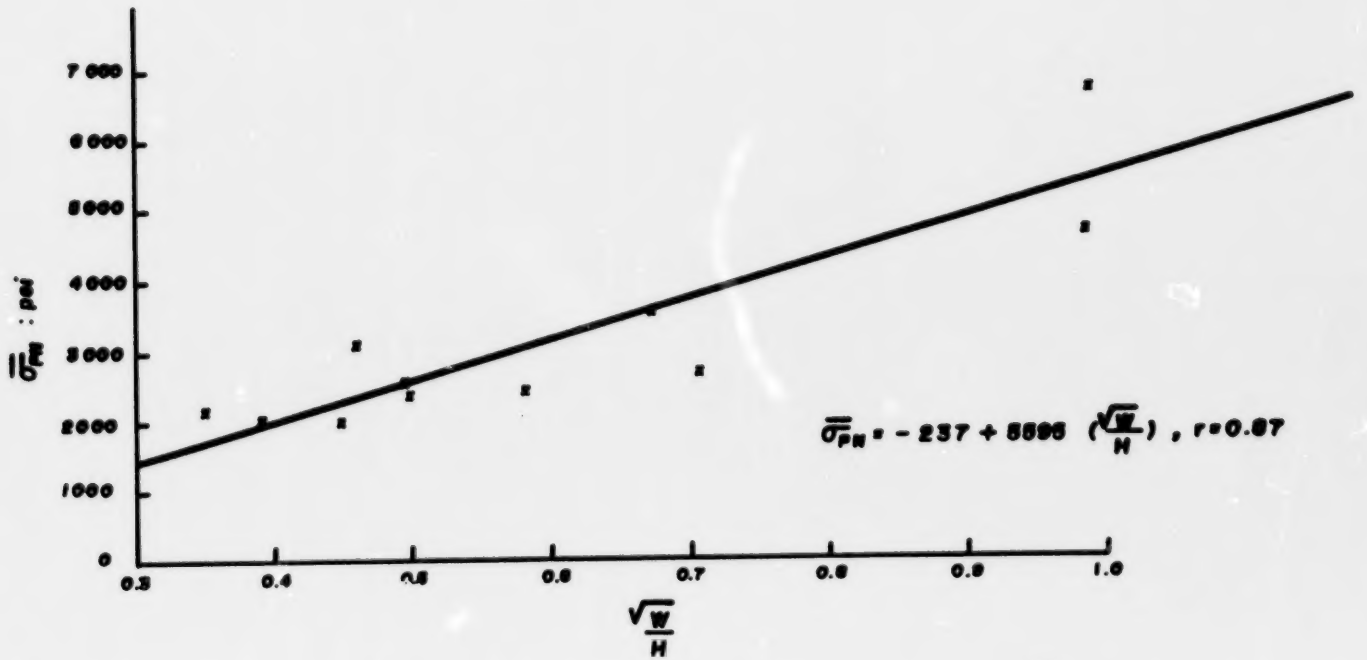

UNIAXIAL RECTANGULAR – $\bar{\sigma}_{PN}$ vs $(\frac{\sqrt{W}}{H})$

FIGURE 13

TABLE 2
MEAN STRENGTHS FOR UNIAXIALLY LOADED RECTANGULAR PRISMS
CORRELATION WITH MODULUS

Mean Strength σ_p psi	Mean W inches	Mean H inches	$\frac{W}{H}$	$\sigma_p \cdot \frac{H}{W}$	Modulus E x 10^4 psi
1911	0.897	0.959	0.987	1936	6.42
1468	1.001	1.015	0.986	1489	6.84
2026	1.961	1.984	0.706	2918	15.3
1790	3.006	2.982	0.581	3079	14.56
1216	4.036	4.04	0.497	2445	10.86
1232	6.098	5.049	0.447	2755	12.69
2320	0.931	1.44	0.670	3462	13.06
3136	1.909	2.990	0.462	6786	20.16
1363	2.993	4.524	0.382	3564	13.80
1214	1.968	4.026	0.348	3484	11.38
840	0.969	1.998	0.492	1704	7.11

$$\sigma_p\left(\frac{H}{W}\right) = -610 + 0.0305\,E; \quad r = 0.88$$

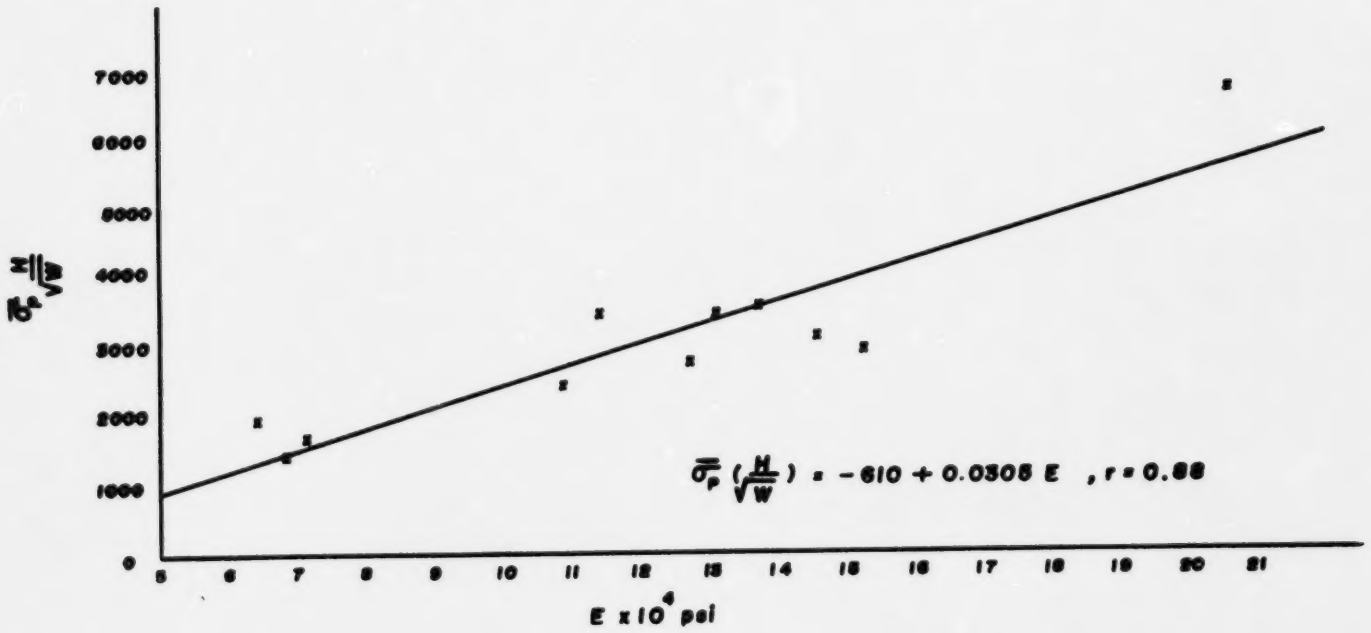

UNIAXIAL RECTANGULAR PRISMS – $\bar{\sigma}_p \left(\frac{H}{\sqrt{W}}\right)$ vs E

FIGURE 14

The linear correlation is given by:-

$$q_p\left(\frac{H}{\sqrt{W}}\right) = -610 + 0.0305\,E$$

with a correlation coefficient r = 0.88.

This is a reasonably good correlation and it can be concluded that normalisation of the data to a constant modulus prior to examination of the size/shape effects was justified.

3.4 Group A3: Uniaxial tests on circular prisms

3.4.1 Deviations from the program plan

The following table compares the number of tests planned with these actually performed

H inches	Dia W inches	H/W	planned #	Actual #
1	1	1	3	0
2	2	1	3	4
3	3	1	3	4
1½	1	1½	3	0
3	2	1½	3	4
4½	3	1½	3	3
2	1	2	3	0
4	2	2	3	5
6	3	2	3	0
5	3	1.7	0	3
			27	23

No 1 inch diameter specimens were prepared due to a tendency to snap off during drilling. The proposed 6 x 3 inch specimens were replaced by 5 inch x 3 inch specimens; the larger specimens could not be obtained.

3.4.2 Results

Appendix A3 tabulates the results of these 23 tests. All strength data was normalised to a constant modulus, E = 20 x 10^4 psi. Analysis of the size/shape effects was carried out using the mean normalised prism strenth, $\bar{\sigma}_{pN}$.

3.4.3 Prism strength/shape effects

In the light of the results from the previous section a correlation between σ_{pN} and $\sqrt{\frac{W}{H}}$ only was sought (W in this case being the specimen diameter).

This correlation (Figure 15) yielded the following equation:-

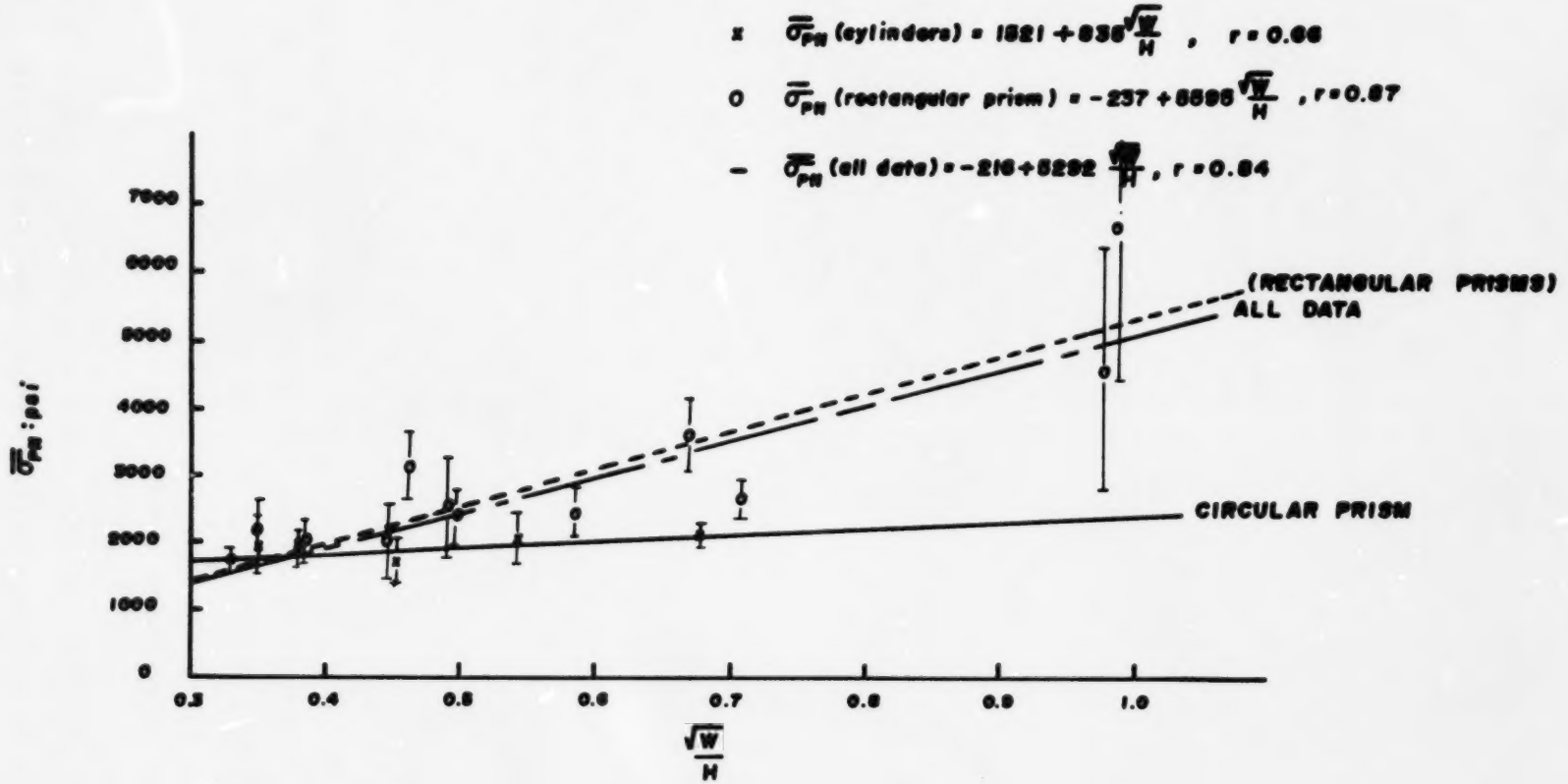

$\overline{\sigma_{PN}}$ versus $\sqrt{\frac{W}{H}}$, FOR CYLINDRICAL, RECTANGULAR AND ALL OTHER PRISMS

FIGURE 18

EJC 86

$$\bar{\sigma}_{pN} = 1521 + 835\sqrt{\frac{W}{H}}$$

with a correlation coefficient, r = 0.66

This equation shows little resemblence to that for the rectangular prims, namely

$$\bar{\sigma}_{pN} = -237 + 5595\sqrt{\frac{W}{H}},\ 4 = 0.87$$

This latter equation is also plotted on Figure 15.

Visual examination of this Figure shows that the cylindrical prism data appears to fall within the scatter band of the rectangular prism data. Hence it may be concluded that within the accuracy of the measurement data, there would appear to be no need to correct the circular prism data to conform to the rectangular prism data. This was confirmed by considering all the data together which yielded the following equation:

$$\bar{\sigma}_{pN} = -216 + 5292\sqrt{\frac{W}{H}} \quad ; \quad r = 0.84$$

This is very close to that for the rectangular prism data only and the correlation coefficient is not significantly changed. Hence to may be concluded that, within the limits of the experimental accuracy, the cylindrical and rectangular prism results may be considered to be the same.

3.4.4 Correlation of all data with modulus

$\bar{\sigma}_p \left(\frac{H}{\sqrt{W}}\right)$ versus modulus E was plotted (Figure 16) for all the cube, rectangular prism and cylindrical prism results. (Table 3 gives the relevant data).

The resulting equation is

$$\bar{\sigma}_p \frac{H}{\sqrt{W}} = -341 + 0.0265\,E \quad ; \quad r = 0.87$$

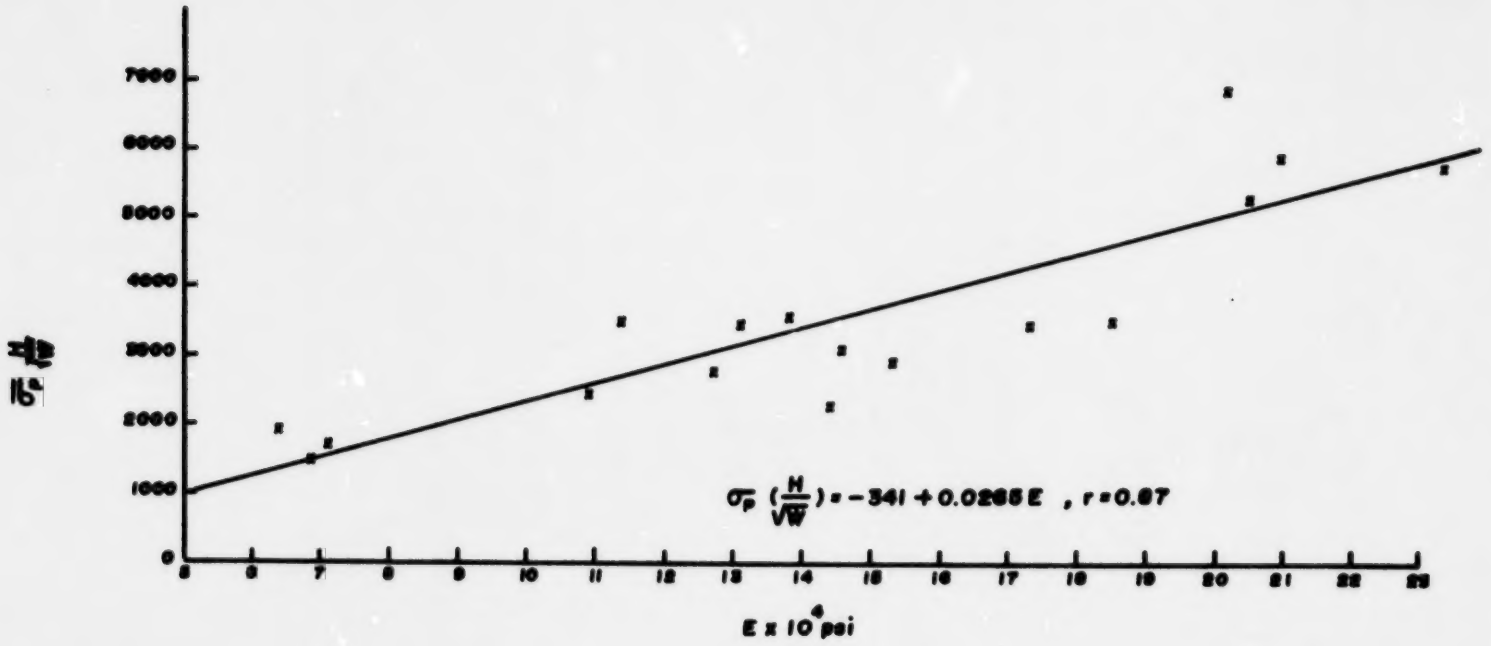

$\sigma_{FN}\frac{H}{\sqrt{W}}$ versus E, FOR ALL PRISMS

FIGURE 16

KJC 88

TABLE 3
MEAN STRENGTHS FOR ALL UNIAXIALLY LOADED PRISMS
CORRELATION WITH MODULUS

Mean Strength σ_p psi	Mean W inches	Mean H inches	$\frac{W}{H}$	Modulus E x 10^4 psi	$\bar{\sigma}_p \frac{H}{W}$
1911	0.897	0.959	0.987	6.42	1936
1468	1.001	1.015	0.986	6.84	1489
2060	1.961	1.984	0.706	15.3	2918
1790	3.005	2.982	0.581	14.56	3079
1216	4.036	4.04	0.497	10.86	2445
1232	5.098	5.049	0.447	12.69	2755
2320	0.931	1.440	0.670	13.06	3462
3136	1.909	2.990	0.462	20.16	6786
1363	2.993	4.524	0.382	13.80	3564
1214	1.968	4.026	0.348	11.38	3484
840	0.969	1.998	0.492	7.11	1704
1507	2.113	2.148	0.677	14.4	2226
1577	2.114	3.21	0.453	18.51	3481
2072	2.115	4.14	0.351	20.95	5903
1839	3.0	3.195	0.542	17.33	3393
2207	2.996	4.566	0.379	23.3	5823
1755	3.0	5.235	0.331	20.48	5302

$$\bar{\sigma}_p \frac{H}{W} = -341 + 0.0265\,E \quad ; \quad r = 0.87$$

3.5 Summary and conclusions

1. The experimental prism strength is linearly correlated to the prism modulus, E.

2. Size/shape effects can be distinguished when the data is normalised to the same, constant, modulus.

3. By far the best correlation between the mean normalised strength, σ_{pn}, and the prism dimension is given by the "general" form:-

$$\bar{\sigma}_{pn} \propto \sqrt{\frac{W}{H}} \qquad (1)$$

When normalised to a constant modulus, E = 20 x 10^4 psi, the general form for the coal is given by

$$\bar{\sigma}_{pn} = -216 + 5292 \sqrt{\frac{W}{H}}; \quad \text{correlation coefficient } r = 0.84$$

4. Within the limits of experimental accuracy, no correction factor is distinguishable between cylindrical and rectangular prisms.

5. After correction for the size/shape effects, the strength correlation with modulus for all prisms is given by

$$\bar{\sigma}_p \sqrt{\frac{H}{W}} = -341 + 0.0265E; \quad \text{correlation coefficient } r = 0.87 \qquad (2)$$

6. Hence, from (1) and (2) a general expression relating all the uniaxial prism strengths can be expressed in the form.

$$\frac{\bar{\sigma}_p}{E} = a + b\sqrt{\frac{W}{H}}$$

For this particular coal, this expression is shown in Figure 17 and is given by:-

$$\frac{\bar{\sigma}_p}{E} = 0.00034 + 0.0232\sqrt{\frac{W}{H}}; \quad \text{correlation coefficient } r = 0.85 \qquad (3)$$

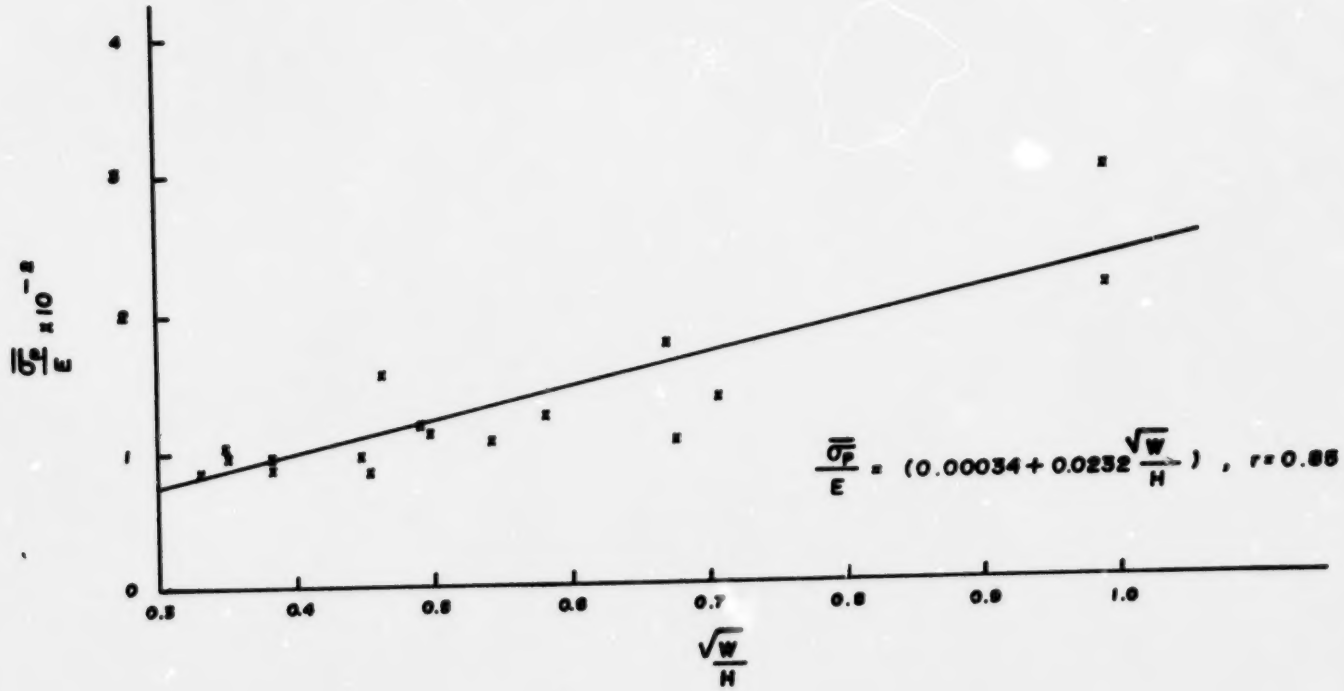

$\frac{\bar{\sigma}_p}{E}$ versus $\sqrt{\frac{W}{H}}$ — ALL DATA

FIGURE 17

For practical purposes, over the experimental range of $\sqrt{\frac{W}{H}}$ from 1 to 0.3, putting a = 0 will only give from 1.5 to 5% error. Hence this relationship can be expressed more simply as

$$\frac{\bar{\sigma}_p}{E} = 0.0232\sqrt{\frac{W}{H}} \qquad (4)$$

4. TRIAXIAL TESTS ON COAL SPECIMENS - GROUP B RESULTS AND ANALYSIS

4.1 Deviation from the program plan

(i) For Group B1 it was planned to test 1 inch diameter by 2 inch high specimens; however it proved to be impossible to drill 1 inch diameter core in the test coal. Consequently these tests were replaced by Group B3 and B4 described below.

(ii) Group B2 tests were carried out as planned with 2 1/8 inch diameter cores of a height of 4.1 inches.

(iii) To replace the group B1 tests it was decided to go to a larger core diameter and specimens of 3" diameter by approximately 4½ inches high were prepared. A limited number of these tests were performed at low confining pressures ($\leq$ 4000 psi). At high confining pressures a great deal of trouble was experienced with splitting of the surrounding membrane which allowed oil to enter the specimen and negated the results. Thus this suite of tests could not be completed.

(iv) It was therefore decided to test a second suite of 2 1/8 inch diameter core but this time with a height of only 2 1/8 inches (i.e. $\frac{H}{W} = 1$); thus examining the triaxial size effects by changing the height rather than the diameter.

The table below compares the number of planned tests with the number actually carried out.

Confining pressure psi	Group B1 H = 2" Planned	Group B1 W = 1" Actual	Group B2 H = 4", Planned	Group B2 W = 2" Actual	Group B3 H = 4½" Planned	Group B3 W = 3" Actual	Group B4 H = 2" Planned	Group B4 W = 2" Actual
0	3	0	3	5	0	3	0	3
1000	-	0	-	2	0	-	0	3
2000	3	0	3	3	0	3	0	3
3000	-	0	-	2	0	-	0	0
4000	3	0	3	3	0	2	0	3
6000	3	0	3	2	0	-	0	3
7500 or 8000	3	0	3	2	0	-	0	2
10000	3	0	3	2	0	-	0	0
	15	0	15	21	0	8	0	17

(v) With the particular design of triaxial cell used it was not possible to carry out the planned triaxial "slip" tests on the failed specimens. Clearance between the cell walls and the specimen was insufficient - this resulted in puncturing of the surrounding membrane allowing oil to enter the specimen. Consequently these proposed tests were abandoned.

4.2 Group B2 results, Triaxial tests on solid coal, (H = 4.1 in, W = 2.1 in.)

4.2.1 Results

Figure 18 shows a typical load deformation curve obtained from these tests. Appendix B1 tabulates the results of these 21 tests.

4.2.2 Strength correlation with modulus

As with the uniaxial test results it was found that the coal modulus varied widely from specimen to specimen. It was believed that the principal stress difference at peak stress might be related to the modulus of the coal; this was examined. Table 4 lists the mean modulus, the mean peak and mean residual stresses at failure, the confining pressure and the mean principal stress difference at failure. Figure 19 shows the resulting correlation. (Note the data from the 4 inch by 2 inch rectangular prisms is also included). A reasonably good correlation coefficient of r = 0.92 is obtained and the relationship is given by:

$$(\bar{\sigma}_p - \bar{\sigma}_3) = -2770 + 0.029\,E, \qquad r = 0.92$$

However, if each individual data item is considered (rather than the mean values) the correlation becomes

$$(\bar{\sigma}_p - \bar{\sigma}_3) = -2702 + 0.0.0279\,E,$$

with a correlation coefficient of only 0.75.

This is a rather poor correlation coefficient and makes it questionable whether

COAL MINING RESEARCH CENTRE

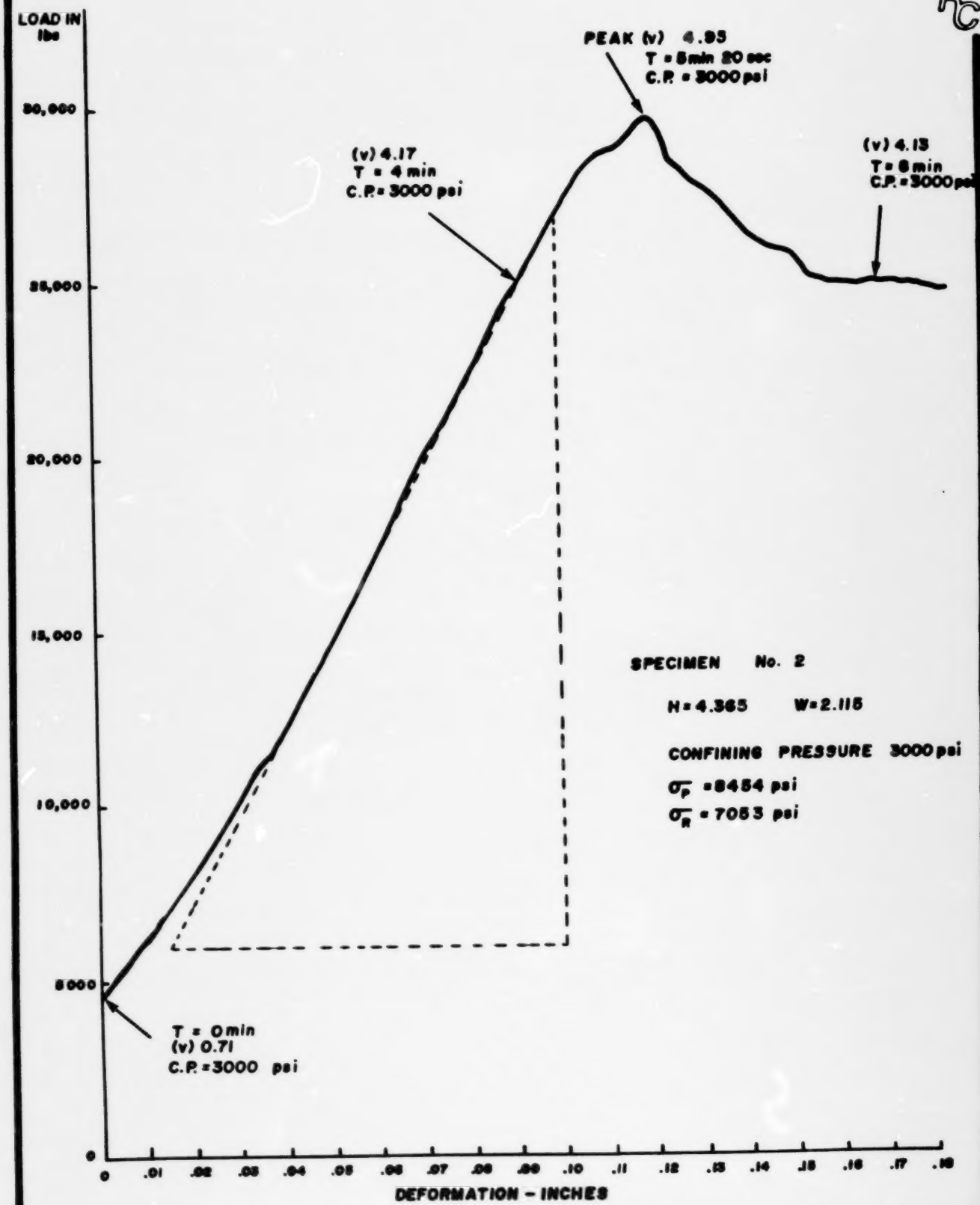

TYPICAL LOAD - DEFORMATION CURVE FOR TRIAXIAL TESTS ON COAL

FIGURE 18

RJC 68

Table 4: Group B2 - Mean Peak and Residual Strength Data

Confining Pressure psi	Mean Peak Strength $\bar{\sigma}_p$ psi	Mean Residual Strength $\bar{\sigma}_R$ psi	Modulus E x 10^4 psi	$\bar{\sigma}_p - \bar{\sigma}_3$ psi	Notes
0	1,214	-	11.38	1,214	Rectangular Prisms 4"x2"
0	2,072	-	20.95	2,072	Circular Cylinders
1,000	5,170	4,112	27.51	4,170	"
2,000	6,698	6,023	28.12	4,698	"
3,000	8,136	7,342	27.13	5,136	"
4,000	8,263	7,666	22.70	4,263	"
6,000	12,298	11,403	29.88	6,298	"
7,500	13,821	12,365	29.51	6,321	"
10,000	17,278	16,745	31.77	7,378	"

$\bar{\sigma}_p - \bar{\sigma}_3 = -2770 + 0.029\,E,$ $\quad r = 0.92$

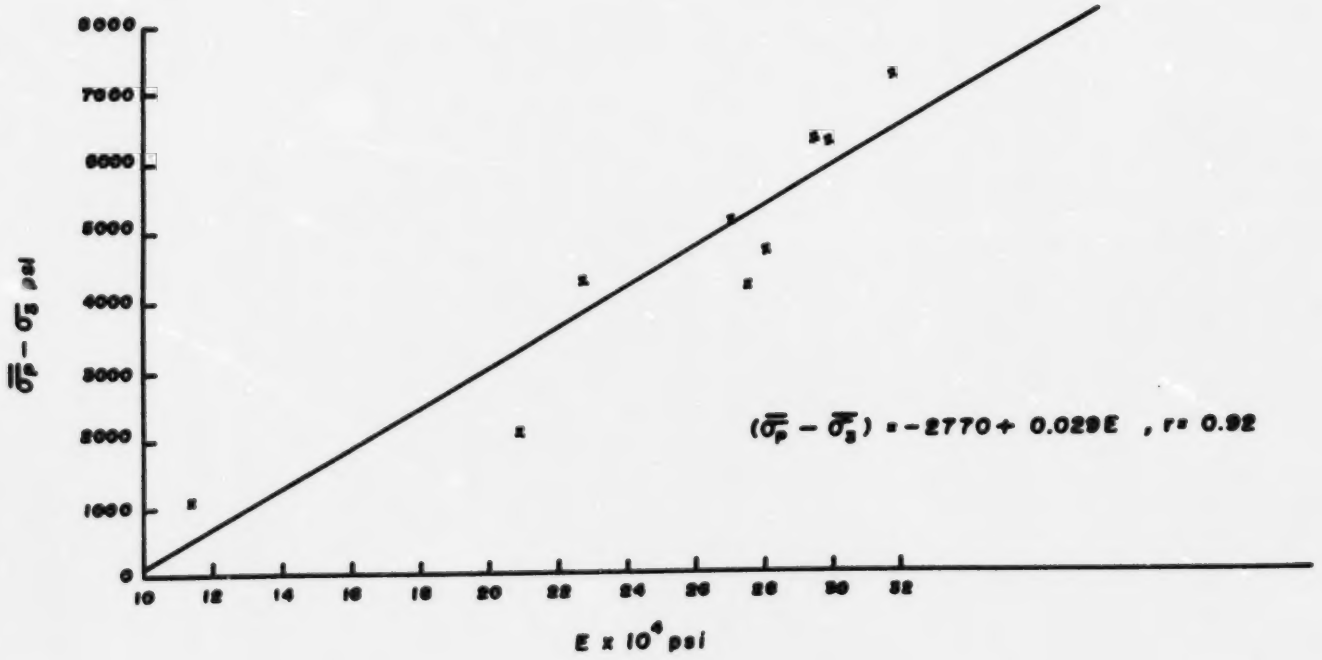

CORRELATION OF PRINCIPAL STRESS DIFFERENCE AT FAILURE WITH MODULUS

FIGURE 19

RJC 86

the data should or should not be "normalised". After due consideration it was decided not to normalise the data, but rather to deal only with the mean raw data.

4.2.3 σ_1/σ_3 relationship at failure

It was assumed that the σ_1, σ_3 relationship at failure is best described by a Mohr envelope of Balmer's form where the relationship is given by:-

$$\sigma_3 = a + b\,\sigma_1^{\,c}$$

Table 5 summarizes the mean peak and residual strength data for this group. For the peak strength data the following relationship was determined:-

$$\sigma_3 = -348 + .0045\ \sigma_1^{\,1.50}$$

with a correlation coefficient r = 0.993.

Figure 20 shows this relationship and measured mean points. The fit is excellent. For the residual strength data the following relationship was determined:-

$$\sigma_3 = 395 + 0.00097\ \sigma_1^{\,1.66} \qquad r = 0.985$$

This relationship and the measured points are also shown in Figure 20. This relationship is also a reasonably good fit to the data.

However it will be immediately noted that the two curves do not intersect but approach each other and then diverge i.e. no transition point is indicated although the closest point of approach is at approximately σ_1 = 11,000 psi σ_3 = 6000 psi.

It is clear that with both curves bending in the same direction it will be very difficult to determine the transition point.

Table 5 - Mean peak and residual strengths - Group B2

Confining pressure	Mean peak stress-psi	Mean residual stress-psi
0	2,072	0
1,000	5,170	4,112
2,000	6,698	6,023
3,000	8,136	7,342
4,000	8,263	7,666
6,000	12,298	11,403
7,500	13,821	12,365
10,000	17,278	16,745

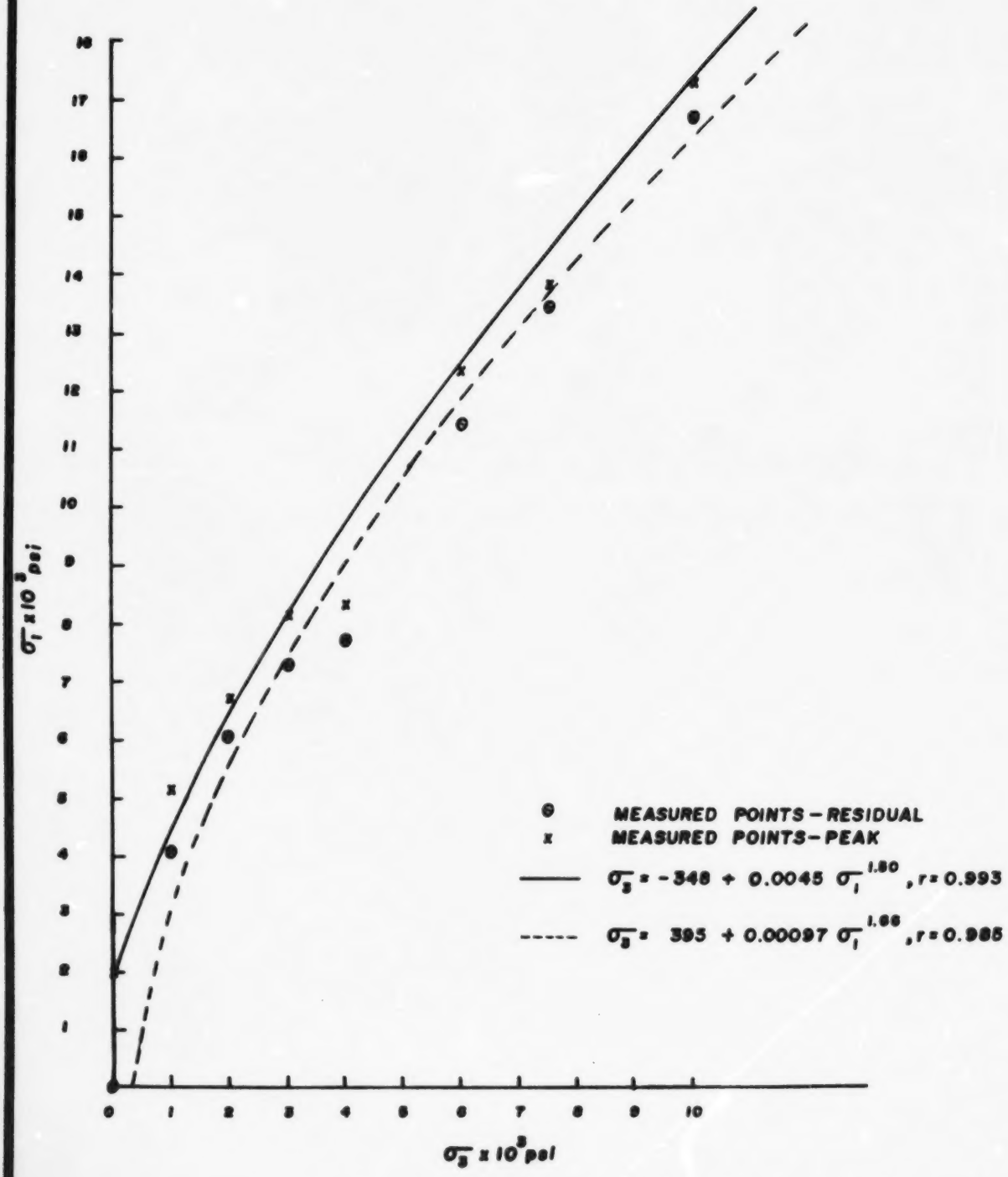
$\sigma_1 \times 10^3$ psi
$\sigma_3 \times 10^3$ psi
0 1 2 3 4 5 6 7 8 9 10
1 2 3 4 5 6 7 8 9 10 11 12 13 14 15 16 17 18
MEASURED POINTS – RESIDUAL
MEASURED POINTS – PEAK
$\sigma_3 = -348 + 0.0045\ \sigma_1^{1.80}$, r = 0.993
$\sigma_3 = 395 + 0.00097\ \sigma_1^{1.88}$, r = 0.985

σ_1 vs σ_3 - GROUP B2 - PEAK AND RESIDUAL STRENGTHS

FIGURE 20

RJC 86

4.3. Group B3 results - Triaxial tests on solid coal (H = 5.01 in W = 3.0 in.)

4.3.1 Results

Appendix B2 tabulates the results of these 9 results. Table 6 summarises the mean peak and residual strength data for the group. Figure 21 shows all data points on a σ_3 vsσ_1 plot. Clearly there is a wide scatter and unsufficient data from this group to allow a statistical analysis to be attempted.

4.4 Group B4 results - Triaxial tests in solid coal (H = 2.175 W = 2.12)

4.4.1 Results

Appendix B3 tabulates the results of these 18 tests. Table 7 summarises the mean peak and residual strength data for this group.

4.4.2 $\sigma_1 - \sigma_3$ relationship at failure

For the peak strength data the following relationship was determined

$$\sigma_3 = -267 + 0.000310\ \sigma_p^{1.797}, \quad r = 0.992$$

For the residual strength data the relationship is:-

$$\sigma_3 = -14.3 + .000293\ \sigma_R^{1.80}, \quad r = 0.991$$

Figure 22 shows these relationships and the measured points.

These two curves are exceedingly close to each other and although they intersect at approximately σ_1 = 15,000 psi, σ_2 = 9,600 psi, clearly this intersection point is not very accurate.

Table 6 - Mean peak and residual strengths - Group B3

Confining pressure	Mean peak stress-psi	Mean residual stress-psi
0	1,755	0
1,000	2,279	1,880
2,000	8,00	25,683
4,000	10,791	9,279

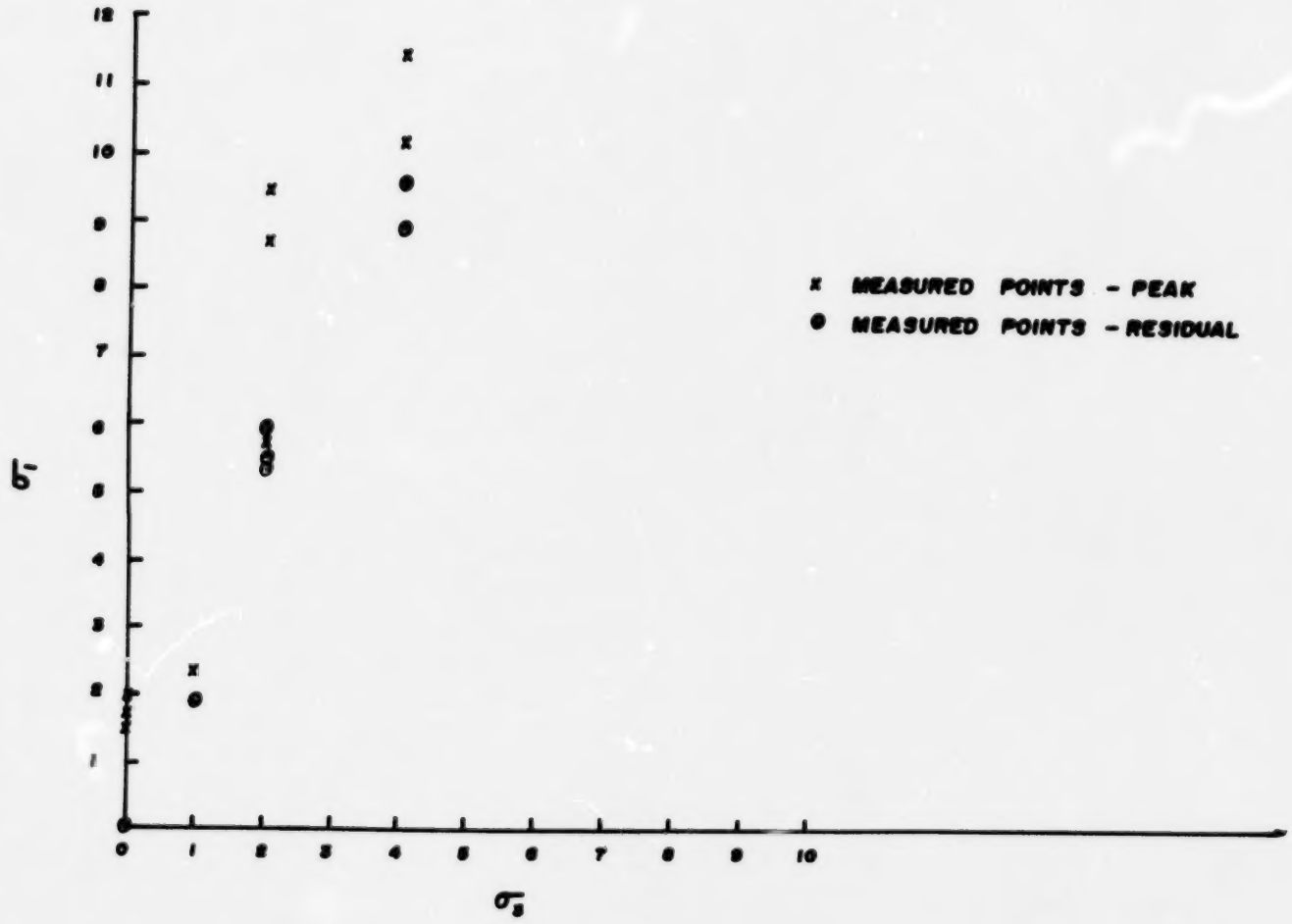

σ1 vs σ3 - GROUP B3 — PEAK AND RESIDUAL

FIGURE 21

KJC 86

Table 7: Mean peak and residual strengths - Group B4

Confining pressure	Mean peak stress-psi	Mean residual stress-psi
0	2,099	0
1,000	5,300	4,910
2,000	7,075	6,843
4,000	8,665	8,542
6,000	11,267	11,030
8,000	13,897	13,897

CMRC

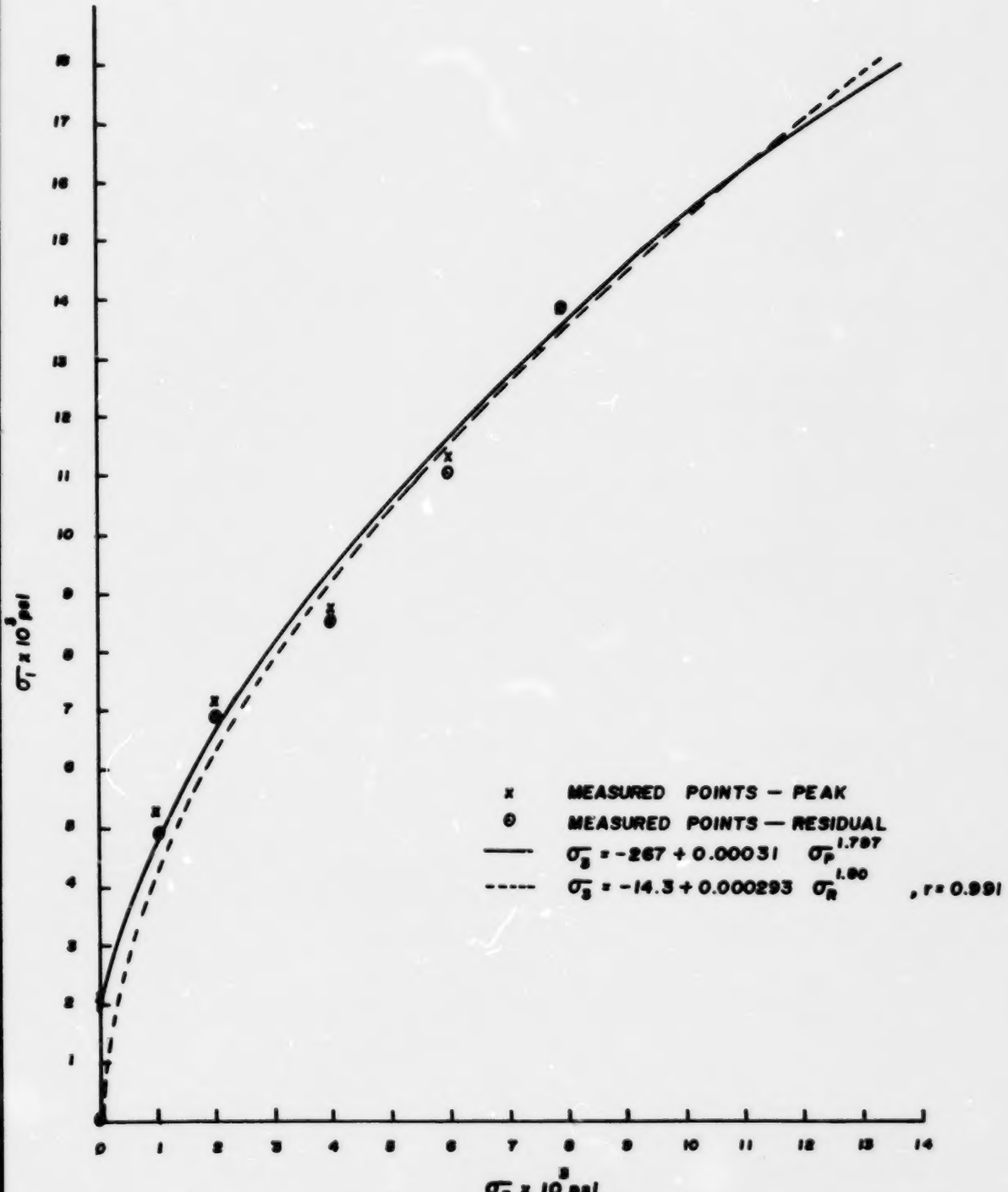

σ_1 vs σ_3 – GROUP B4 – PEAK AND RESIDUAL STRESSES

FIGURE 22

KJC 86

4.5 Comparison of Group B2 and B4 results

4.5.1 Peak strengths

Figure 23 shows a comparison of the peak strength relationships for groups B2 and B4. There is a difference between these curves but whether or not the difference is significant (i.e. whether a size effect has shown up) is not clear. This will be discussed further in section 4.6.

4.5.2 Residual strengths

Figure 24 shows a comparison of the residual strength data for the two groups. There would seem to be very little difference between these two curves. Thus we can tentatively conclude that the residual strength is independent of size. If this is the case then we could better define the relationship by combining the two data groups and also adding the group B3 residual data. This has been done and the relationship derived is:

$$\sigma_3 = -52.3 + 0.0106\ \sigma_3^{1.42}, \qquad r = 0.993$$

Figure 25 shows this relationship and all the measured data. This expression appears to be a reasonable fit for all data.

4.5.3 Transition point

The expression for the peak strengths for groups B2 and B4 have been plotted in Figure 26 and compared with this general expression for all residual data. It is seen that the group B2 data does not indicate a transition point where as the group B4 data indicates a transition point at

$$\sigma_3 = P_{3T} = 7{,}070 \text{ psi}$$

$$\sigma_1 = P1T = 12{,}700 \text{ psi}$$

The validity and the accuracy of this point must be questionable; although this point will be taken as the transition point in the ensuing discussion.

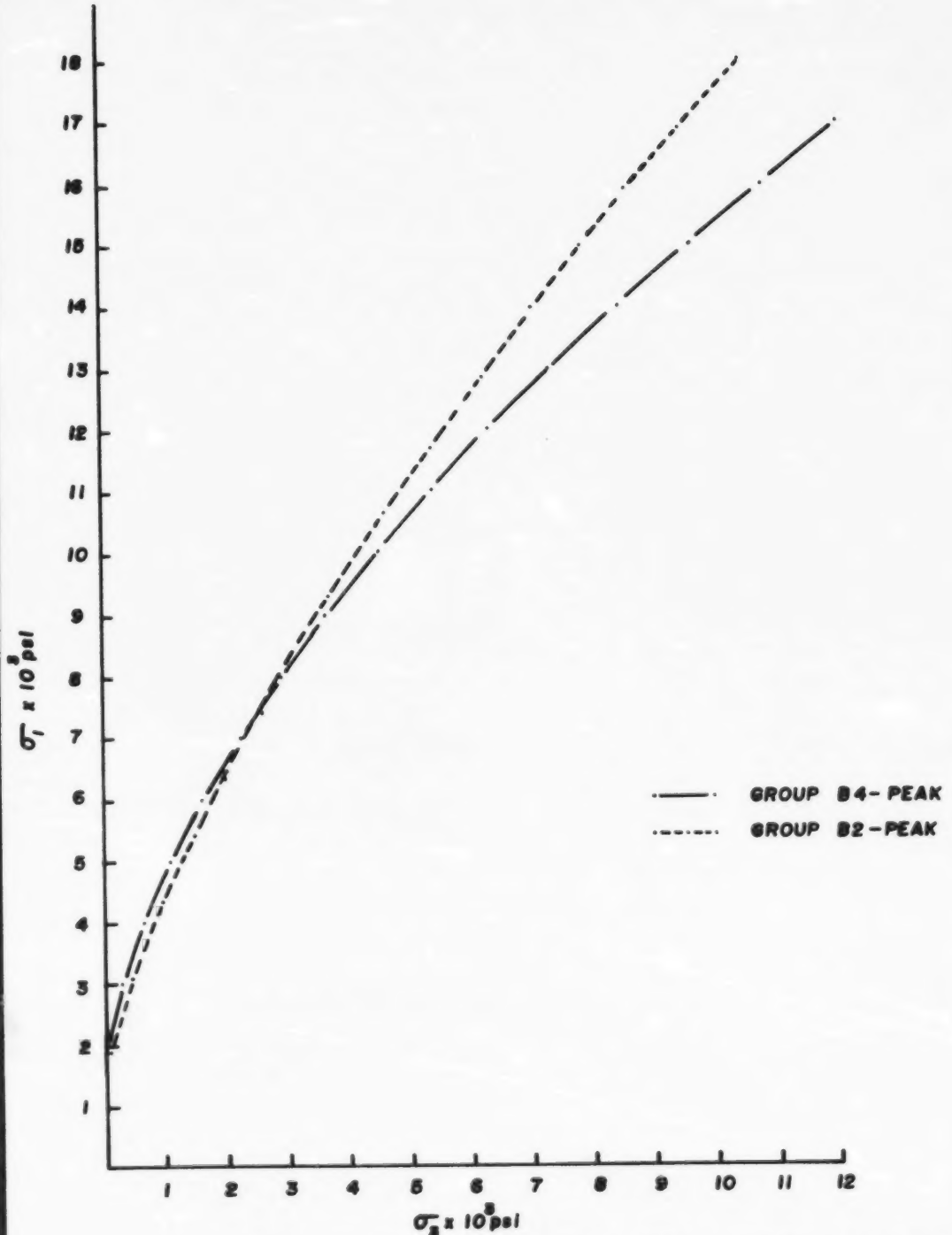

σ_1 vs σ_3 RELATIONSHIPS – PEAK DATA GROUPS B2 AND B4

FIGURE 23

KJC 88

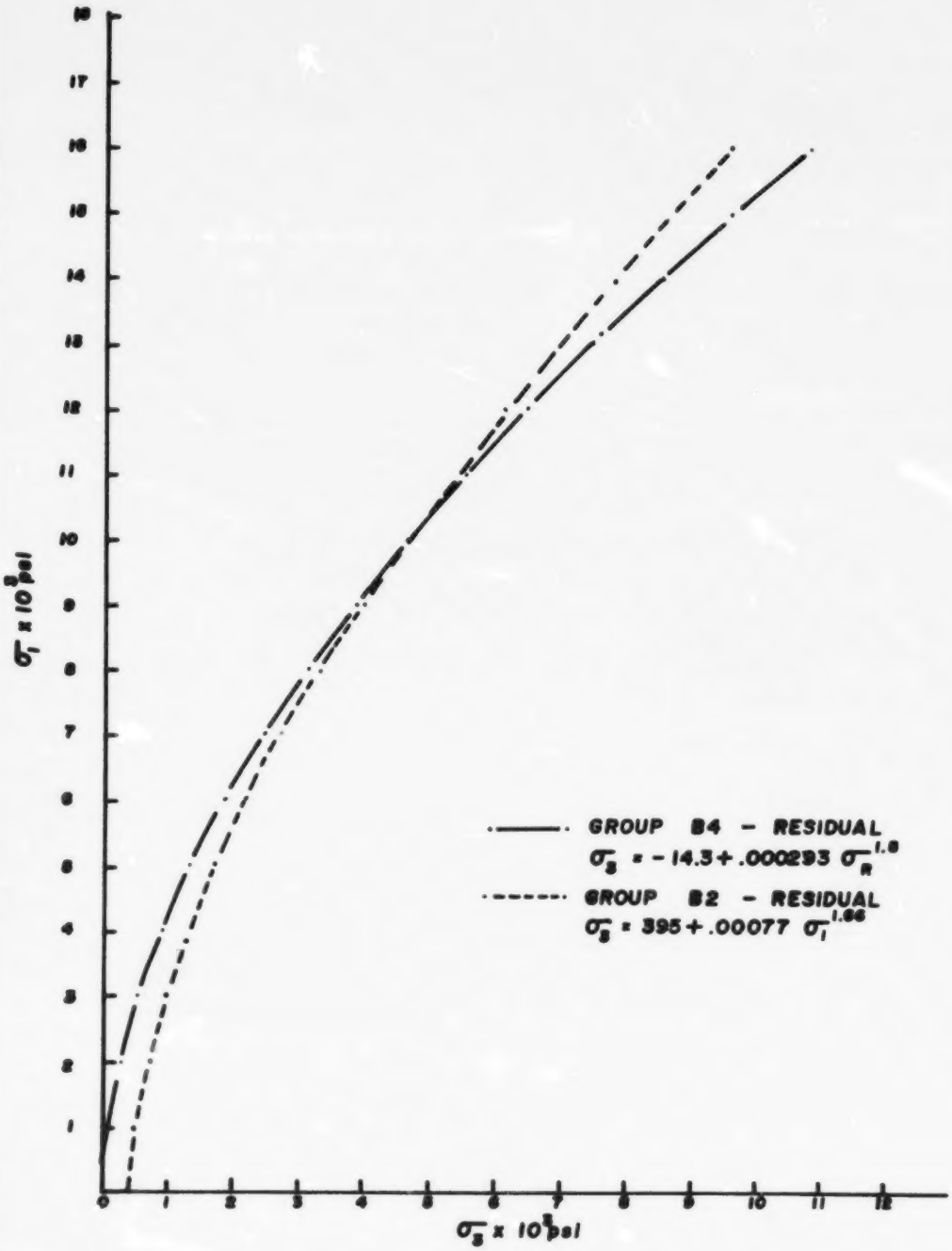
$\sigma_1 \times 10^3$ psi
$\sigma_3 \times 10^3$ psi
GROUP B4 - RESIDUAL
$\sigma_3 = -14.3 + .000293\ \sigma_R^{1.8}$
GROUP B2 - RESIDUAL
$\sigma_3 = 395 + .00077\ \sigma_1^{1.66}$

σ vs. σ RELATIONSHIPS – RESIDUAL DATA - GROUPS B2 & B4

FIGURE 24

KJC 68

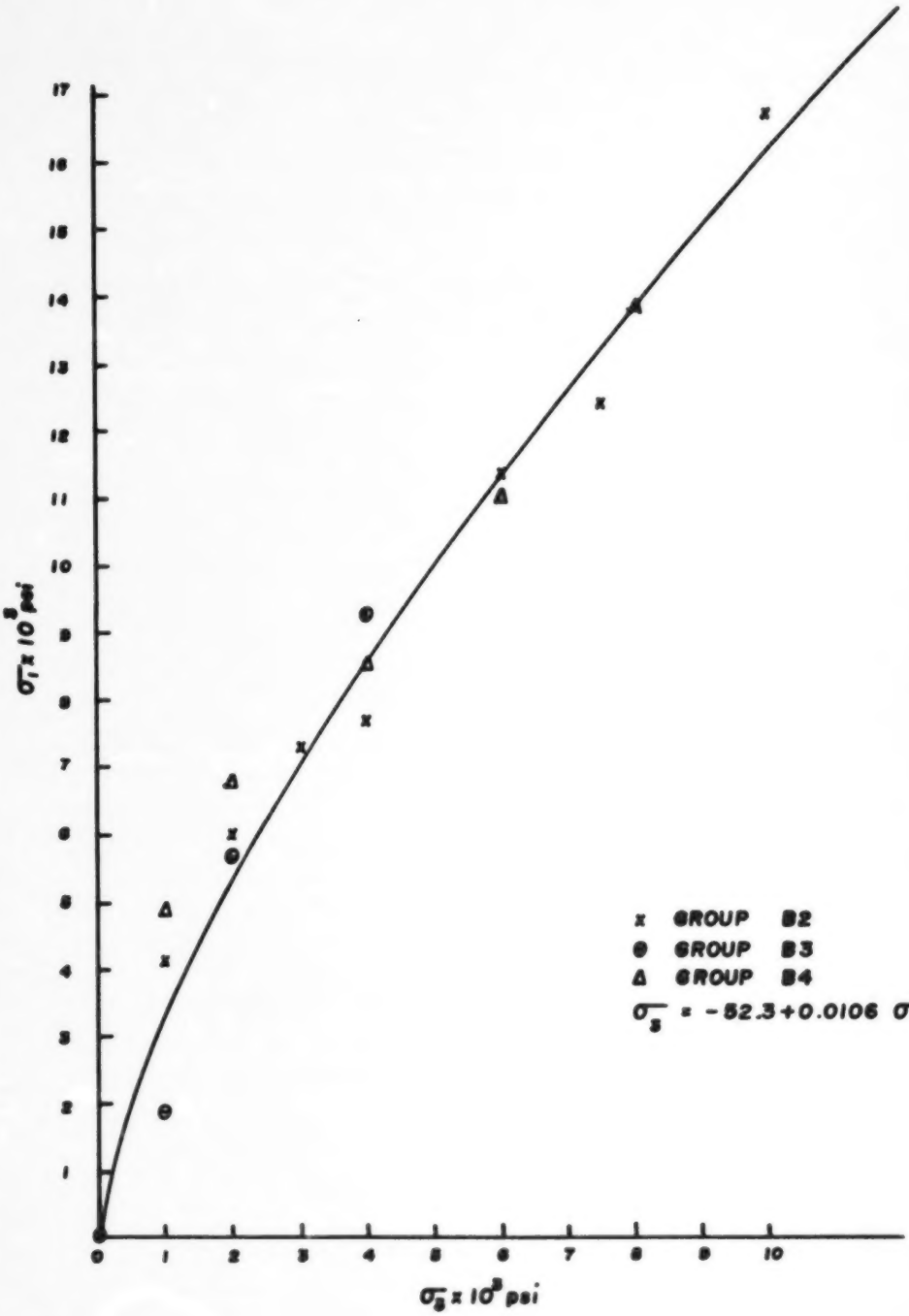

$\bar{\sigma_1}$ vs $\bar{\sigma_3}$ – ALL RESIDUAL DATA

FIGURE 25

KJC 68

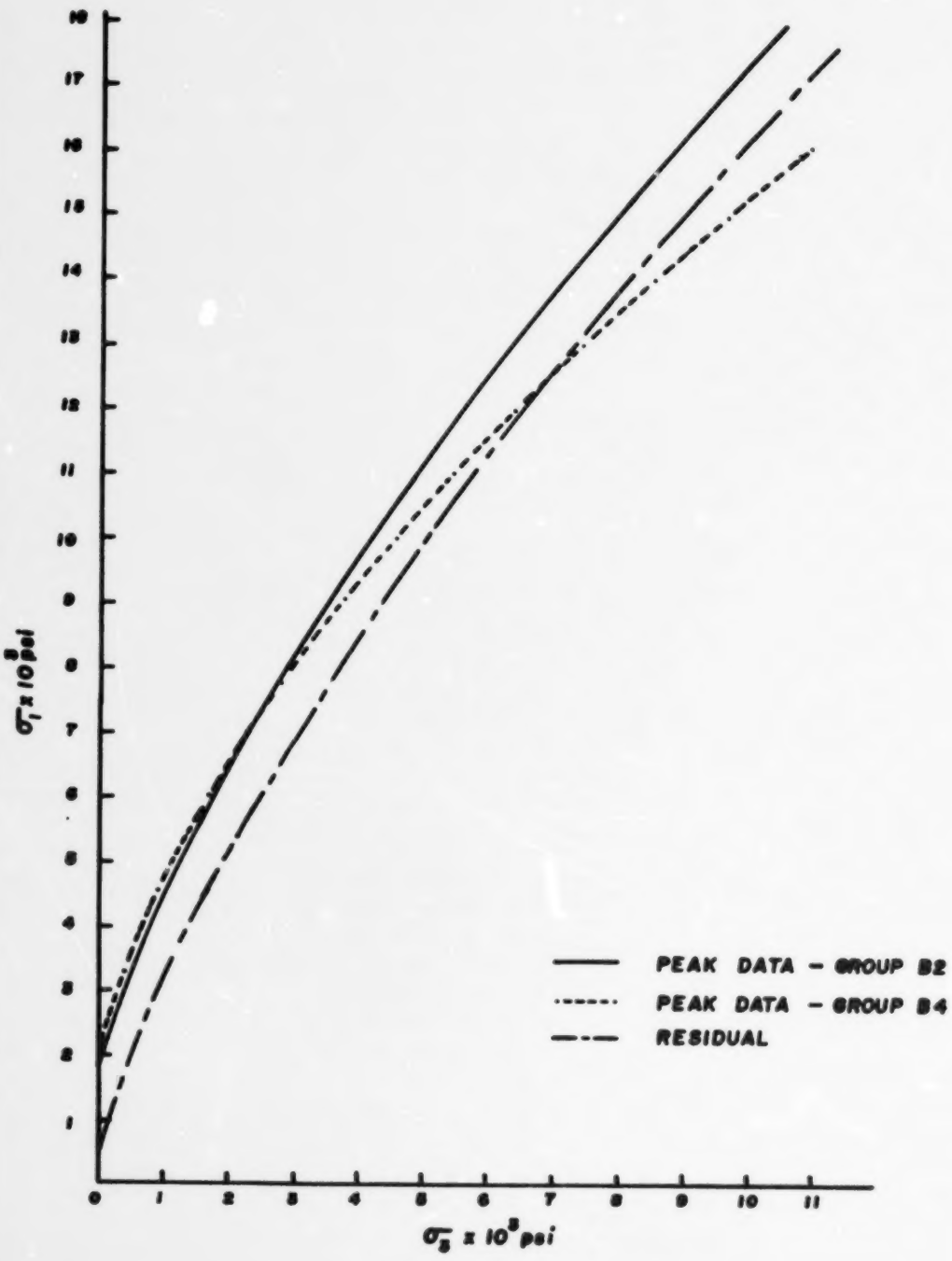

σ_3 vs. σ_1 — PEAK DATA FOR GROUPS B2 & B4 PLUS ALL RESIDUAL DATA

FIGURE 26

4.6 Some theoretical aspects of size effects

It has been shown, for any one size, that the peak stress at failure is related to the confining pressure at failure by the expression

$$\sigma_3 = A + B\ \sigma_p^{\ c} \qquad (1)$$

Now when $\sigma_3 = 0$ then $\sigma_p = \sigma_{pc}$ where σ_{pc} is the unaxial prism strength

$$\text{Thus} \quad -A = B\ \sigma_{pc}^{\ c} \qquad (2)$$

substituting from (2) into (1) gives:-

$$\sigma_3 = B\ \left(\sigma_p^{\ c} - \sigma_{pc}^{\ c}\right) \qquad (3)$$

Further, at the transition point, $\sigma_3 = P_{3T}$ and $\sigma_p\ P_{1T}$, thus substituting into (3) gives

$$B = \frac{P_{3T}}{\left(P_{1T}^{\ c} - \sigma_{pc}^{\ c}\right)} \qquad (4)$$

Hence substituting from (4) into (3) gives the general relationship

$$\sigma_3 = P_{3T} \quad \left\{ \frac{\left[\sigma_p^{\ c} - \sigma_{pc}^{\ c}\right]}{\left[P_{1T}^{\ c} - \sigma_{pc}^{\ c}\right]} \right\} \qquad (5)$$

but it was already established, from the uniaxial test results (section 3) that

$$\sigma_{pc} = k\ \frac{\sqrt{W}}{H} \qquad (6)$$

Hence, substituting for σ_{pc} form (6) into (5) gives the general relationship:-

$$\sigma_3 = P_{3T} \left\{ \frac{\sigma_p^{\ c} - \left(\frac{k\sqrt{W}}{H}\right)^c}{P_{1T}^{\ c} - \left(\frac{k\sqrt{W}}{H}\right)^c} \right) \qquad (7)$$

Consider now the residual strength curve; this may be expressed in a similiar form by:

$$\sigma_3 = A_R + B_R \sigma_R^{CR} \qquad (8)$$

Let us assume, as is tentatively indicated by the results, that there are no size effects on residual strength, then when $\sigma_3 = 0$, $\sigma_R = 0$ since the residual strength is zero under uniaxial conditions. Thus, substituting into (8) gives

$$A_R = 0 \qquad (9)$$

Further, at the transition point $\sigma_3 = P_{3T}$, $\sigma_R = P_{1T}$

Thus $$B_R = \frac{P_{3T}}{P_{1T}^{CR}} \qquad (10)$$

Hence substituting into (8) gives the general expression:-

$$\sigma_3 = P_{3T} \left\{ \frac{\sigma_R^{CR}}{P_{1T}^{CR}} \right\} \qquad (11)$$

Comparing equations (7) and (11) it is seen that they are the same provided that when $C = C_R$ then $\frac{k\sqrt{W}}{H}$ is put equal to zero. i.e. equation (11) represents a lower limit of equation (7).

Thus if we assume that c is a function of size and that C_R is the lower limit of C then one expression can represent both peak and residual relationships.

Assume that $C = \alpha + \beta \frac{\sqrt{W}}{H}$ represents the function of C with size. Then when $C = C_R$, there is no size effect, consequently $\beta = 0$ and $\alpha = C_R$

Hence $$C = C_R + \beta \frac{\sqrt{W}}{H} \qquad (12)$$

In addition, suppose we have a set of test results for size W_1, H_1, then C and hence β can be determined: i.e.

$$\beta = (C_1 - C_R) \frac{H_1}{\sqrt{W_1}} \qquad (13)$$

and substituting from (13) into (12) gives:-

$$C = C_R + (C_1 - C_R) \frac{H_1}{\sqrt{W_1}} \cdot \frac{\sqrt{W}}{H} \qquad (14)$$

i.e. from a knowledge of C_R and C_1 from tests at one size, we could estimate the C for any other size, using equation (14).

i.e. we have a general relationship

$$\sigma_3 = P_{3T} \left\{ \frac{\sigma_1^{\,c} - \left(k \frac{\sqrt{W}}{H}\right)^c}{P_{1T}^{\,c} - \left(k \frac{\sqrt{W}}{H}\right)^c} \right\} \qquad (15)$$

where $C = C_R + (C_1 - C_R) \frac{H_1}{\sqrt{W_1}} \cdot \frac{\sqrt{W}}{H}$ (16)

and this expession would predict the peak stress relationship at failure by putting $\sigma_1 = \sigma_p$ and the residual stress relationship by putting $\sigma_1 = \sigma_R$ and $\frac{k\sqrt{W}}{H} = 0$.

The experimental results will now be examined in the light of these the theoretical considerations.

4.7 Comparison of the results with the theoretical considerations

4.7.1 Group B2 and Group B4 results

Assume that P_{1T} = 12,700 and P_{3T} = 7,070 psi (as indicated by the B4 results). Assume that, for all the residual data we have C_R = 1.42 (Figure 25). From equation 16, using the B2 results, that C_2 = 1.50, W_2 = 2.1, H_2 = 4.1, $\frac{\sqrt{W_2}}{H_2}$ = 0.35 then for a unit cubical specimen (C_c) we would predict (W = 1, H = 1)

$$C_C = 1.42 + (1.5 - 1.42)\ \frac{1}{.35} = 1.65$$

and from the B4 results $C_4 = 1.797$, $W_4 = 2.12$, $H_4 = 5.0$, $\frac{\sqrt{W_4}}{H_4} = 0.67$, then we would predict for a unit cube

$$C_C = 1.42 + \frac{1.797-1.42}{.67} = 1.98$$

These two predictions are not exactly close, however let us take the mean value as being the best estimate

$$\text{i.e. } C_C = \frac{1.65+1.98}{2} = 1.815$$

Then substituting into equation (15) the general expression for C for any $\frac{\sqrt{W}}{H}$ is given by

$$C = 1.42 + (1.815 - 1.42)\frac{\sqrt{W}}{H}$$

$$\text{i.e. } C = 1.42 + .395\frac{\sqrt{W}}{H}$$

This can then be used in equation (16) to predict the relationship for any specimen size, W, H. For peak strength

$$\sigma_3 = P_{3T}\left\{\frac{\sigma_p{}^c - (\frac{k\sqrt{W^c}}{H})}{P_{1T}{}^c - (\frac{k\sqrt{W^c}}{H})}\right\}$$

and for residual stresses

$$\sigma_3 = P_{3T}\left\{\frac{\sigma_R{}^c}{P_{1T}{}^c}\right\}$$

Now from section 3, equation (1) $k = 5{,}290$

4.7.2 Comparision of general expression with Group B2, B3 and B4 results

We can therefore use this general expression "predict" the Group B2, B3 and B4 results and compare them with the actual measurements.

It should be noted that for group B2 $\frac{W}{H} = \frac{2.1}{4.1} = 0.35$ and also, for group B3, $\frac{W}{H} = \frac{3.0}{5.0} = 0.35$. i.e. $\frac{W}{H} = 0.35$ for both data sets. Thus Group B2 and group B3 results should both fall on the same curve.

For $\frac{W}{H} = 0.35$ then $C = 1.42 + .395\frac{W}{H} = 1.56$

Thus σ_p should be given by

$$\sigma_3 = P_{1T}\left\{\frac{\sigma_p^{1.56} - k\left(\frac{W}{H}\right)^{1.56}}{P_{1T}^{1.56} - k\left(\frac{W}{H}\right)^{1.56}}\right\}$$

with $P_{1T} = 12{,}700$; $P_{3T} = 7{,}070$ $k = 5{,}290$, $\frac{W}{H} = 0.35$ this reduces to:-

$$\sigma_3 = 7{,}070\left\{\frac{\sigma_p^{1.56} + (1{,}850)^{1.56}}{12{,}700^{1.56} + (1{,}850)^{1.56}}\right\}$$

Figure 27 plots this expression and compares it to the measured peak strengths for group B2 and Group B3 data. This appears to be a not unreasonable fit to the date.

Likewise for Group B4, $\frac{W}{H} = 0.67$ then

$$c = 1.42 + .395 \times .67 = 1.68$$

and σ_p should be given by:-

$$\sigma_3 = 7{,}070\left\{\frac{\sigma_p^{1.68} - \left(k\frac{W}{H}\right)^{1.68}}{P_{1T}^{1.68} - \left(k\frac{W}{H}\right)^{1.68}}\right\}$$

with $P_{1T} = 12{,}700$, $P_{3T} = 7{,}070$, $k = 5290$ and $\frac{W}{H} = 0.67$

Figure 28 plots this expression and compares it to the measured peak strength for Group B4. Again this appears to be a reasonable fit to the data.

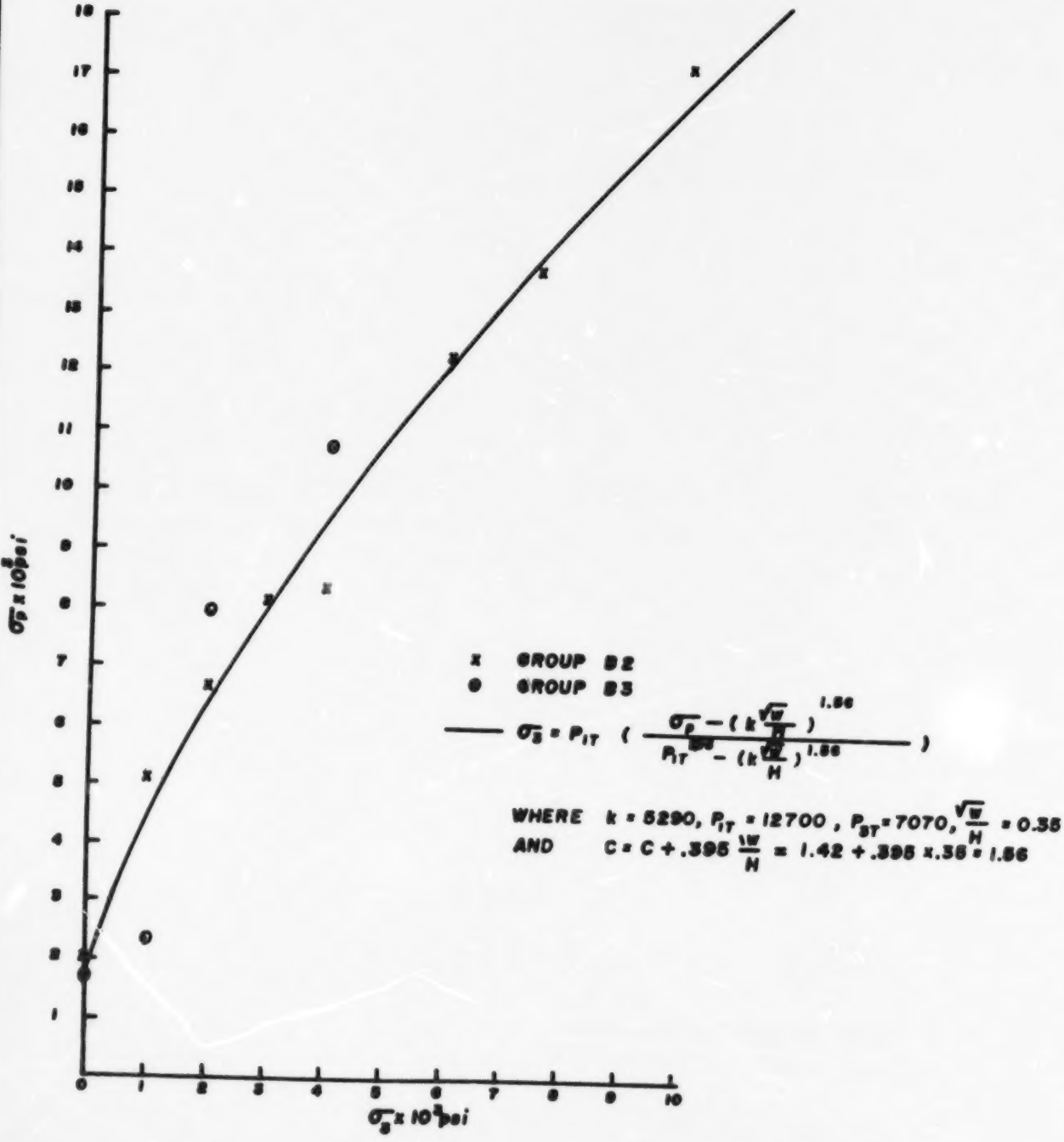
$\sigma_s \times 10^3$ psi
$\sigma_s \times 10^3$ psi
x GROUP B2
● GROUP B3
$\sigma_s = P_{1T} \left(\frac{\sigma_p - (k\frac{\sqrt{w}}{H})^{1.86}}{P_{1T} - (k\frac{\sqrt{w}}{H})^{1.86}} \right)$
WHERE $k = 5290$, $P_{1T} = 12700$, $P_{ST} = 7070$, $\frac{\sqrt{w}}{H} = 0.38$
AND $C = C + .395\frac{\sqrt{w}}{H} = 1.42 + .395 \times .38 = 1.86$

COMPARISOM OF GROUP B2 AND B3 PEAK STRENGTH DATA WITH THE GENERAL EXPRESSION

FIGURE 27

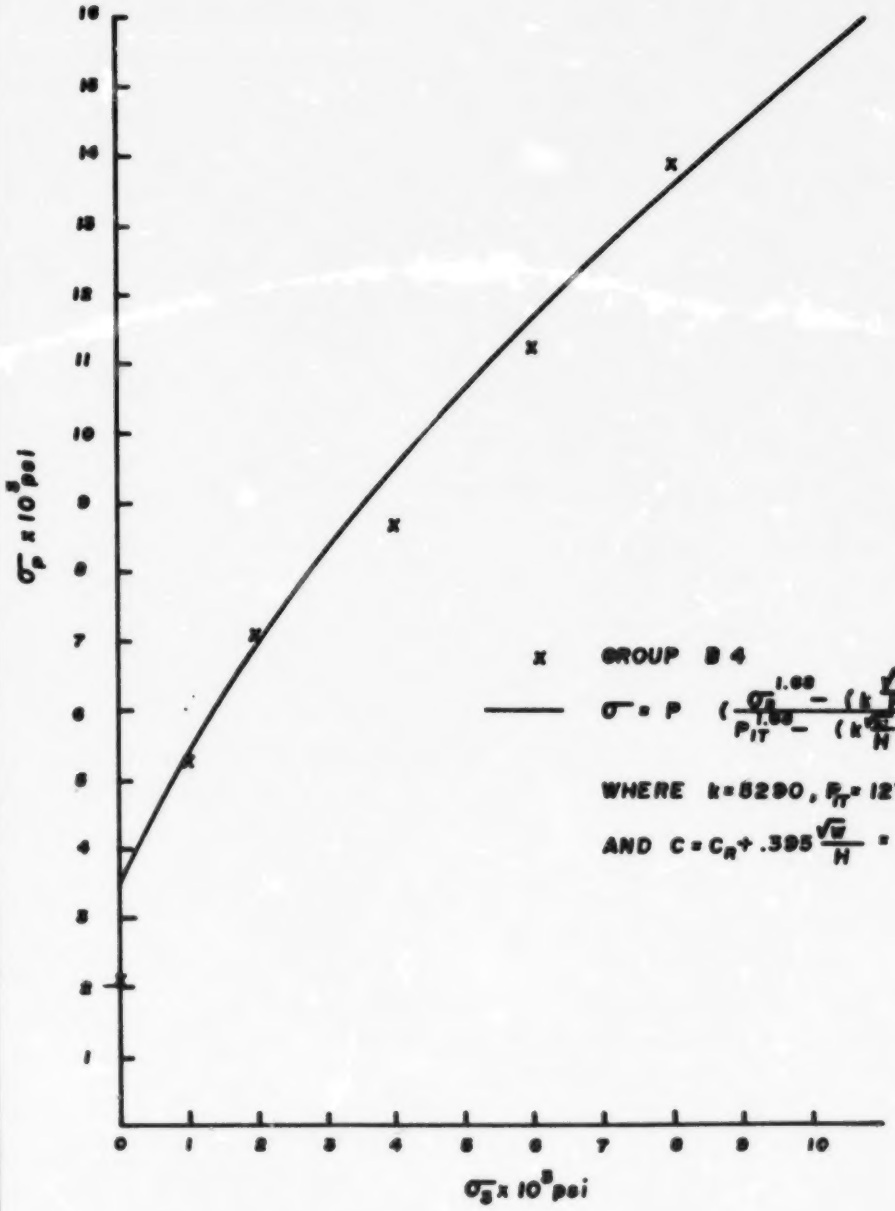
$\sigma_p \times 10^3$ psi
$\sigma_3 \times 10^3$ psi
0 1 2 3 4 5 6 7 8 9 10
1 2 3 4 5 6 7 8 9 10 11 12 13 14 15 16
x GROUP B 4
$\sigma = P \left(\frac{\sigma_3^{1.68} - \left(k \frac{\sqrt{w}}{H}\right)^{1.68}}{P_{1T}^{1.68} - \left(k \frac{\sqrt{w}}{H}\right)^{1.68}} \right)$
WHERE $k = 8290$, $P_{1T} = 12700$, $P_{3T} = 7070$, $\frac{\sqrt{w}}{H} = 0.67$
AND $C = C_R + .395 \frac{\sqrt{w}}{H} = 1.42 + .395 \times .67 = 1.68$

COMPARISOM OF GROUP B4 PEAK STRENGTH DATA WITH THE GENERAL EXPRESSION

FIGURE 28

KJC 85

The general expression for all residual data will be given by $C_R = 1.42$:-

$$\sigma_3 = 7{,}070 \frac{\sigma_R^{1.42}}{12{,}7000^{1.42}}$$

Figure 29 compares this expression with the residual strength data from all groups. Again this appears to be a reasonable fit to the data.

4.8 Limits of application of the general expression

It was shown in part 2 of this report (Appendix B) that for UNIAXIAL tests on coal prisms, the prism strength σ_{pc} is given by:

$$\sigma_{pc} = k\frac{W}{H}$$

and that the following limits were imposed on the validity of the expression:

$$0.125 < \frac{W}{H} < 1.4$$

The above expression is a simplified form ($\sigma_3 = 0$) of the general expression and it is reasonable to suppose that limits of applicability also apply to the general expression. Whether or not these limits change under triaxial conditions is not known; consequently it will be provisionally assumed that the above uniaxial limits also apply under triaxial conditions. However, it is recommended that these limits be investigated as part of some future testing program.

Figure 30 illustrates how the general expression predicts the peak and residual strengths for the test coal within these limits.

It will be noted that the lower limit $\frac{W}{H} = 0.125$, is for all practical purposes the same as the residual strength ($\frac{W}{H} = 0$), except under uniaxial conditions. Hence the lower limit $\frac{W}{H} = 0.125$ probably is acceptable as a definition of the residual strength. This implies that as the specimen size gets larger, the strength tends towards a constant value defined by the residual strength.

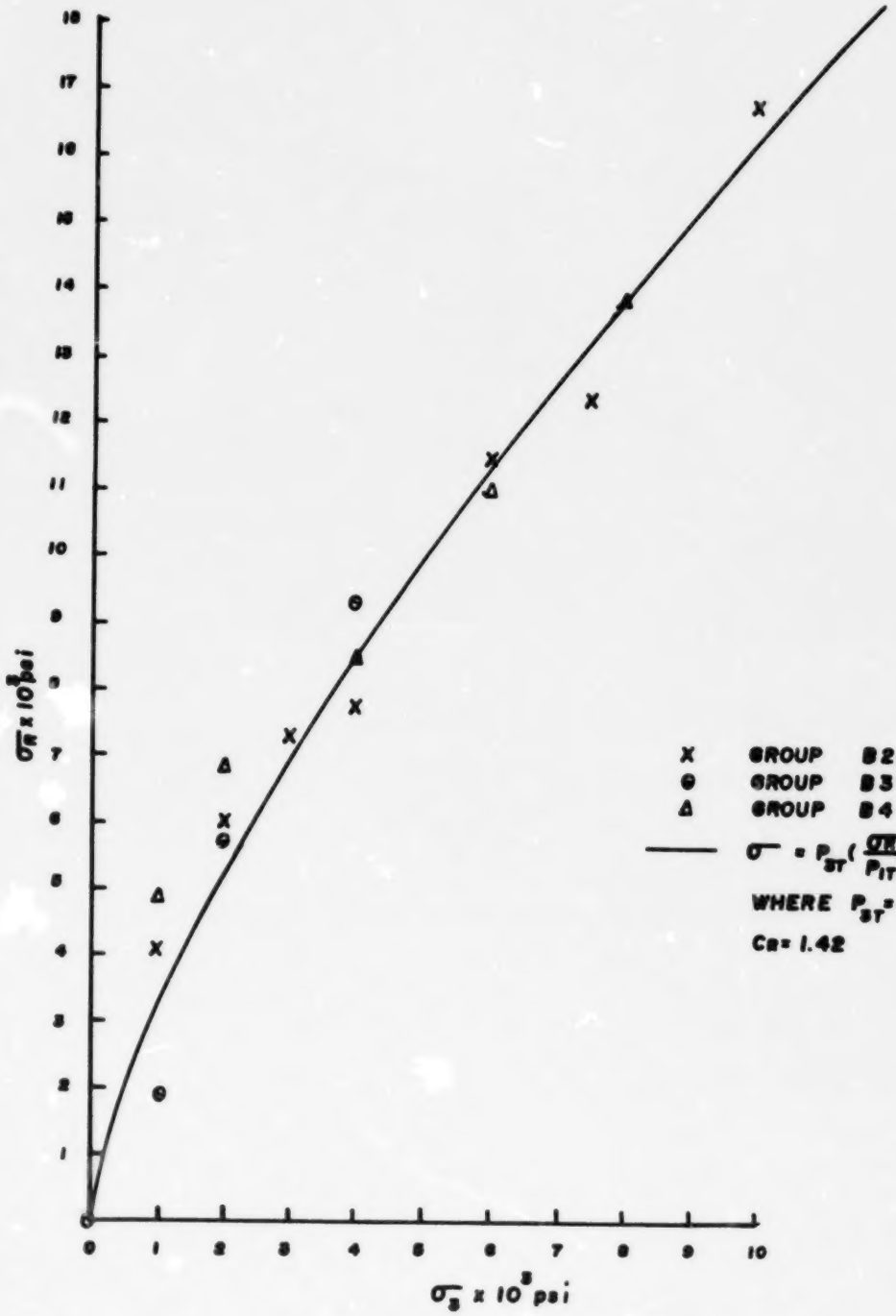

COMPARISOM OF ALL RESIDUAL STRENGTH WITH THE GENERAL EXPRESSION

FIGURE 29

KJC 68

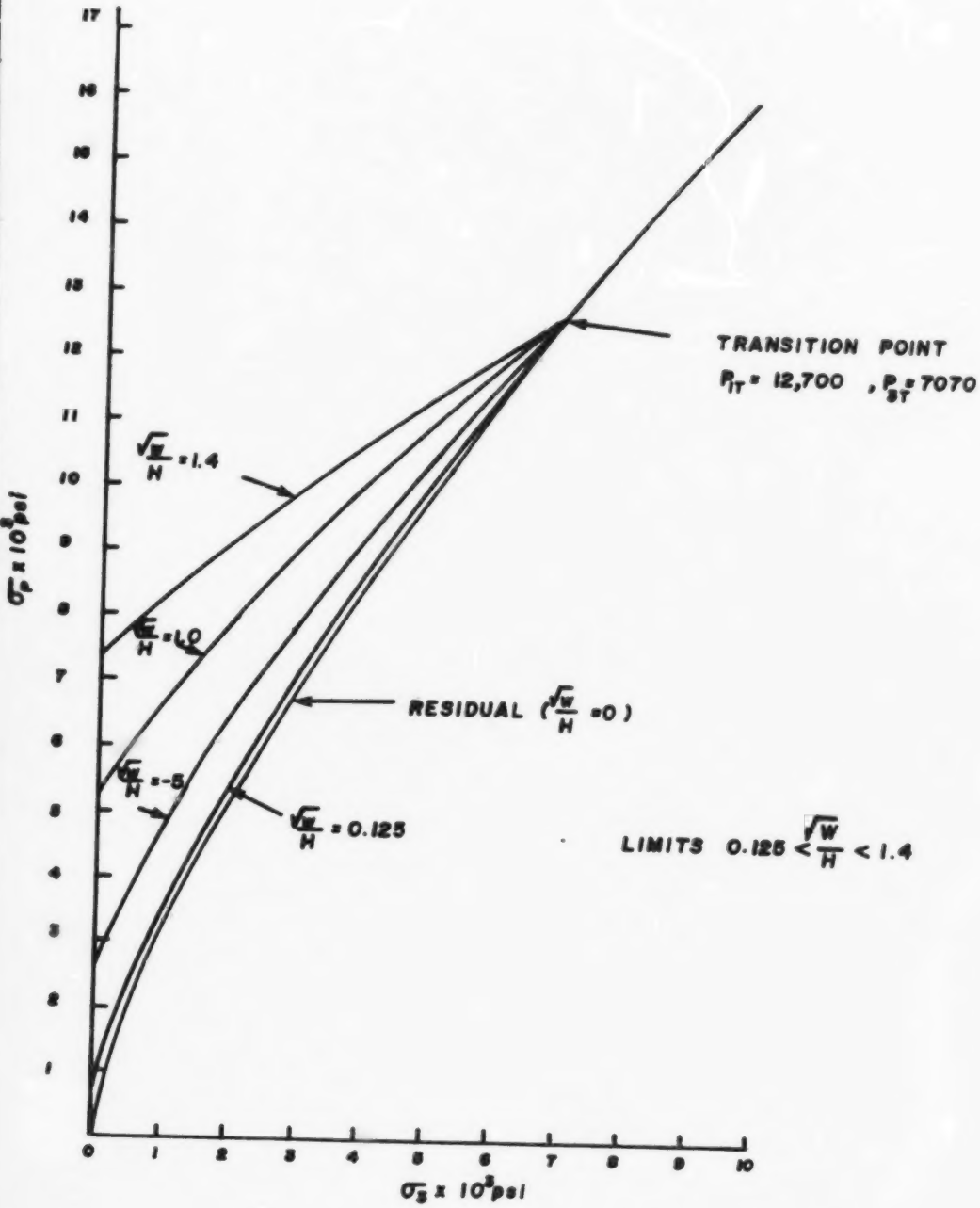
TRANSITION POINT
P_{1T} = 12,700 , P_{ST} = 7070
$\frac{\sqrt{W}}{H}$ = 1.4
$\frac{\sqrt{W}}{H}$ = 1.0
$\frac{\sqrt{W}}{H}$ = 0.5
$\frac{\sqrt{W}}{H}$ = 0.125
RESIDUAL ($\frac{\sqrt{W}}{H}$ = 0)
LIMITS $0.125 < \frac{\sqrt{W}}{H} < 1.4$
$\sigma_p \times 10^3$ psi
$\sigma_s \times 10^3$ psi
0 1 2 3 4 5 6 7 8 9 10
1 2 3 4 5 6 7 8 9 10 11 12 13 14 15 16 17

EFFECT OF SIZE ON THE PEAK AND RESIDUAL STRENGTHS OF THE TEST COAL

FIGURE 30

KJC 88

At the upper limit $\frac{W}{H} = 1.4$; i.e. $W = (1.4\ H)^2 = 1.96H^2 \sim 2H^2$, i.e. $\frac{W}{H} = 2H^2$. This limit is therefore only likely to be encountered with the testing of small specimens e.g. the variation of $\frac{W}{H}$ with the H at the limit is given below

H inches	W/H at limit
0.5	1
1	2
2	3
3	6

However, it is seen that as H increases W/H increases very rapidly and it is unlikely that specimens with a high W/H ratio can be treated as "uniaxial" specimens since confining pressure is likely to build up in the core. In this case, the upper limit may be better defined by the "critical width to avoid catestrophic failure" developed in the pillar model (Pt 1 report, page 92): This should be investigated further in the future.

4.9 Tentative Conclusions

(1) A general relationship given by:

$$\sigma_3 = P_{3T} \left\{ \frac{\sigma_1^{\,c} - k\left(\frac{W}{H}\right)^c}{P_{1T}^{\,c} - k\left(\frac{W}{H}\right)^c} \right\}$$

appears to fit all the peak and residual strength measurements, where

$$c = C_R + (C_1 - C_R)\frac{H1}{W1} \cdot \frac{W}{H}$$

where P_{3T} = the confining pressure at the transition point

P_{1T} = the major principal stress at the transition point

W = specimen width

H = specimen height

C_1 is the parameter obtained from measurements at height H_1 and W_1

C_R is the parameter obtained from the residual strength curve

k is the "unit cube" strength for coal (uniaxial, H = 1 inch, W = 1 inch)

σ_1 is equal to σ_p for the peak strength.

(2) For the residual strength, σ_R, this expression will also apply provided that $(k\frac{\sqrt{W}}{H})$ is put equal to zero and $\sigma_1 = \sigma_R$.

(3) For the test coal, k = 5,290, C_R = 1.42 and $C = 1.42 + 0.395\frac{\sqrt{W}}{H}$

(4) Limits on the applicability of this general equation must be set. Provisionally the limits $0.125 < \frac{\sqrt{W}}{H} < 1.4$ are indicated from past work under uniaxial conditions.

For all practical purposes the lower limit (0.125) is identical to the residual strength curve. This indicates that as a specimen (pillar) size is increased so the strength approaches a constant value for any σ_3. i.e. that the size effects disappear with increasing size and the peak strength approaches the residual strength.

The upper limit, $\frac{\sqrt{W}}{H} = 1.4$, is only likely to be encountered when testing small (laboratory size) specimens. Past work indicates that, for uniaxial tests, this limit is correct. However, this limit may change under triaxial conditions. This requires further investigation; consideration should be given as to whether this upper limit might better be defined in terms of the "critical width to avoid catestrophic failure" developed in pillar model (pt 1 report, page 92).

(5) The determination of the transition point, P_1, P_{3T}, is difficult and cannot be done accurately because both the peak and residual strength curves bend in the same direction making it difficult to determine their intersection accurately.

(6) For the test coal it was estimated that P_{1T} = 12,700 psi, P_{3T} = 7,070 psi.

(7) The implications of the general expression derived are important:-

(i) As confining pressure increases, the variation of specimen strength with size diminishes until the brittle-ductile transition point is reached. There are no size effects beyond this point.

(ii) The maximum "size effect" occurs under uniaxial conditions.

(iii) As the size increases, (i.e. as $\frac{\sqrt{W}}{H}$ tends to zero), the strength decreases and becomes assymptotic to the residual strength curve.

(iv) The residual strength is unaffected by size.

(8) The assumption used in the pillar model that the coefficient of friction, μ_B, for sliding on fractured coal surfaces (the slope of the residual stress Mohr envelope) is a constant is not valid. μ_B diminishes with increasing normal stress across the surface. Consequently the equations defining the transition point, used in the pillar model, should be re-written taking this into account.

However, if a full suite of triaxial test data is not available, then the assumption that μ_B = constant is probably acceptable as a first approximation. This assumption will tend to underestimate P_{1T} and P_{3T}.

(9) The implicit assumption used in the past that size effects observed under uniaxial condition are directly applicable to triaxial conditions is wrong. Size effects diminish and eventually disappear as both size and confining pressure increase.

It is recommended that:-

(1) The pillar model developed in Pt. 1 report be modified to make use of the improved and refined failure criteria for coal.

(2) Further investigation should be carried out on the limits of applicability of the general expression derived for the effect of size on coal specimens.

It should be noted that the variability of data from the test coal was very large; consequently these conclusions can only be regarded as tentative. It is recommended that further tests be carried out with a less variable coal or perhaps with a mudstone or similar less variable sedimentary rock.

5. TRIAXIAL TESTS ON RECOMPACTED BROKEN COAL

5.1 Equipment and procedures

The re-compacted coal specimens were prepared by crushing the coal and sieving it to minus 1/10 inch in size. The crushed coal was placed on bolted split steel molds of the appropriate diameter and then re-compacted by loading to the appropriate pressure in the press. The specimens were then extracted by opening the split molds.

The triaxial tests on the re-compacted specimens were carried out using the same apparatus and system as for the solid coal specimen (see section 3.1). The uniaxial tests on these specimens were carried out in a Whykham-Farrance loading frame in which the load was measured by a proving ring and the deformation by L.V.D.T.'s (Figure 31).

5.2 Deviations from the program plan

It was planned (see section 2) to carry out tests on specimens re-compacted under three different re-compaction pressures; at two different sizes H/W=2, W=1 and W/H=2, W=2; with 3 specimens at each of six different confining pressures for a total of 108 tests.

In practice, because of the consistency of the results at the highest and lowest re-compaction pressures, the intermediate re-compaction pressure was eliminated as being unnecessary. Seven, rather than the planned six, confining pressures were used. Table 8 compares the planned and actual number of tests; a total of 91 tests were carried out.

5.3 Results

Figure 32 shows a typical load-deformation curve obtained from these tests. Appendices C1, C2, C3 and C4 tabulate the detailed results. Table 9 summarises the mean data from each of these test groups.

Figure 33 shows the σ vs σ_1 relationship for all of these tests plotted on the same figure.

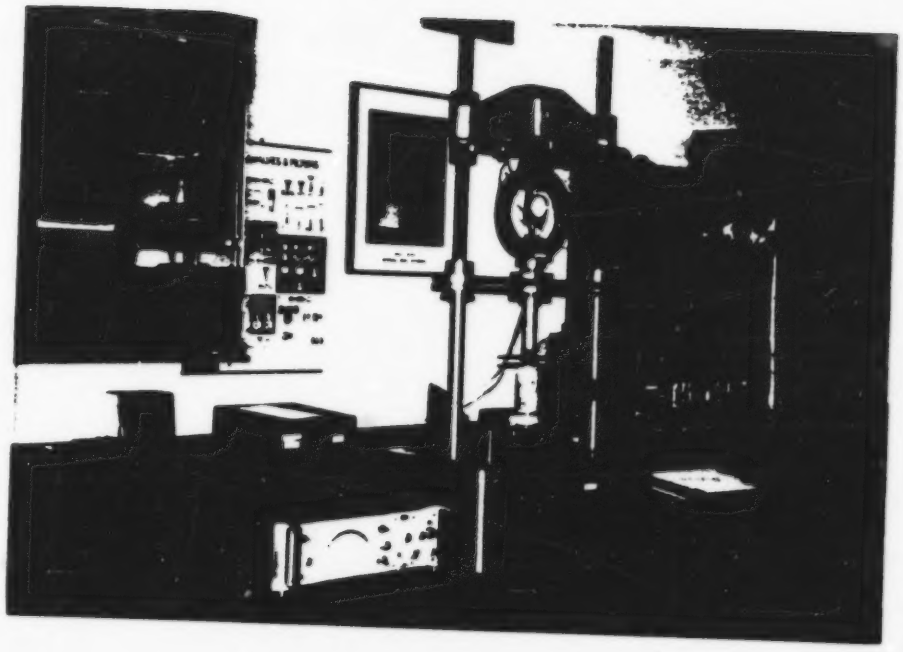

FIGURE 31: Whykham-Farrance loading frame for uniaxial tests on re-compacted coal specimens

Table 8: Comparison of Planned and Actual number of Tests
Re-compacted Coal Samples

Group H/W, W	C1 H/W=2 W=1 inch						C2 H/W=2 W= 2 inch					
Group Re-compaction	C1.1 35,000 psi		C1.2 30,000 psi		C1.3 25,000 psi		C2.1 35,000 psi		C2.2 30,000 psi		C2.3 25,000 psi	
Confining Pressures	Planned	Actual	# tests P	A	P	A	P	A	P	A	P	A
0	3	6	3	-	3	6	3	11	3	-	3	6
500	0	4	0	-	0	3	0	2	0	-	0	2
1,000	3	3	3	-	3	3	3	3	3	-	3	3
2,000	3	3	3	-	3	4	3	3	3	-	3	2
4,000	3	3	3	-	3	3	3	2	3	-	3	2
6,000	3	3	3	-	3	1	3	2	3	-	3	0
8,000	3	3	3	-	3	3	3	3	3	-	3	2
Total	18	25	18	0	18	23	18	26	18	0	18	17

Total planned = 108

Total actual = 91

CMRC

SAMPLE NO. 1

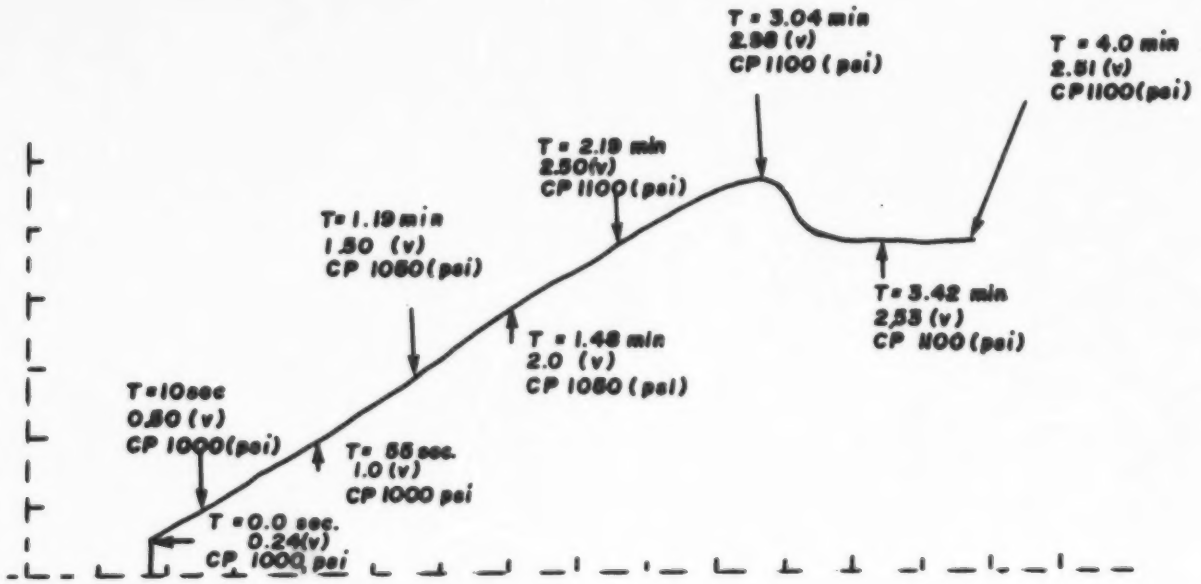

RE-COMPACTION PRESSURE — 25000 psi
CONFINING PRESSURE — 1000psi
SCALE : X AXIS = 0.044 inches / cm
Y AXIS = 3160 lbs / cm

TRIAXIAL TEST ON RE-COMPACTED BROKEN COAL

FIGURE 32

KJC 68

TABLE 9: RECOMPACTED COAL SPECIMENS - TRIAXIAL DATA

Group	C1.1
Diameter	0.84 in
H/D	2.4
Recompaction Pressure	35,000 psi

Confining Pressure

σ_3	σ_p	E x 10^4	$\sigma_p - \sigma_3$
0	110	.159	110
500	2359	1.57	1859
1000	4000	3.55	3000
2000	7435	5.51	5435
4000	12320	8.65	8320
6000	16370	10.88	10370
8000	17810	12.32	9810

Group	C1.3
Diameter	0.84
H/D	2.4
Recompaction Pressure	25,000

σ_3	σ_p	E x 10^4	$\sigma_p - \sigma_3$
0	48	.116	48
500	2513	2.58	2013
1000	4274	3.53	3274
2000	7034	6.99	5034
4000	12295	8.56	8295
6000	15750	9.75	9750
8000	18452	12.97	10452

Group	C2.1
Diameter	2.125
H/D	2
Recompaction Pressure	35,000 psi

σ_3	σ_p	E x 10^4	$\sigma_p - \sigma_3$
0	114	.283	114
500	2770	4.04	2270
1000	4523	6.23	3523
2000	7479	7.35	5479
4000	11730	8.78	7730
6000	15177	10.38	9177
8000	17603	11.75	9603

TABLE (Continued)

Group	C2.3
Diameter	2.125 in
H/D	2.0
Recompaction Pressure	25,000 psi

Confining Pressure

σ_3	σ_p	$\varepsilon \times 10^4$	$\sigma_p - \sigma_3$
0	125	.39	125
500	3128	3.85	2628
1000	4604	4.0	3604
2000	8311	5.88	6311
4000	12546	7.5	8546
6000	-	-	-
8000	17180	10.61	9180

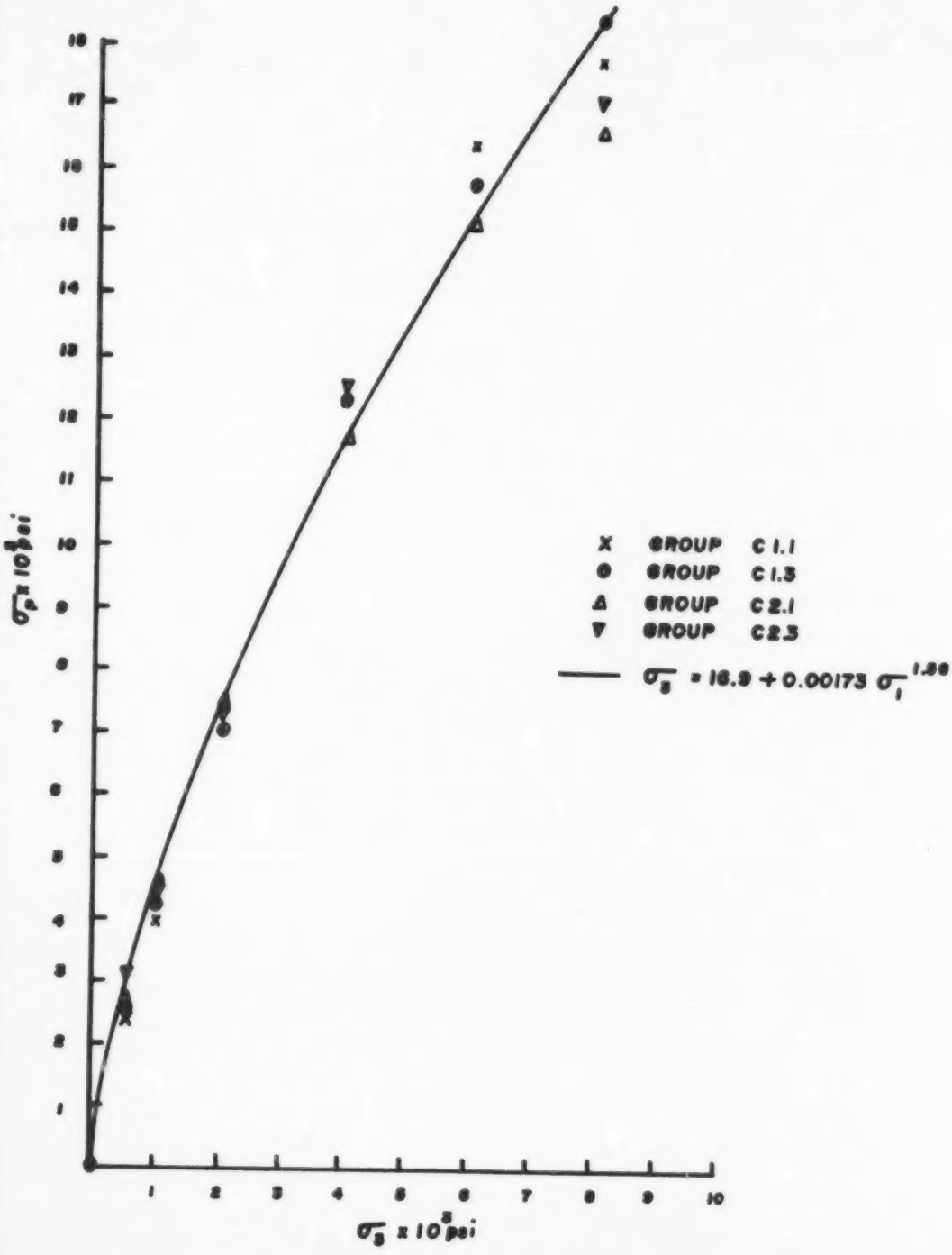

σ vs σ – ALL RECOMPACTED PEAK STRENGTHS

FIGURE 33

RJC 68

It is seen that:-

(i) There is no "size effect". i.e. there is no apparent difference between the strengths of the W = 1 inch and W = 2 inch specimens.

(ii) There is no "re-compaction" pressure effect. i.e. there is no apparent difference between the strengths when the re-compaction pressure was 25,000 psi and when it was 35,000 psi.

(iii) All the data can be described by a relationship given by:-

$$\sigma_3 = 16.9 + 0.00178 \ \sigma_p^{1.56}$$

5.4 Comparison of results with the residual strengths for solid coal tests

Figure 34 compares the above expression for the re-compacted coal samples with that obtained for the residual strength relationship for the solid coal specimens. There is apparently no relationship between these two curves.

5.5 Broken coal properties

The pillar model assumes that the "broken coal" behaves as a Coulomb Navier material, i.e. the σ_3 vs σ_1 relationship is assumed to be linear. Clearly this linear relationship is not exactly true. However, Figure 35 shows the re-compacted broken coal data correlated in linear from which yields:-

$$\sigma_1 = 1920 + 2.186 \ \sigma_3, \quad r = 0.98$$

This correlates coefficient is good and to a first approximation this linear assumption is acceptable. If ϕ_B is the angle of internal fraction for broken coal and P_B is its uniaxial strength then from this curve we have

$$P_B = 1920 \text{ psi}$$

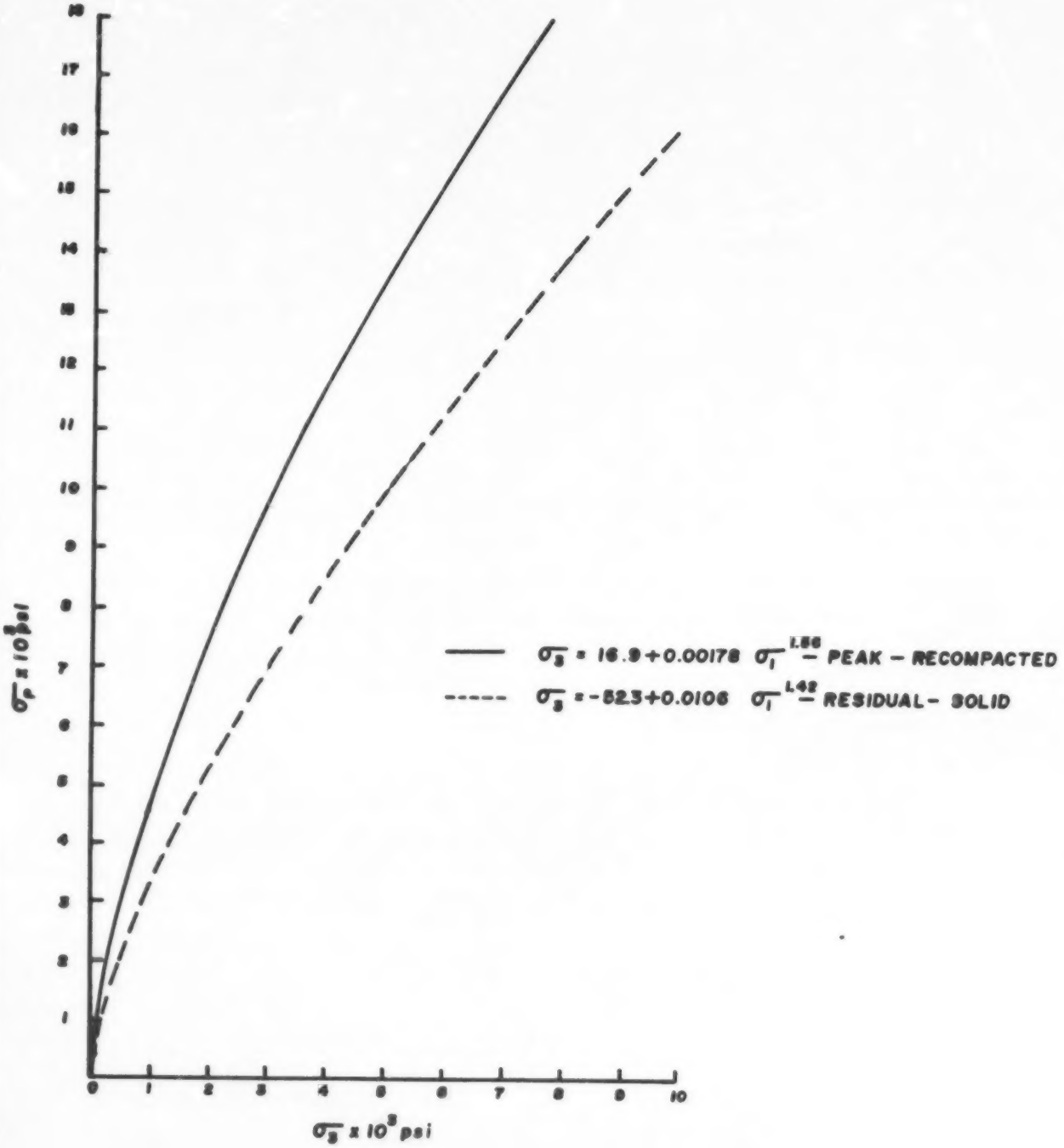
$\sigma_3 = 16.9 + 0.00178\ \sigma_1^{1.86}$ PEAK - RECOMPACTED
$\sigma_3 = -523 + 0.0106\ \sigma_1^{1.42}$ RESIDUAL - SOLID
$\sigma_3 \times 10^3$ psi
$\sigma_1 \times 10^3$ psi

COMPARISON OF RECOMPACTED STRENGTHS WITH SOLID COAL RESIDUAL STRENGTH

FIGURE 34

RJC 88

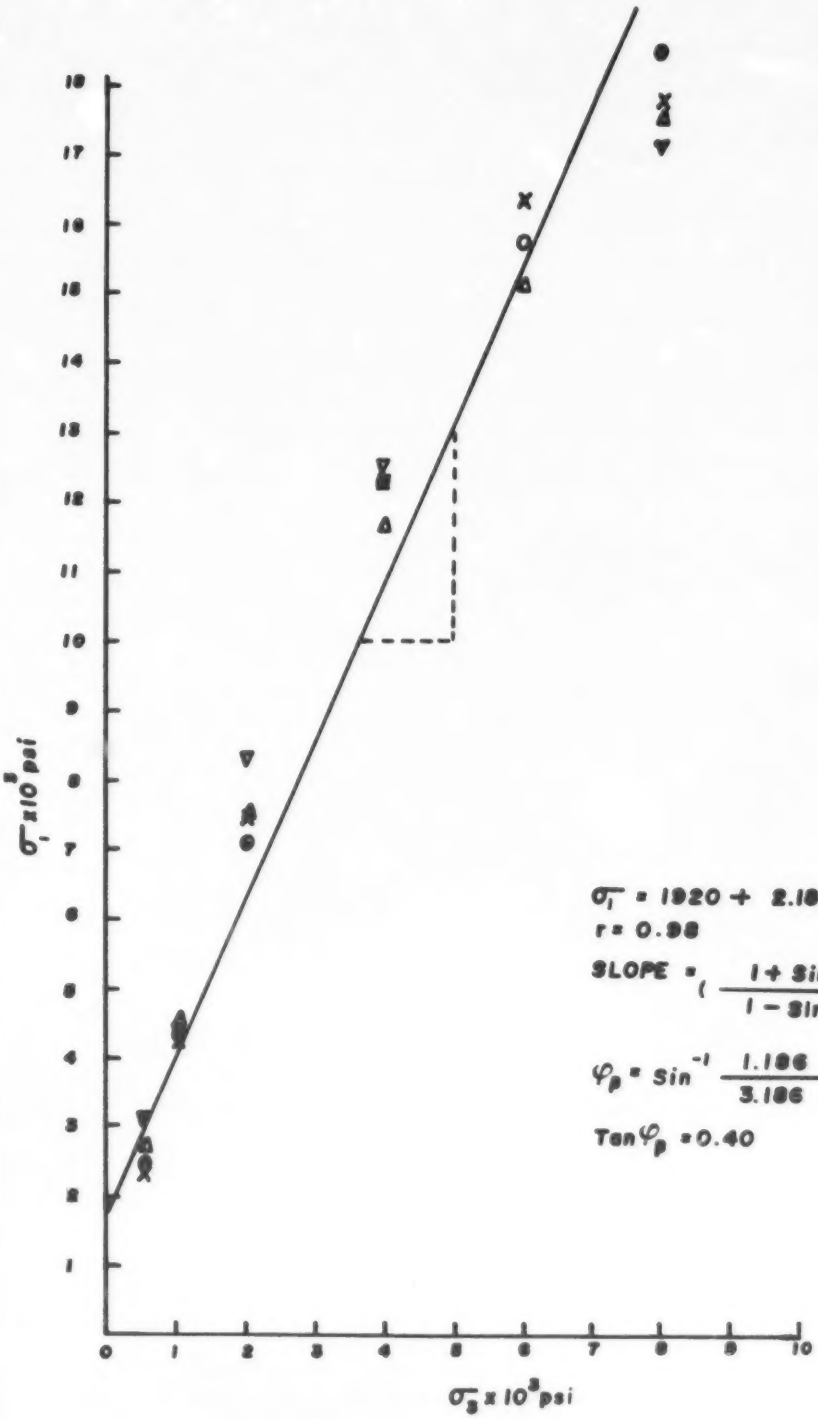
σ_1 x 10^3 psi
σ_3 x 10^3 psi
$\sigma_1 = 1920 + 2.186\ \sigma_3$
r = 0.98
SLOPE = $\left(\frac{1+\sin\varphi_p}{1-\sin\varphi_p}\right) = 2.186$
$\varphi_p = \sin^{-1}\frac{1.186}{3.186} = \sin^{-1}.372 = 21.8°$
$\tan\varphi_p = 0.40$

σ_1 vs σ_3 FOR PEAK RECOMPACTED COAL SAMPLES, ASSUMING A LINEAR RELATIONSHIP

FIGURE 38

KJC 68

$$\text{Slope of curve} = 2.186 = \frac{(1 + \sin \phi_B)}{(1 - \sin \phi_B)} \quad \text{from which}$$

$$\phi_B = \sin^{-1}(0.372) = 21.8^\circ$$

and $\tan \phi_B = 0.40$

Clearly this linear relationship over estimates the value P_B; it would be better to assume that P_B is giving by the mean of all the uniaxial tests on the broken coal. This is given by:-

P_B = 101 psi standard deviation = 64

whether this value of P_B is accurate is also doubtful.

5.6 Coefficient of sliding friction of coal on coal

It was also postulated in the pillar model that the sliding coefficient of friction of coal are coal, μ_β was a constant. This is the slope of the residual strength Mohr envelope. It was shown in section 4 that in fact the curve in non-linear and thus μ_β is not a constant. However, if as a first approximation we assume linearity, then figure 36 shows this correlation which is given by:-

$$\sigma_1 = 1740 + 1.567\ \sigma_3, \quad r = 0.97$$

from this curve the slope = 1.567 from which

$$\frac{(1 + \sin \phi)}{(1 - \sin \phi)} = 1.567 \qquad \phi = \sin^{-1} 0.221 = 12.8^\circ$$

$$\mu_B = \tan \phi = 0.23$$

This angle of sliding friction seems to be very low, as is the coefficient μ_B.

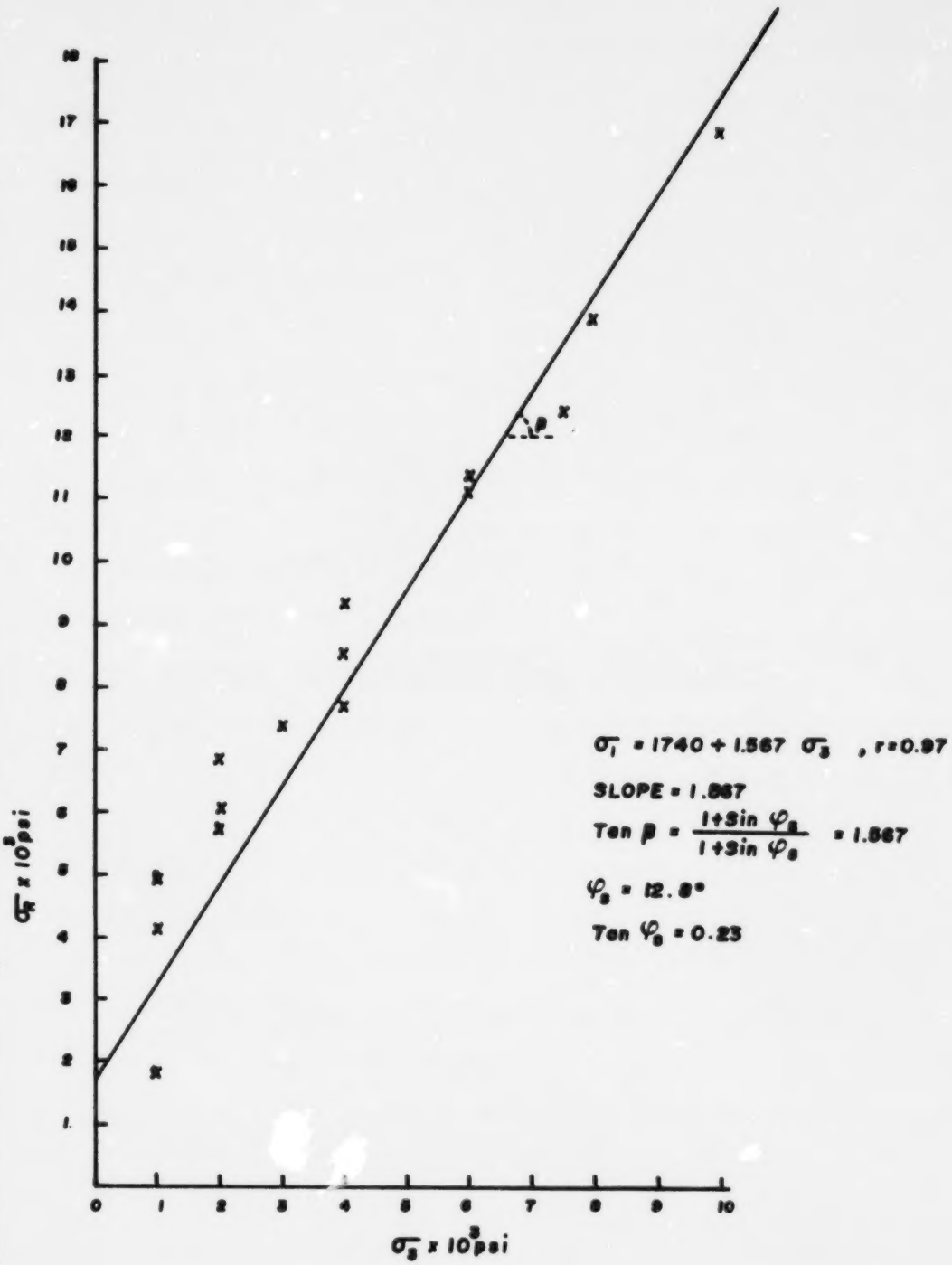
$\sigma_1 = 1740 + 1.567\ \sigma_3$, r=0.97
SLOPE = 1.567
Ten β = $\frac{1+\sin \varphi_s}{1+\sin \varphi_s}$ = 1.567
φ_s = 12.8°
Ten φ_s = 0.23
σ_1 x 10^3psi
σ_3 x 10^3psi
β

σ_1 vs σ_3 FOR RESIDUAL STRENGTHS, ASSUMING A LINEAR RELATIONSHIP

FIGURE 36

KJC 88

Even if we consider only the data below the transition point (σ_1 = 12,700, σ_3 = 7,070) then the resulting linear correlation is:-

$$\sigma_1 = 1345 + 1.79\,\sigma_3 \qquad r = 0.95$$

which gives $\phi = 16.4^{o}$ and $\mu_B = 0.295$

Clearly the angle of sliding friction is not equal to the coefficient of internal friction for broken coal.

5.7 Transition point relationship to μ_B

One of the relationships developed in the pillar model was:-

$$P_{1T} = \frac{A}{2} + \frac{A}{2\mu_B}\left(1 + (1+\mu_B^2)^{\frac{1}{2}}\right) + \left(\frac{A^2}{2} + \frac{A^2}{2\mu_B}\left[1 + (1+\mu_B^2)^{\frac{1}{2}}\right]\right)^{\frac{1}{2}}$$

where A for small specimens is given by $A = \frac{k}{2\sqrt{H}}$ (see Pt 2 report pg 8).

Now from the test results on uniaxial cubes k = 5290

Hence, for a 2 inch high specimen A = 1870

if we assume μ_B = 0.23 then the above equation yields.

P_{1T} = 45,000 psi

and P_{3T} = 28,460 psi (see equ. 73, Pt. 2 report)

This is very different from the transition point estimated from the measurements.

If we assume μ_B = 0.295 (from the data below the transition point) this yields.

P_{1T} = 29440 psi

P_{3T} = 16340 psi

This is still very different from the measured value.

Alternatively if we assume P_{1T} equals the measured value of 12,700 psi and solve for μ_B = this gives μ_B = 0.50 ϕ = 26.5° which is not in agreement with either value given above. Clearly, this equation for P_{1T} requires re-defining using the re-defined failure criteria.

5.8 Tentative conclusion

(1) The σ_1 vs σ_3 relationship for re-compacted broken coal has no apparent relationship to that for the residual strength of the solid coal specimen.

(2) The assumption made in the pillar model that the broken coal behaves as a linear Coulomb Navier material is not strictly true; the σ_1 vs σ_3 relationship is best expressed in a curvilinear form.

(3) If we assume, to a first approximation, that the material is linear, then the angle of internal friction of re-compacted broken coal is 21.8° as compared to that obtained from the residual strength curve of 12.8° (or 16.5° if data below the transition point only is used). Clearly the suggestion made in the model that μ_B (the coefficient of friction on fractured surfaces) might equal $\tan^{-1}$ (angle of internal friction of broken coal), is not valid.

(4) The uniaxial compressure strength of broken coal (P_B) is grossly overestimated by the assumption of linearity. A value of P_B given by the mean of the uniaxial tests (100 psi) is probably closer to the true value, although the accuracy of this measurement must also be doubtful.

(5) The prediction of the transition point from the equation:-

$$P_{1T} = \frac{A}{2} + \frac{A}{2\mu_B}\left(1 + (1+\mu_B^2)^{\frac{1}{2}}\right) + \left(\frac{A^2}{2} + \frac{A^2}{2\mu_B}\left[1 + (1+\mu_B^2)^{\frac{1}{2}}\right]\right)^{\frac{1}{2}}$$

is not acceptable. This equation should be defined using the non- linear expressing and the parameter C and C_R. This should be done in the near future.

6. Group D - Shear box tests - cut coal specimens

6.1 Equipment and procedures

Figure 37 shows the Leonard Farnell direct shear box machine used for these tests. In this shear box the top and bottom halves of the specimen are supported (cemented) in two metal boxes with the cut face of the coal forming the interface between. The lower box rides on roller bearings and the upper box is placed so that the two cut surfaces are matches. A normal load is then placed across the joint through a dead weight and lever system. A shearing rate is selected and lower box is driven beneath the upper box at a constant rate. The shear resistance between the joint surfaces is transmitted through a proving ring and recorded either manually or automatically. The vertical displacments were measured with a dial gauge and the horizontal displacment with an L.V.D.T.

The shearing rate selected for these tests was 25 mm per minute. The surfaces were cut by a diamond saw, producing a relatively flat surface (as confirmed by sample profile measurements). Eight specimens were prepared, the surface areas ranging from $.260 \times 10^{-3}$ m^2 (4.03 sq. inches) to 4.35×10^{-3} m^2 (6.75 sq. inches).

Tests were carried out with seven or eight normal loads applied. The minimum normal load being 200 N (45 lbs) and the maximum normal load being 5200 N (1170 lbs). The maximum normal stress applied was therefore 2000 KN/m^2 (290 psi).

6.2 Results

Appendix D tabulates the results. It was noted that in no case was there significant dilitation between the cut surfaces during the tests.

Figures 38 to 45 show the test results and Figure 46 show the $\tau - \sigma$ curve for all tests grouped together. Table 10 summarizes the linear correlations obtained from each of these tests and from all the data grouped together.

From these tests if is seen that a linear correlation of the form

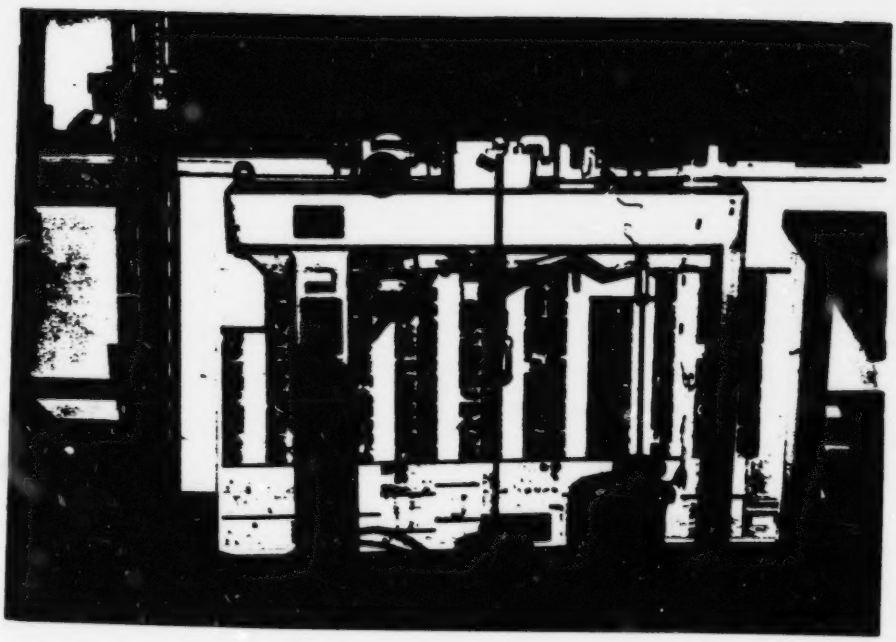

FIGURE 37: Shear Test Apparatus

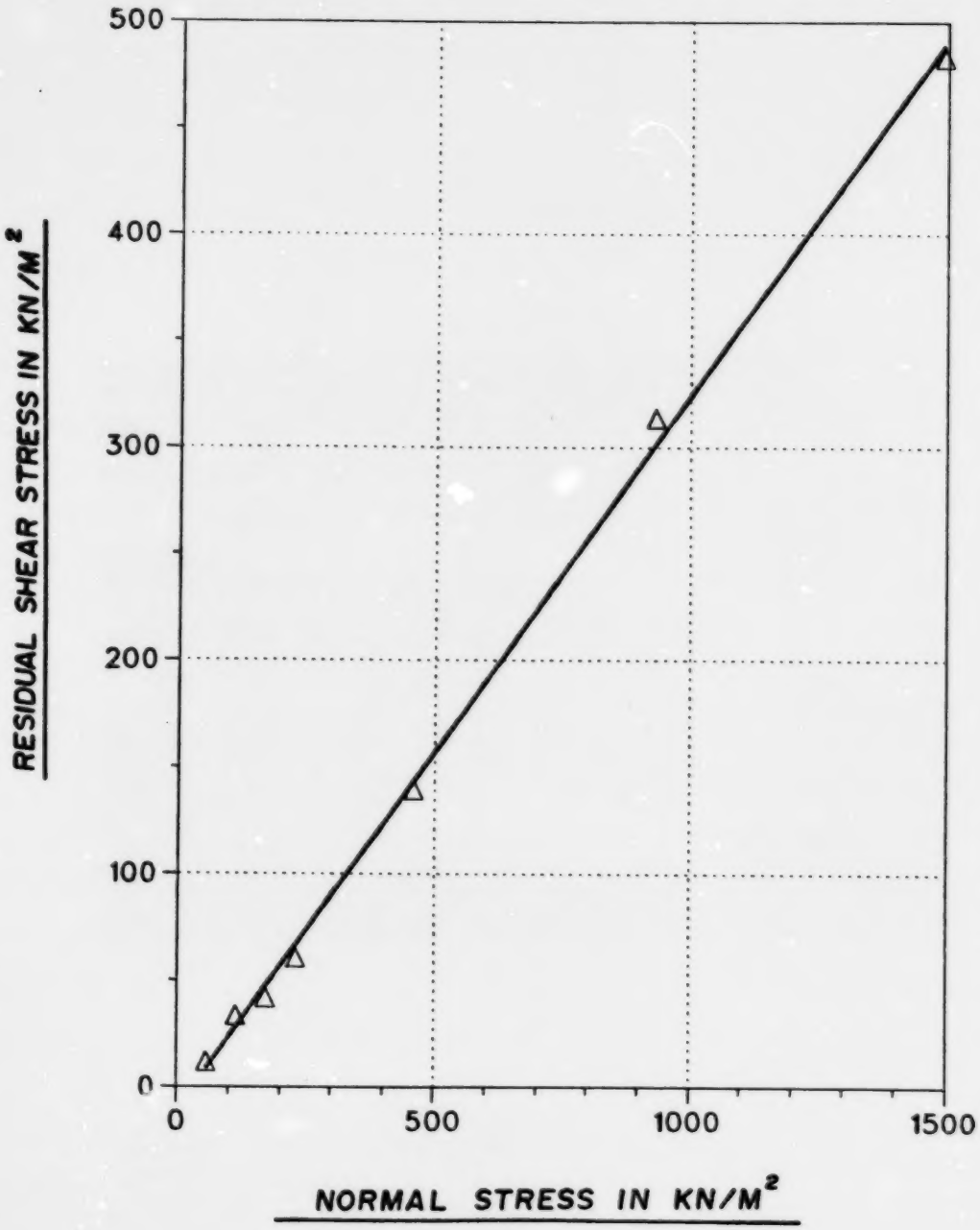

SHEAR TEST # 1

FIGURE 38

RJC 88

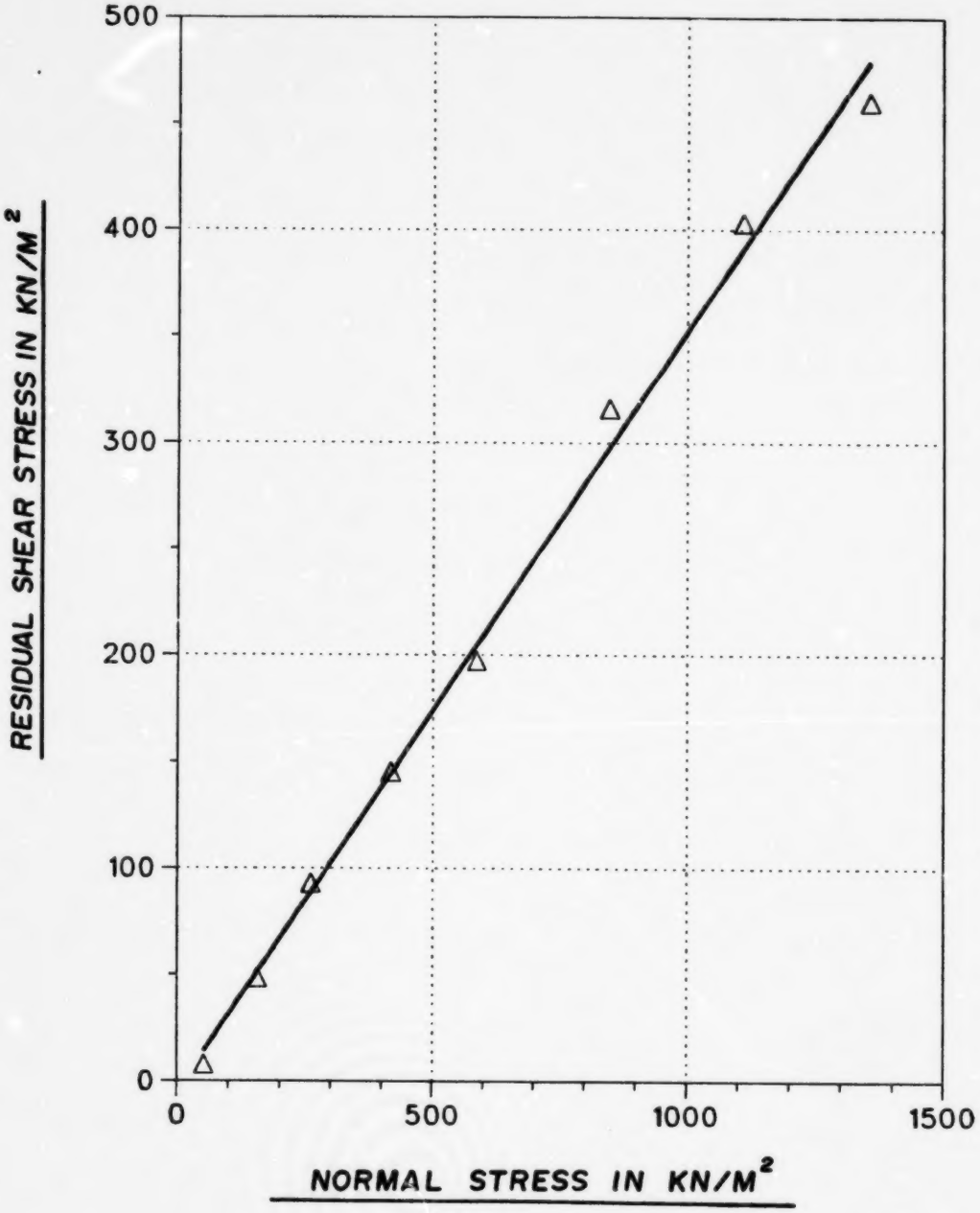

SHEAR TEST # 2

FIGURE 39

KJC 88

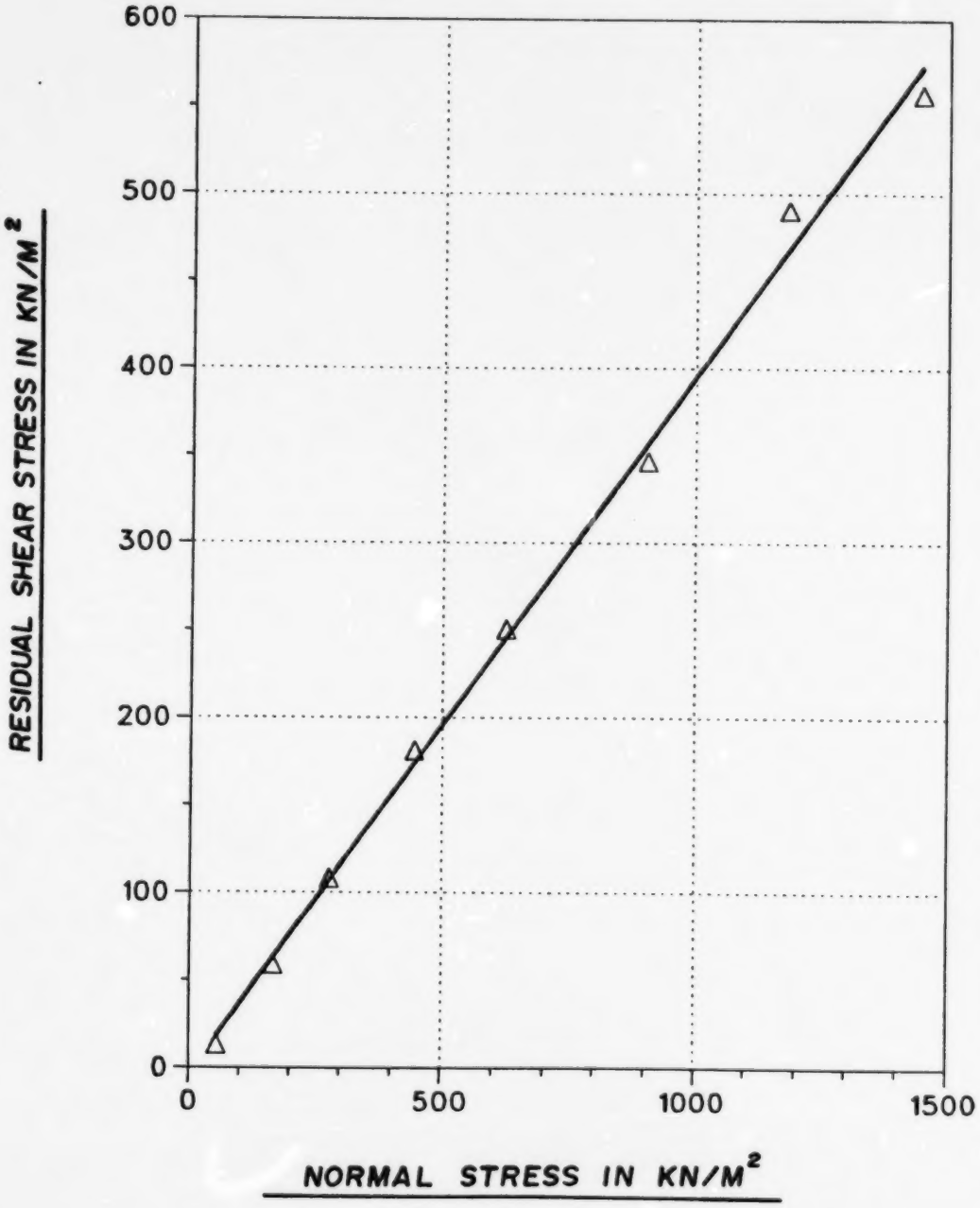

SHEAR TEST # 3

FIGURE 40

KJC 88

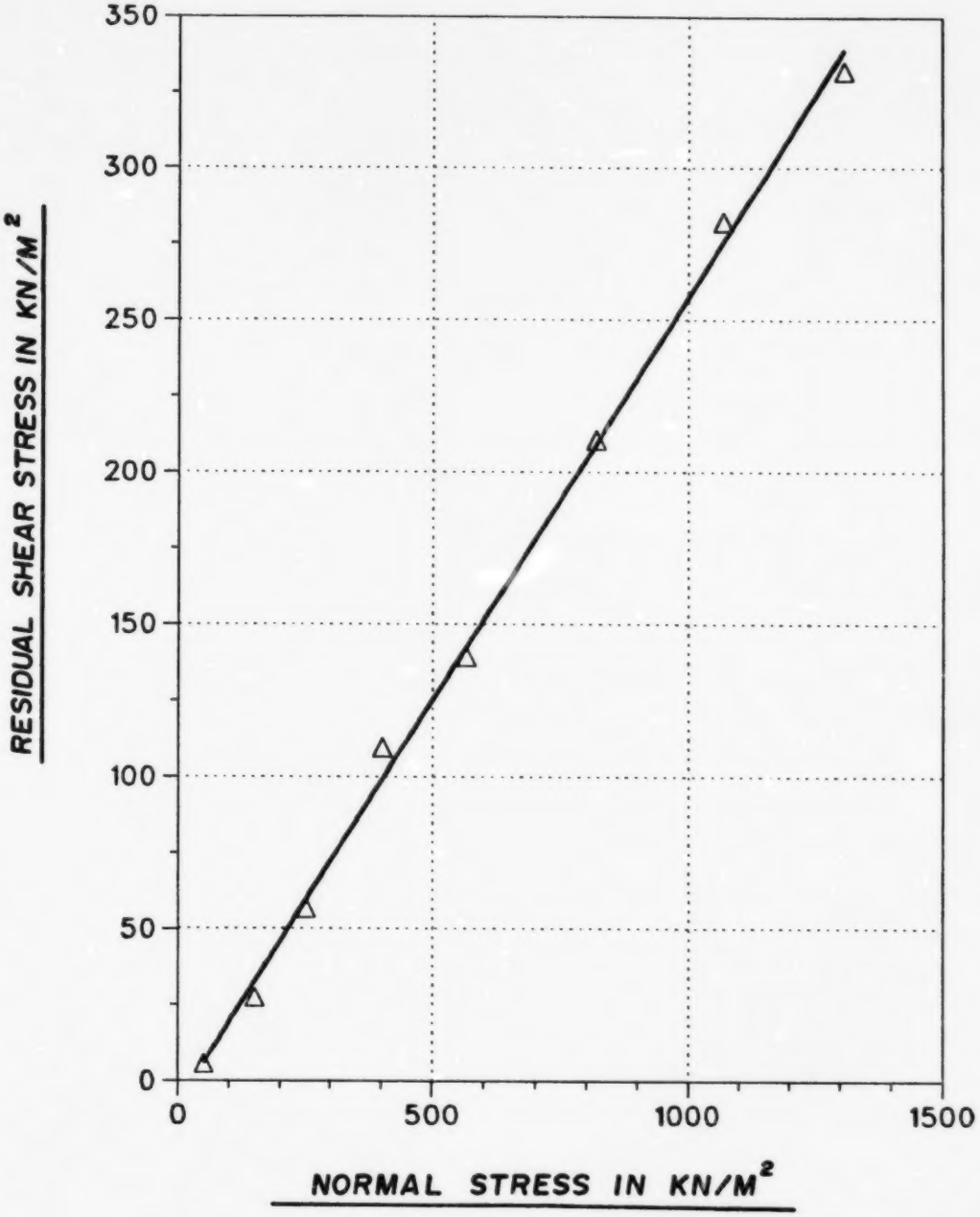

SHEAR TEST # 4

FIGURE 41

KJC 88

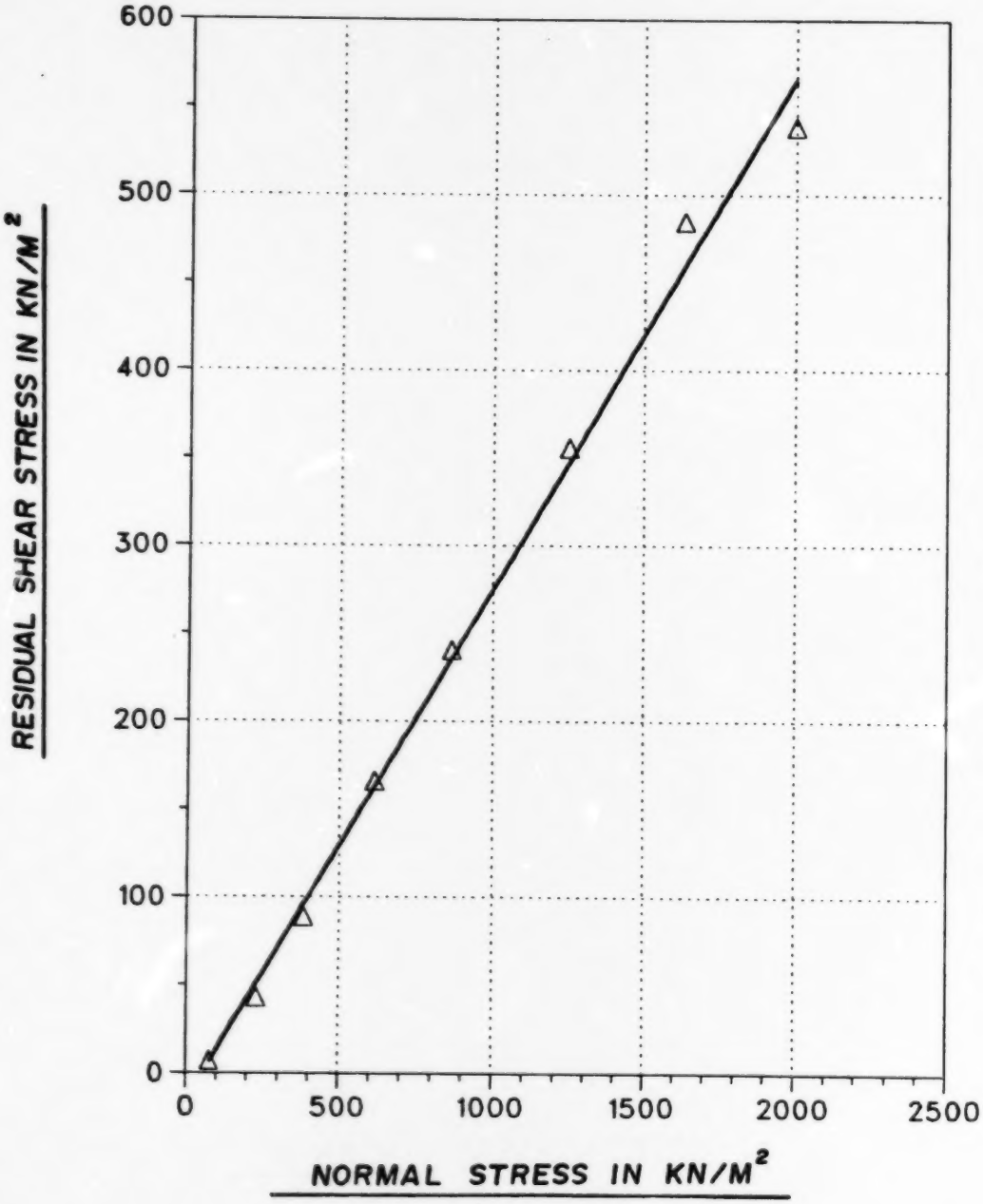

SHEAR TEST # 5

FIGURE 42

KJC 88

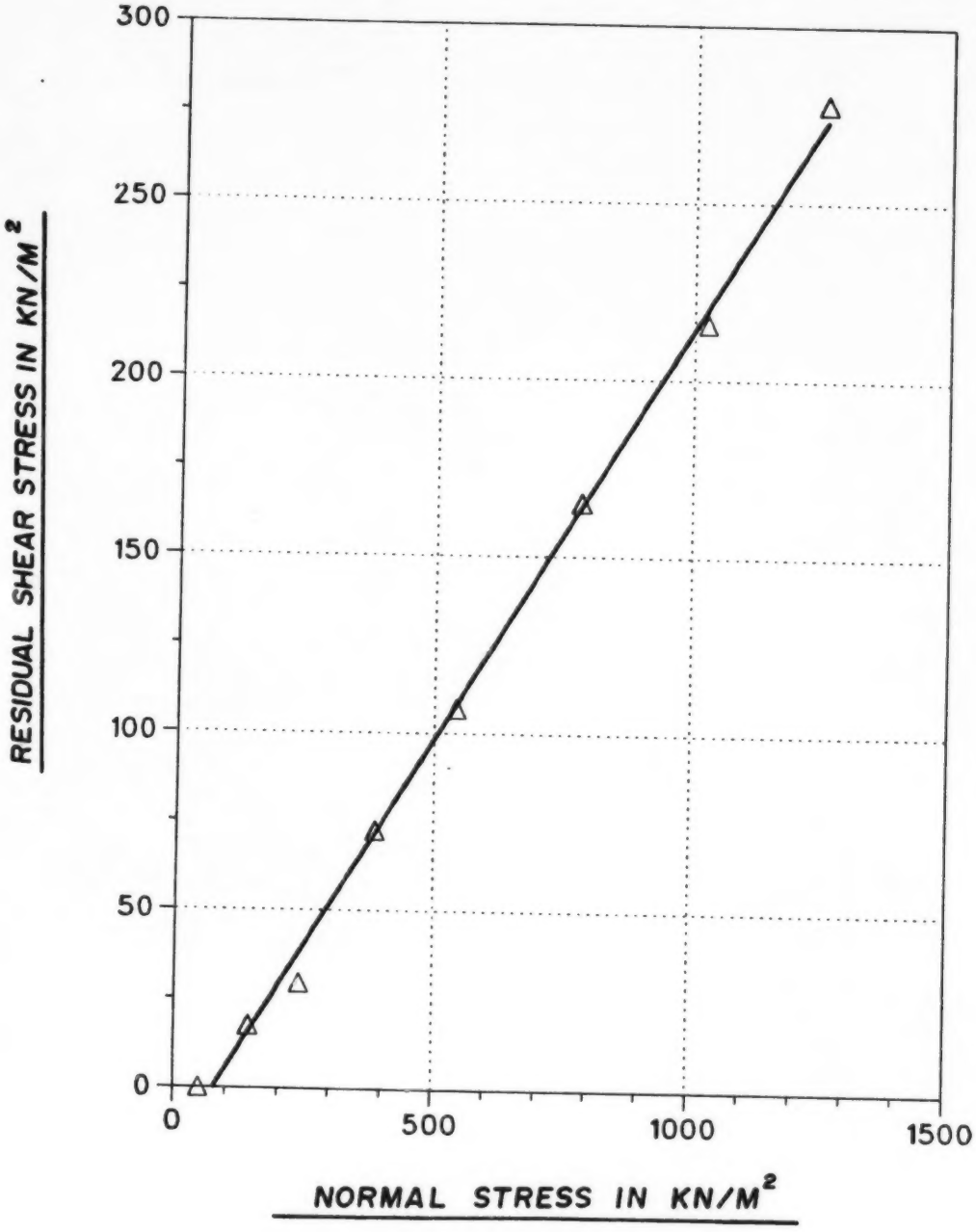

SHEAR TEST #6

FIGURE 43

KJC 88

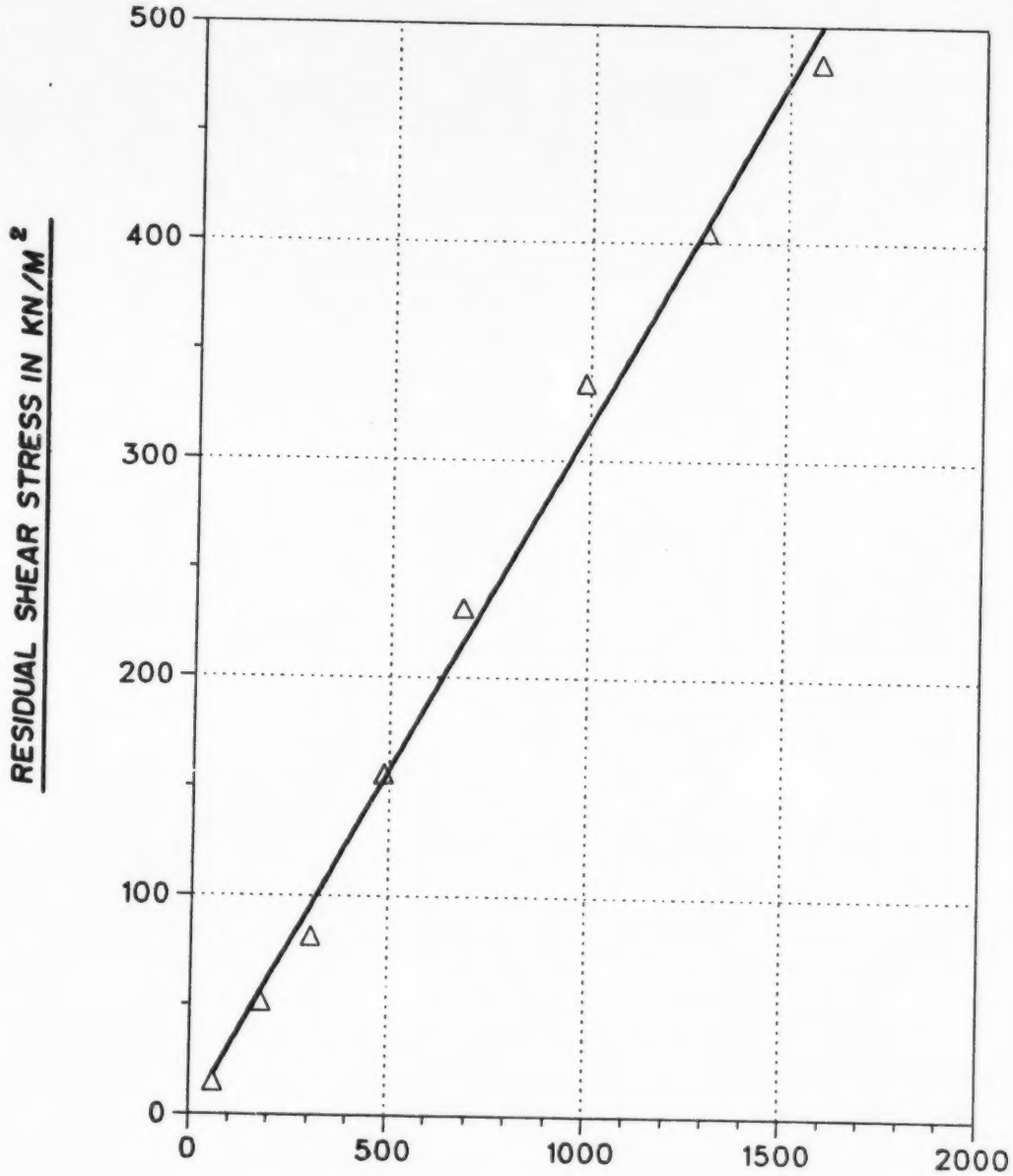

SHEAR TEST # 7

FIGURE 44

EJC 88

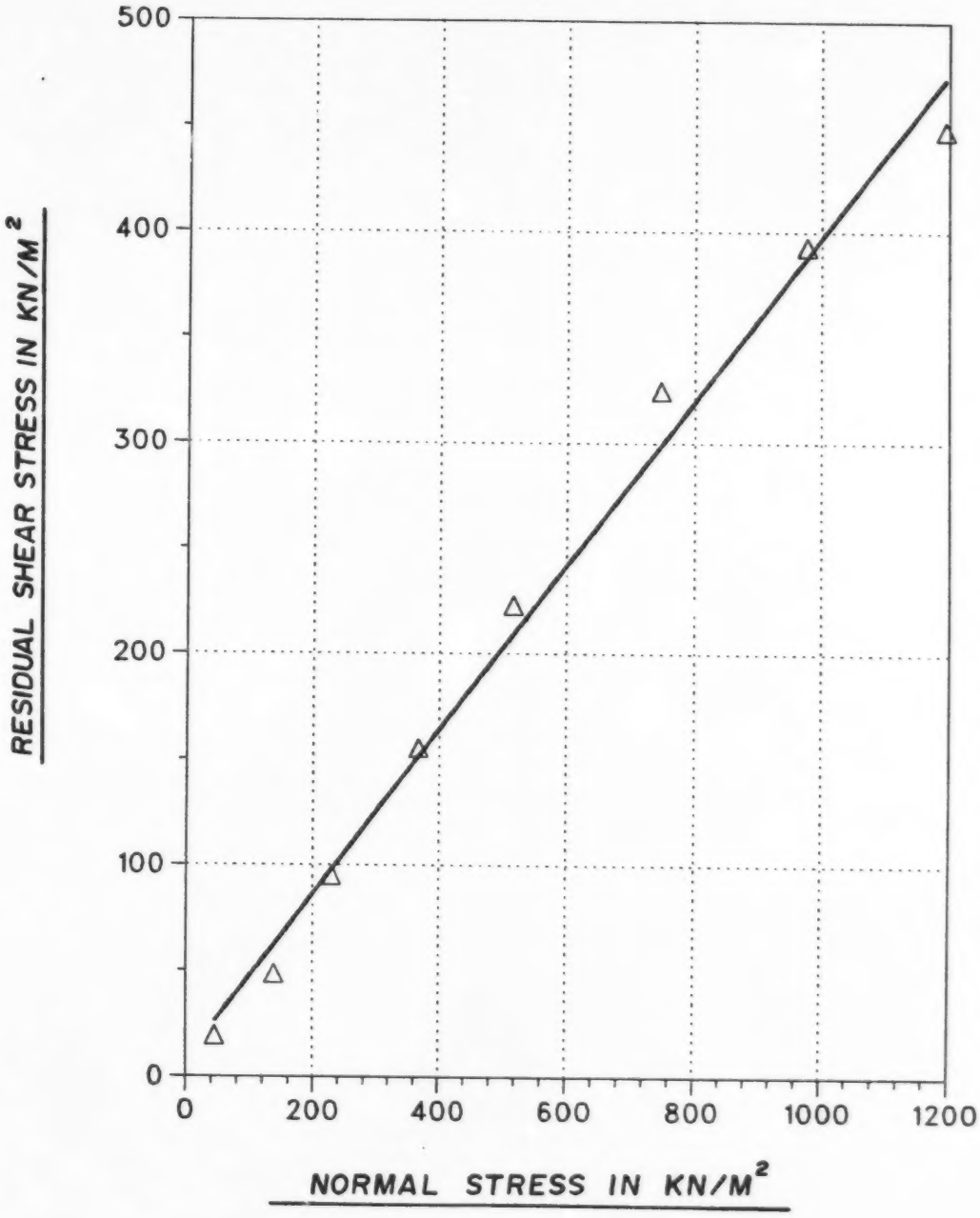

SHEAR TEST # 8

FIGURE 45

KJC 88

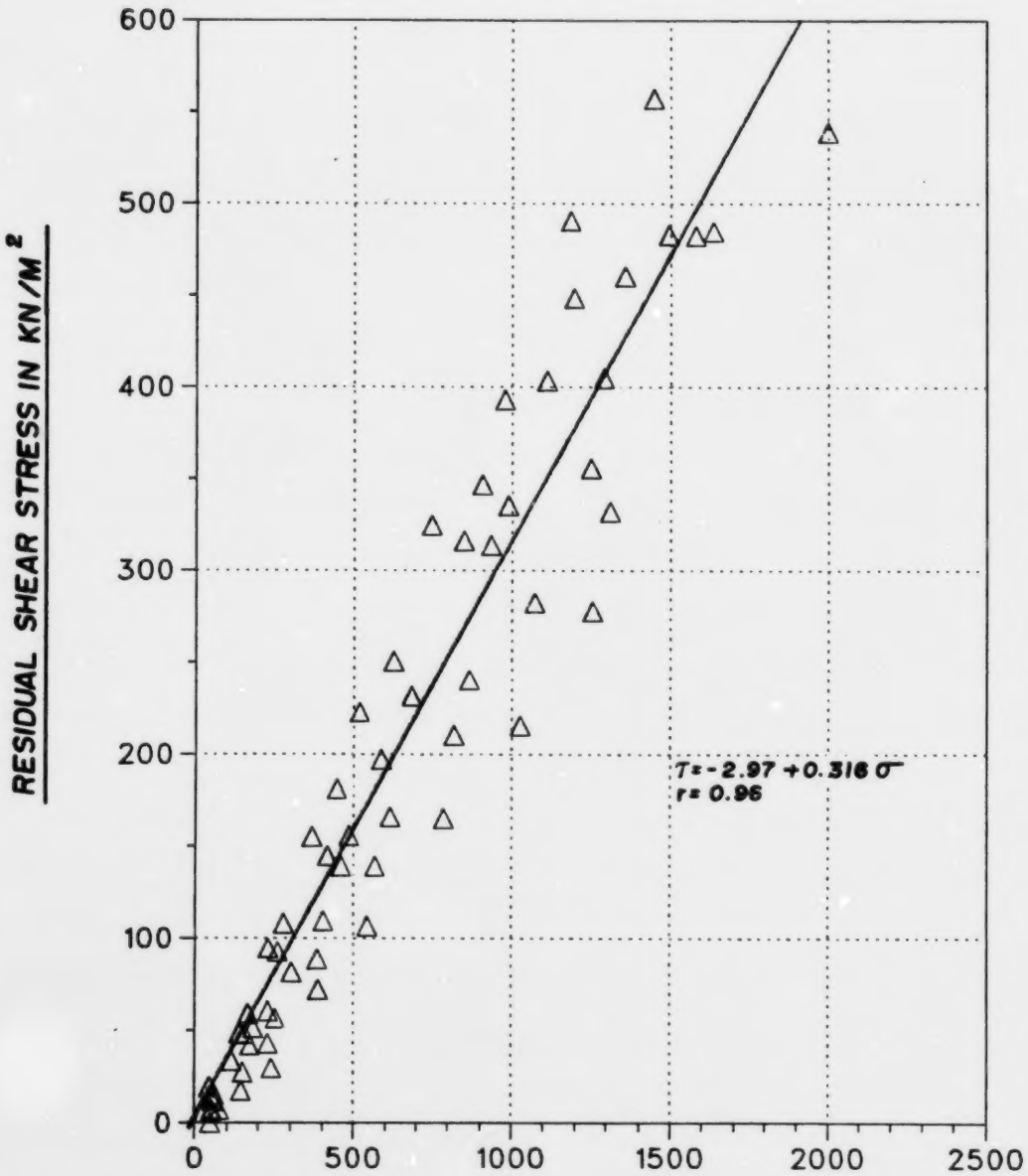

SHEAR TEST-ALL

FIGURE 46

KJC 88

$$\tau = a + b\,\sigma$$

gives an excellent fit to all data.

The coefficient of sliding friction of coal on coal is given by $\tan^{-1} b$ and has a mean value of 17.5°, a range of 13.1 to 21.7°, and a standard deviation of 3°.

Table 10: Linear $\tau - \sigma$ correlation from shear box tests

$\tau = a + b\,\sigma$ (kN/m^2)

Test #	a	b	$\tan^{-1} b$	Correlation coefficient r
1	-10.2	0.334	18.5	0.999
2	-4.4	0.356	19.6	0.997
3	-3.6	0.398	21.7	0.998
4	-7.6	0.264	14.8	0.998
5	-15.6	0.290	16.2	0.997
6	17.9	0.232	13.1	0.999
7	0.42	0.316	17.5	0.997
8	8.23	0.389	21.2	0.995
All data	-2.95	0.315	17.5	0.957

6.3 Comparison with broken coal and residual strength properties

From the shear box tests, the coefficient of sliding friction of coal on coal, is determined as $\tan(17.5^\circ) = 0.315$

From the residual strength curves, the coefficient of sliding friction of coal between the fractured surfaces (assuming a linear σ_3 vs σ_1 relationship) was found (section 5.6) to be $\tan(12.8^\circ) = 0.23$. However, if only the data below the transition point is considered this angle becomes $\phi = 16.4$ i.e. $\mu = \tan\phi = 0.295$.

This is in relatively close agreement to that obtained from the shear box tets. Hence, for this coal, we can take $\phi = 17^\circ$ i.e. $\mu = 0.306$.

From the tests on broken, re-compacted, coal the angle of internal friction was determined (section 5.5) to be $\phi_B = 21.8^\circ$ i.e. $\tan\phi_B = 0.40$.

Clearly the coefficient of friction of coal sliding on coal is significantly different from the angle of internal friction of re-compacted broken coal samples and thus it is not valid to assume that $\mu_B = \tan^{-1} \phi_B$.

6.4 Tentative Conclusions

(1) The angle of sliding friction of coal on coal determined from the shear box tests is close to that determined from the residual strength curve, provided that only the residual strengths below the transition point are considered. A value of $\mu_B = \tan^{-1} 17^o = 0.306$ can be taken for this test coal.

(2) The coefficient of internal friction of broken coal is different from that of coal fracture surfaces sliding one upon the other. Thus we cannot assume $\mu = \tan^{-1} \phi_B$. μ and ϕ_B must be determined from different experimental test procedures. A value of $\phi_B = 21.8^o$ can be assumed for this broken coal.

7. Uniaxial model pillars (H/W <) - Group E

7.1 Deviation from the program plan

It was planned to test a total of 27 uniaxial plate specimens as detailed in section 2. The range of height - width ratio planned were 1/3, 1/6 and 1/10. It proved to be very difficult to prepare these specimens and in fact only one height (1.3 inches) could be used. Two specimens each at H/W = 0.46 (≃ ½) and (H/W) = 0.3 (≃ 1/3) and three specimens at H/W = 0.14 (≃ 1/7) were tested.

7.2 Results

Figure 47 shows photographs of two of the 1/7 specimens after uniaxial testing. Appendix E tabulates the results. Figure 48 shows a typical load - deformation curve for these tests. Table 11 summarizes these results.

7.3 Comparison with uniaxial prism results

From the general expression for prism strength, when $\sigma_3 = 0$, then

$$\sigma_p = k\sqrt{\frac{W}{H}}$$

and k was estimated as ≃ 5290 psi. This expression is however valid only between the limits $.125 < \sqrt{\frac{W}{H}} < 1.4$. Table 12 shows the comparision between the measured strengths and those calculated using this expression. It is seen that there is no agreement between the results even for the case where $\sqrt{\frac{W}{H}}$ is within the limits presented above.

7.4 Comparison with the prism strength formulae derived from the pillar model

Assuming that for laboratory specimen loaded in the press, that there is a uniform stress distribution across the specimen (pillar) then it was shown (report Pt. 1 and Pt. 2) that the model approach yielded the follow strength equations:-

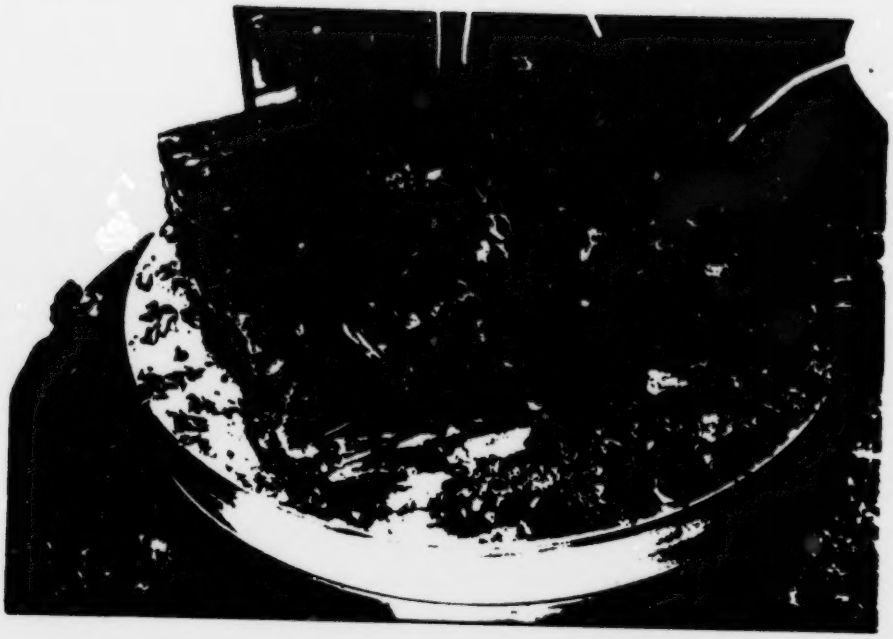

FIGURE 47: "Plate" specimens after testing

CMRC

FIGURE 48: UNIAXIAL TEST ON A COAL PLATE
SIZE 9 IN x 9 IN x 1 IN HIGH

X-AXIS = 8.3×10^{-3} IN PER CM

Y-AXIS = 30,000 LB PER CM

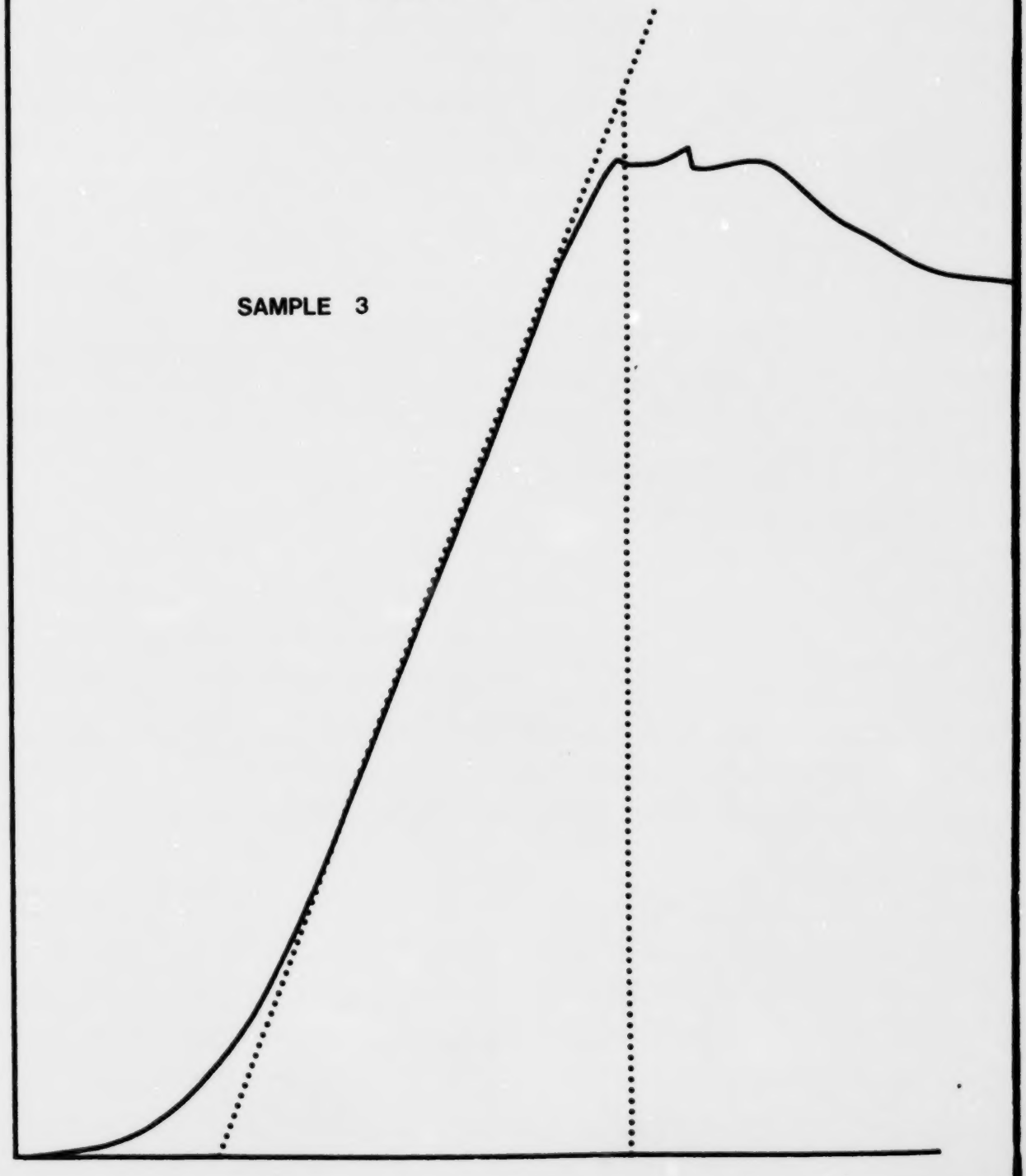

Table 11: Summary of plate specimen results

Specimen #	H = 2h	W = 2w	$\frac{W}{H}$	$\frac{W}{H}$	Peak strength psi	Modulus $Ex10^{-4}$ psi
1	1.3	8.95	6.9	2.3	6458	14.7
2	1.32	9.0	6.81	2.27	7080	16.2
3	1.27	9.0	7.08	2.36	6674	14.7
4	1.31	2.75	2.09	1.26	2417	16.1
5	1.26	2.80	2.22	1.33	1555	14.0
6	1.30	4.34	3.33	1.60	3796	19.3
7	1.38	4.40	3.18	1.52	2937	16.8

Table 12: Comparison of plates with prisms

Specimen	W/H	$\sigma p = k\ W/H$	σp measured
1	2.3	12167	6458
2	2.27	12010	7080
3	2.36	12484	6674
4	1.26	6665	2417
5	1.33	7035	1555
6	1.60	8464	3796
7	1.52	8040	2937

Table 13: Comparison with Formulae - P_B = 100 psi P_{IT} = 12,700

Specimen #	Calculated Strength	Measured Strength
1	6610	6458
2	6549	7080
3	6781	6674
4	442	2417
5	480	1555
6	1014	3796
7	917	2937

Table 14: Comparision with Formulae P_B = 390 psi, P_{IT} = 12,700

Specimen #	Calculated Strength	Measured Strength
1	9292	6458
2	9233	7080
3	9399	6674
4	1725	2417
5	1872	1555
6	3954	3796
7	3576	2937

Minimun pillar strength is given by:

$$\sigma_{s\ min} = \sigma_c \tag{1}$$

where is σ_c the uniaxial compressive of the prism of that dimension.

When $d_T > w$ (where $w = \frac{W}{2}$, the semi pillar width) the pillar fractures at a strength given by

$$\sigma_{SF} = \frac{P_B\ \theta}{2w} \left\{ \frac{h}{\tan \phi_B} \left[e^{(w/h)\ \gamma \tan \phi_B} - 1 \right] - b \right\} \tag{2}$$

and when $d_T < w$, the pillar yields at a strength given by:

$$\sigma_{SY} = \frac{P_B\ \phi}{2_w} \left\{ \frac{h}{\tan \phi_B} \left[e^{(dt/h)\ \gamma \tan \phi_B} - 1 \right] - dt \right\} + \frac{(w-dt)}{w} P_{1T} \tag{3}$$

where w is the semi-pillar width, h is the semi pillar height, dt is the depth of the transition point which is given by:-

$$dt = \frac{h}{\gamma \tan \phi_B} \log_e \left\{ \frac{2P_{1T}}{\theta\ P_B} + \frac{1}{\gamma} \right\}$$

and $\theta = \dfrac{(1 - \sin \phi_B)}{\sin \phi_B}$ and $\gamma = \dfrac{(1 + \sin \phi_B)}{(1 - \sin \phi_B)}$

and P_{1T} is the major principal stress at the transition point.

Now, for the test coal, let us assume that:

(1) From the tests on broken re-compacted coal $\phi_B = 21.8^o$ and $P_B = 100$ psi

(2) From the triaxial tests, group B4, $P_{1T} = 12{,}700$ psi then for this coal $\theta = 1.69$ and $\alpha = 2.18$ and for all the test plates $h \sim 0.65$ inches thus $d_t \sim 3.74$ inches

i.e. in this case for specimen 1-3, dt < w and equation 3 applies

for specimen 4-7, dt > w and equation 2 applies.

Table 13 compares the calculations with the measured strengths using these numbers. It is seen that the strength of the fractured specimens is grossly underestimated where as that for the yielding specimens gives a reasonable fit to

the data.

Now it is unfortunate that determination of both P_B and P_{1T} are very inaccurate. Let us therefore examine the effect of changing these values.

To give a possible fit to the fractured specimens (#'s 4 - 7) it would be necessary to raise P_B to 390 psi. This has been done in table 14. In this case, a much better fit is obtained for specimens 4 - 7 but the yielding strengths of specimens 1 - 3 are now grossly overestimated.

Finally let us keep P_3 at 390 psi and drop P_{1T} to 8000 psi. Table 15 shows the results of these calculations. These calculations are as close as we are likely to get a fit to all the experimental data.

7.5 Tentative conclusions

We can conclude therefore that:

(1) Using the values of ϕ_B, P_B and P_{1T} obtained from the triaxial tests in broken and solid coal in the equations derived from the pillar model do not give a good prediction of the plate test results.

(2) However, the accuracy of the determinations of P_B and P_{1T} is not good. It is possible to use the formulae to get a much better fit to the experimental data for plate specimens if P_B and P_{1T} are judiciously changed.

Possibly back analysis of plate tests where $dt > b$ (i.e. fracture occurs) might be a better way of estimating P_B. However it is clear that P_B is always going to be difficult to determine with any accuracy.

It is thought that P_{1T} ought to be able to be determined more accurately than was the case in the triaxial tests in solid coal. Perhaps this would be the case with a less variable material (and should be investiated by further testing); however the fact that P_{1T} is given by

Table 15: Comparison with Formulae - P_B = 390 psi P_{1T} = 8,000

Specimen #	Calculated Strength	Measured Strength	% Diff
1	6385	6458	-1.1
2	3376	7080	-11.1
3	6442	6674	-3.6
4	1725	2417	-40.0
5	1872	1555	+16.9
6	3954	3796	+4.0
7	3576	2937	+17.8

the intersection of two curves bending in the same direction is always going to make this point difficult to determine accurately.

(3) The "prediction" of the plate test results also assumed that ϕ_B was a constant. This is only a first approximation. The pillar (specimen) strength formulae should be re-expressed taking into account both the non-linearity of ϕ_B and also the non-linerity of μ_B (which defines P_{1T}). The data should be re-examined when this has been done.

8. CONCLUSIONS AND RECOMMENDATIONS

The test coal proved to be extremely variable, thus considerable difficulty was experienced in interpreting the results. Consequently all conclusions given here must be considered as tentative and not proven facts.

8.1 With respect to uniaxial prism tests

(1) The experimentally determined prism strengths are linearly correlated to the specimen modulus. This allowed the data to be normalised to a common modulus and thus allow the size/shape effects on strength to be more clearly seen.

(2) An expression $\sigma_{pN} = k \sqrt{\frac{W}{H}}$ describes this uniaxial test data, where W is the minimum prism width, H is its height, σ_{pN} is the normalised prism strength.

(3) Taking into account the modulus E of the specimen, an expression

$$\frac{\sigma_p}{E} = a + b\sqrt{\frac{W}{H}}$$

fits the data. For all practical purposes a = 0 and the expression

$$\frac{\sigma_p}{E} = b\sqrt{\frac{W}{H}}$$

gives an acceptable fit to the data.

8.2 With respect to the triaxial tests on solid coal specimens

(1) The experimentally determined principal stress difference $(\sigma_p - \sigma_3)$ at failure is possibly linearly correlated with the specimen modulus; however in view of this doubt and the fact that under triaxial conditions the modulus variation was not as large as with the uniaxial test specimens, no normalisation of data was carried out.

(2) A general relationship given by

$$\sigma_3 = P_{3T}\left\{\frac{\sigma_1^{\,c} - \left(k\sqrt{\frac{W}{H}}\right)^c}{P_{1T}^{\,c} - \left(k\sqrt{\frac{W}{H}}\right)^c}\right\}$$

appears to describe both the peak and the residual strength measurements within the limits of experimental accuracy, where

$$C = C_R + (C_1 - C_R) \frac{H_1}{\sqrt{W_1}} \cdot \frac{\sqrt{W}}{H}$$

where P_{3T} is the confining pressure at the transition point
P_{1T} is the major principal stress at the transition point
W is the specimen width
H is the specimen height
C_1 is a parameter determined from a suite of tests with specimens of height H_1, width W_1
C_R is a parameter obtained from the residual strenth curve of this same suite of specimens
k is the "unit cube" strength for the coal (uniaxial, W = H = 1 inch)

and $\sigma_1 = \sigma_p$ to describe the peak strength at failure

(3) To determine the residual strength σ_R is put equal to σ_1 in this expression and $(k \frac{\sqrt{W}}{H})$ is put to zero.

(4) Some limits must be placed in the range of applicability of this expression. Provisionally the limits $0.125 < \frac{\sqrt{W}}{H} < 1.4$ are indicated from past work with uniaxially tested specimens.

For all practical purposes the lower limit (0.125) is identical to the residual strength curve. This indicates that as a specimen (pillar) size increases so the strength approximates to a constant value for any σ_3. i.e. size effects decrease with increasing size and the peak strength approaches the residual strength.

The upper limit, $\frac{\sqrt{W}}{H} = 1.4$, is only likely to be encountered when testing small, laborating size specimens. Past work indicates that, for uniaxial tests, this limit is correct, however it is conceivable that this limit may change with triaxial stress conditions. Consideration should also be given as to whether this limit might be better defined in terms of "the critical width to avoid catestrophic failure" developed in the pillar model.

(5) The determination of the transition point (P_{3T}, P_{1T}) is difficult and, with this test coal at least, was very inaccurate. Even with a less variable rock, it will be difficult to define accurately since both the peak and residual strength curves bend in the same direction and thus their point of intersection will always be prone to error.

(6) The implications of the general expression given above are very important:-

i. As the confining pressure increases, the variation of specimen strength with specimen size decreases until the brittle ductile transition point is reached. There are no size effects beyond this point.

ii. The maximum "size effect" on strength occurs under uniaxial conditions.

iii. As the size increases, i.e. as $\frac{\sqrt{W}}{H}$ tends to zero (or perhaps to 0.125), the strength decreases and becomes assymptotic to the residual strength cruve.

iv. The residual strength is independent of size effects.

(7) The assumption used in the pillar model that the coefficient of sliding friction, μ_B, for coal fracture surfaces is a constant is not valid. μ_B diminishes with increasing normal stress across the fracture surface. Consequently the equation in the pillar model defining the transition point should be re-determined using a non linear relationship.

(8) The implicit assumption used in the past that the size effects observed under uniaxial stress conditions are directly applicable to triaxial conditions is wrong. Size effects diminish and eventually disappear as both size and confining pressure increase.

8.3 With respect to triaxial tests on broken coal specimens

(1) The σ_1 vs σ_3 relationship for recompacted broken coal at failure appears to be independent of specimen size and re-compaction pressure (within the range tested) and is best described by a relationship of the form

$$\sigma_{3_B} = a + b\ \sigma_{1_B}^{c_B}$$

(2) It is doubtful whether this test will yield an accurate value of the uniaxial compressive strength, P_B, of broken coal required by the model.

(3) An assumption of a linear relationship is possibly acceptable in this case (although it requires further investigation); thus ϕ_B for input into the model can be estimated from these results.

(4) The σ_1 vs σ_3 relationship at failure for broken coal has no apparent relationship to that for the residual stresses for solid coal specimens. Hence the suggestions made in the earlier reports that μ_B might equal $\tan^{-1} \phi_B$ is not valid.

8.4 With respect to the shear box tests

(1) The angle of sliding friction of coal surfaces obtained from the shear box tests is close to that determined from the residual strength curve for the solid coal specimens (provided that a linear assumption is made in the latter case and only data below the transition point considered).

(2) These shear box tests are limited to low normal stresses. It is seen from the residual strength curves that this angle of friction changes with increasing normal stress. Hence the shear box test is probably not a good method for defining μ. It will be better to use the residual strength curve and to re-define the transition point using a non-linear relationship.

8.5 With respect to the model pillars (plates)

(1) Using the values of ϕ_B, P_B and P_{1T} estimated from the previous tests in the model equations allowed a prediction to be made of the results. The agreement between the "predicted" and measured results was poor.

(2) However, it was shown that by varying P_B and P_{1T} a passable fit of the prediction to the experimental results could be obtained. In view of the fact that the accuracy of determination of P_B and P_{1T} was poor in the earlier tests, it is seen that the model pillar predictions are not totally out of line with the model. However, these results do not validate the model.

8.6 Recommendations

(1) Further testing should be carried out using a less variable coal or another relatively weak sedimentary rock such as mudstone. The following points should be noted in the planning of this test program.

i. There would appear to be little point in including shear box tests in such a program.

ii. Great care should be taken in the experiments to try to better define the residual stresses. Perhaps, after failure, the specimen should be unloaded and then re-loaded at the same confining pressure in order to better define σ_R.

iii. With a less fractured material such as mudstone it may be easier to prepare plate specimens of a suitable size and of varying heights. A larger number of such tests would help considerably in assessing whether the model can be used as a prediction test.

(2) The pillar model should be modified by:-

i. Re-defining the transition point in terms of non-linear equations for both the peak and residual strengths using the general expression developed in the triaxial tests given in this report. (note: the non-linear peak stress relationship currently used in the model ,

$$\tau = A\ \sigma + \frac{A^2}{4}\ ,$$

is most unsatisfactory).

ii. Re-defining the broken coal properties in terms of a non-linear σ_1 vs σ_3 relationship.

iii. On the basis of the above, developing the new equations to define pillar strengths, residual stress capacity, critical pillar deminsions etc.

(3) Having modified the pillar model as recommended in (2) above, the data in this report should be re-examined. Likewise the data developed in (1) above should also be used in the assessment.

9. REFERENCES

(1) Barron, K., "An analytical approach to the design of pillars in coal. Part I: The Analytical model". Dept. Supply and Services, Ottawa, Contract No. ISQ80-00161 report, January 1983.

(2) Barron, K., "An analytical approach to the design of pillars in coal. Part 2: Application of the model to case histories." Dept. Supply and Services, Ottawa, Contract No. ISQ80-00161 report, March 1983.

(3) Salamon, M.D.G., and Munro, H.H., "A study of the strength of coal pillars", Journal of the S. African Institute of Mining and Metallurgy, pp 55-67, September 1967.

(4) Steart, F.A. "Strength and Stability of pillars in coal mines", J. Chemical, Metallurgical and Mining Society of S. Africa, pp 309-325, 1954.

(5) Holland C.T. and Gadey, F.L. "Some aspects of permanent support of overburden on coal beds", Proc. West Virginia Coal Mining Institute, pp 43-66, 1957.

Acknowledgements

The project was funded CANMET, EMR, with Dr. M. Das as scientific authority. The author would like to express his thanks to CANMET for their aid and, in particular, to Dr. Das for his suggestions, contribution and patience during this work.

Much assistance in the testing and specimen preparation was given by D. Green, K. Chekerda, and S. Thornton of CMRC and by R. Krzanowski and E. Ferguson of the University of Alberta. To each of them the author expresses his appreciation.

The manuscript was typed by Anita Wright and Ardith Nash with much patience with the authors' writing.

Appendix A1: Uniaxial cube strength tests - Group A1

Specimen #	Height H inches	Depth D inches	Width W * inches	H/W	X-Section Area sq. inches	Unit WT x 10 lbs/cu in	σ_p Peak Strength psi	σ_R Residual Strength psi	Modulus E x 10 psi	σ_{pN}* Normalised Peak psi
1-1	0.957	0.984	0.787	1.216	0.775	5.26	620	---	1.05	11809
1-2	0.992	0.898	0.767	1.293	0.689	4.95	1220	---	4.50	5422
1-3	0.976	1.000	0.929	1.050	0.933	4.76	2830	---	9.42	6008
1-4	0.921	0.933	0.908	0.932	0.922	4.74	2670	---	8.48	6297
1-5	0.940	0.996	0.909	1.034	0.906	4.85	1655	---	4.92	6727
1-6	0.965	0.908	0.961	1.004	0.949	5.02	1707	---	6.55	5212
1-7	0.961	0.909	0.937	1.026	0.852	5.04	2680	---	10.04	5338
Mean	0.959	0.958	0.897	1.079	0.861	4.95	1912	---	6.42	6688
S.D	0.023	0.044	0.086	0.127	0.096	0.18	843	---	3.19	2325
2-1	1.022	1.026	0.995	1.030	1.021	4.79	1784	---	8.26	4126
2-2	0.978	1.019	1.002	0.968	1.021	5.19	1838	---	---	---
2-3	1.033	1.020	1.000	1.033	1.020	4.89	873	---	3.71	4436
2-4	1.020	1.007	1.021	0.999	1.028	4.86	1517	---	3.46	8768
2-5	1.021	1.010	1.000	1.021	1.010	4.95	1663	---	5.43	6125
2-6	1.030	1.025	0.990	1.040	1.010	5.03	1596	---	7.20	4433
2-7	1.030	1.009	0.990	1.040	0.999	4.97	1862	---	11.13	3346
2-8	1.026	1.025	1.000	1.026	1.026	5.17	1405	---	9.40	2989
2-9	0.972	1.019	1.006	0.966	1.025	4.73	1229	---	6.83	3598
2-10	1.023	1.025	1.011	1.012	1.036	5.23	1042	---	6.17	3377
Mean	1.015	1.019	1.002	1.014	1.020	4.98	1468	---	6.84	4578
S.D	0.023	0.007	0.009	0.028	0.011	0.17	344	---	2.52	1825
1	1.937	2.094	2.007	0.965	4.205	4.97	1783	---	13.73	2597
2	1.981	2.055	1.902	1.043	3.908	4.97	2210	---	14.78	2998
3	1.980	2.047	1.941	1.020	3.968	4.99	1362	---	11.78	2328
4	2.035	2.098	1.992	1.021	4.180	4.84	2885	---	21.00	2747
Mean	1.983	2.074	1.961	1.012	4.063	4.94	2060	---	15.30	2666
S.D	0.040	0.026	0.048	0.033	0.151	0.07	650	---	4.01	277

* Normalised to E=20 x 10 psi

Appendix A1: Uniaxial cube strength tests - Group A1

Specimen #	Height H inches	Depth D inches	Width W * inches	H/W	X-Section Area sq. inches	Unit WT x 10 lbs/cu in	σ_p Peak Strength psi	σ_R Residual Strength psi	Modulus E x 10 psi	σ_{pN} * Normalised Peak psi
1	2.976	3.016	3.016	0.987	9.096	5.09	1954	---	19.19	2036
2	2.992	2.995	2.957	1.012	8.710	5.02	696	---	6.02	2312
3	3.043	3.035	3.016	1.009	9.150	4.89	1402	---	13.94	2011
4	2.948	3.008	2.976	0.991	8.938	4.76	2183	---	15.80	2918
5	3.008	3.090	3.110	0.965	9.610	5.00	2035	---	16.24	2506
6	3.066	3.027	2.957	1.037	8.950	5.06	2467	---	17.00	2800

Mean	2.982	3.027	3.005	1.000	9.078	4.98	1790	---	14.56	2443
S.D.	0.096	0.034	0.058	0.025	0.300	0.13	648	---	4.56	398

1	3.984	4.007	4.000	0.966	16.030	5.10	1340	---	11.24	2304
2	3.984	4.078	4.007	1.023	16.350	5.26	760	---	5.16	2045
3	4.000	4.000	3.966	1.009	15.84	5.15	1257	---	12.46	2017
4	4.079	4.129	4.011	1.017	16.570	4.93	1510	---	14.60	2068

Mean	4.040	4.012	4.036	1.004	16.200	5.11	1216	---	10.86	2354
S.D.	0.057	0.048	0.062	0.026	0.325	0.13	322	---	4.05	426

1	5.047	5.078	5.059	0.998	25.640	5.08	1184	---	14.82	1598
2	5.051	5.035	5.137	1.003	25.870	4.77	1288	---	10.56	2424

Mean	5.049	5.056	5.098	1.000	25.760	4.92	1232	---	12.69	2011
S.D.	0.003	0.030	0.055	0.003	0.162	0.20	68	---	3.01	584

* Normalised to E=20 x 10 psi

Appendix A2: Uniaxial tests on rectangular prisms with a square base - Group A2 H/W = 1.0

Specimen #	Height H inches	Depth D inches	Width W * inches	H/W	X-Section Area sq. inches	Unit WT x 10 lbs/cu in	σ_p Peak Strength psi	σ_R Residual Strength psi	Modulus E x 10 psi	σ_{pN}^* Normalised Peak psi
1-1	0.957	0.984	0.787	1.216	0.775	5.26	620	---	1.05	11809
1-2	0.992	0.898	0.767	1.293	0.689	4.95	1220	---	4.50	5422
1-3	0.976	1.000	0.929	1.050	0.933	4.76	2830	---	9.42	6008
1-4	0.921	0.933	0.988	0.932	0.922	4.74	2670	---	8.48	6297
1-5	0.940	0.996	0.989	1.034	0.986	4.85	1655	---	4.92	6727
1-6	0.965	0.988	0.961	1.004	0.949	5.02	1707	---	6.55	5212
1-7	0.961	0.989	0.937	1.026	0.852	5.04	2680	---	10.04	5338
Mean	0.959	0.958	0.897	1.079	0.861	4.95	1912	---	6.42	6688
S.D	0.023	0.044	0.086	0.127	0.096	0.18	843	---	3.19	2325
2-1	1.022	1.026	0.995	1.030	1.021	4.79	1704	---	8.26	4126
2-2	0.970	1.019	1.002	0.968	1.021	5.19	1838	---	---	---
2-3	1.033	1.020	1.000	1.033	1.020	4.89	823	---	3.71	4436
2-4	1.020	1.007	1.021	0.999	1.028	4.86	1517	---	3.46	8768
2-5	1.021	1.010	1.000	1.021	1.010	4.95	1663	---	5.43	6125
2-6	1.030	1.025	0.990	1.040	1.010	5.03	1596	---	7.20	4433
2-7	1.030	1.009	0.990	1.040	0.999	4.97	1862	---	11.13	3346
2-8	1.026	1.025	1.000	1.026	1.026	5.17	1405	---	9.40	2989
2-9	0.972	1.019	1.006	0.966	1.025	4.73	1229	---	6.83	3598
2-10	1.023	1.025	1.011	1.012	1.036	5.23	1042	---	6.17	3377
Mean	1.015	1.019	1.002	1.014	1.020	4.98	1468	---	6.84	4578
S.D	0.023	0.007	0.009	0.028	0.011	0.17	344	---	2.52	1825
1	1.937	2.094	2.007	0.965	4.205	4.97	1783	---	13.73	2597
2	1.901	2.055	1.902	1.043	3.908	4.97	2218	---	14.78	2998
3	1.980	2.047	1.941	1.020	3.960	4.99	1362	---	11.78	2328
4	2.035	2.090	1.992	1.021	4.180	4.84	2885	---	21.88	2747
Mean	1.983	2.074	1.961	1.012	4.063	4.94	2060	---	15.38	2666
S.D	0.060	0.026	0.060	0.033	0.151	0.07	650	---	4.81	277

* Normalised to E=20 x 10 psi

Appendix A2: Uniaxial tests on rectangular prisms with square base - Group A2

Specimen #	Height H inches	Depth D inches	Width W * inches	H/W	X-Section Area sq. inches	Unit WT x 10 lbs/cu in	σ_p Peak Strength psi	σ_R Residual Strength psi	Modulus E x 10 psi	σ_{pN} * Normalised Peak psi
1	2.976	3.016	3.016	0.987	9.096	5.09	1954	---	19.19	2036
2	2.992	2.995	2.957	1.012	8.710	5.02	696	---	6.02	2312
3	3.843	3.035	3.016	1.009	9.150	4.89	1402	---	13.94	2011
4	2.948	3.000	2.976	0.991	8.930	4.76	2183	---	15.00	2910
5	3.000	3.090	3.110	0.965	9.610	5.00	2035	---	16.24	2586
6	3.866	3.027	2.957	1.037	8.950	5.06	2467	---	17.00	2800

Mean	2.982	3.027	3.005	1.000	9.070	4.98	1790	---	14.56	2443
S.D.	0.096	0.034	0.050	0.025	0.300	0.13	640	---	4.56	398

1	3.984	4.007	4.000	0.966	16.030	5.10	1340	---	11.24	2384
2	3.984	4.078	4.007	1.023	16.350	5.26	760	---	5.16	2945
3	4.000	4.000	3.966	1.009	15.84	5.15	1257	---	12.46	2017
4	4.079	4.129	4.011	1.017	16.570	4.93	1510	---	14.60	2060

Mean	4.040	4.012	4.036	1.004	16.200	5.11	1216	---	10.86	2354
S.D.	0.057	0.048	0.062	0.026	0.325	0.13	322	---	4.05	426

1	5.047	5.078	5.059	0.998	25.648	5.08	1184	---	14.82	1598
2	5.051	5.035	5.137	1.003	25.870	4.77	1200	---	10.56	2424

Mean	5.049	5.056	5.098	1.000	25.760	4.92	1232	---	12.69	2011
S.D.	0.003	0.030	0.055	0.003	0.162	0.20	60	---	3.01	584

* Normalised to E=20 x 10 psi

Appendix A2 : Uniaxial tests in rectangular prisms - square base - Group A2

Specimen #	Height H inches	Depth D inches	Width W * inches	H/W	X-Section Area sq. inches	Unit WT x 10 lbs/cu in	σ_p Peak Strength psi	σ_R Residual Strength psi	Modulus E x 10 psi
1	1.504	0.984	0.945	1.59	0.93	5.130	2710	---	15.19
2	1.453	0.964	0.945	1.540	0.911	4.860	2305	---	13.64
3	1.397	0.917	0.870	1.610	0.798	4.950	1955	---	12.84
4	1.409	1.023	0.964	1.460	0.987	4.900	2316	---	10.59
Mean	1.441	0.972	0.931	1.550	0.907	4.960	2320	---	13.06
S.D	0.048	0.044	0.042	0.067	0.079	0.001	308	---	1.92

1	3.012	1.964	1.945	1.550	3.821	4.870	2748	---	19.10
2	2.941	1.984	1.917	1.54	3.803	5.400	2397	---	18.75
3	3.063	2.062	1.981	1.61	3.921	4.900	3854	---	21.43
4	2.945	2.000	1.874	1.57	3.755	5.000	3547	---	21.38
Mean	2.990	2.002	1.909	1.570	3.825	5.060	3136	---	20.16
S.D.	0.050	0.042	0.029	0.031	0.069	0.240	678	---	1.44
1	4.543	3.050	3.012	1.508	9.186	5.070	1182	---	14.49
2	4.461	3.035	2.937	1.519	8.913	4.880	1211	---	10.43
3	4.567	3.071	3.031	1.507	9.308	5.020	1695	---	16.50
Mean	4.524	3.052	2.993	1.511	9.135	5.000	1363	---	13.80
S.D.	0.056	0.018	0.049	0.007	0.202	0.090	288	---	3.09
1	4.008	2.047	1.992	2.008	4.078	4.830	897	---	8.40
2	4.039	1.968	1.949	2.072	3.837	5.030	1094	---	9.05
3	4.031	1.929	1.913	2.107	3.698	5.280	862	---	10.12
4	4.019	2.035	1.968	2.051	3.989	4.870	1308	---	15.77
5	4.043	2.027	2.027	1.995	4.109	4.870	1910	---	13.57
Mean	4.026	2.001	1.968	2.047	3.941	4.980	1214	---	11.38
S.D.	0.017	0.051	0.043	0.046	0.175	0.190	428	---	3.16
1	1.992	1.024	0.949	2.100	0.971	5.090	1359	---	9.88
2	1.972	0.984	0.957	2.060	0.942	5.390	446	---	2.80
3	2.000	1.012	1.000	2.000	1.012	4.960	716	---	8.65
Mean	1.998	1.007	0.969	2.05	0.975	5.140	840	---	7.11
S.D.	0.014	0.021	0.027	0.05	0.035	0.002	469	---	3.70

Appendix A3: Uniaxial tests in circular prisms - Group 3A
(Dia. 2 1/8 inches)

Specimen #	Height H inches	Width W = inches	H/W	X-Section Area sq. inches	Unit WT x 10 lbs/cu in	σ_p Peak Strength psi	σ_R Residual Strength psi	Modulus E x 10 psi	σ_{pN}^* Normalised Peak psi
1	2.22	2.118	1.048	3.523	5.500	1268	---	13.72	1836
2	2.150	2.108	1.029	3.464	5.100	1853	---	16.29	2275
3	2.250	2.114	1.064	3.518	4.800	1966	---	18.88	2091
4	1.975	2.120	0.932	3.530	5.400	951	---	8.81	2159
Mean	2.148	2.113	1.017	3.506	5.200	1587	---	14.48	2090
S.D	0.128	0.009	0.059	0.030	0.136	483	---	4.27	186
1	3.200	2.100	1.520	3.464	5.200	1645	---	19.35	1780
2	3.29	2.125	1.548	3.547	5.400	980	---	14.67	1360
3	3.275	2.118	1.546	3.523	5.100	1771	---	22.37	1583
4	3.007	2.116	1.450	3.517	4.700	1894	---	17.64	2147
Mean	3.210	2.114	1.518	3.512	5.100	1577	---	18.51	1697
S.D.	0.093	0.010	0.042	0.035	0.298	399	---	3.22	351
1	3.837	2.124	1.806	3.543	4.800	1930	---	18.01	2143
2	4.165	2.108	1.980	3.464	5.100	2130	---	---	---
3	4.180	2.115	1.980	3.513	4.900	2152	---	---	---
4	4.330	2.120	2.046	3.530	4.900	2396	---	20.97	2285
5	4.197	2.12	1.980	3.53	4.900	1750	---	23.87	1466
Mean	4.140	2.115	1.968	3.516	4.900	2072	---	20.95	1965
S.D.	0.184	0.009	0.090	0.031	0.100	244	---	2.93	438

Appendix A3: Uniaxial tests in circular prisms - Group 3A
(Dia. 3 inches)

Specimen #	Height H inches	W inches	H/W	X-Section Area sq. inches	Unit WT x 10 lbs/cu in	σ_p Peak Strength psi	σ_R Residual Strength psi	Modulus E x 10 psi	σ_{pN}^* Normalised Peak psi
1	3.12	3.0	1.04	7.069	4.850	1460	---	17.28	1698
2	3.165	3.0	1.055	7.069	4.840	3038	---	23.36	2601
3	2.975	3.0	0.992	7.069	4.9	849	---	8.74	1943
3 (a)	3.300	3.0	1.100	7.069	4.860	2012	---	19.96	2016
Mean	3.195	3.0	1.065	7.069	4.860	1839	---	17.33	2062
S.D.	0.093	0.0	0.031	0.000	0.026	929	---	6.25	385
4	4.488	3.0	1.496	7.069	4.940	2750	---	25.08	2200
5	4.610	3.0	1.536	7.069	5.050	1684	---	19.60	1637
6	4.600	2.988	1.539	7.012	4.950	2267	---	25.30	1792
Mean	4.566	2.996	1.523	7.05	4.980	2287	---	23.30	1876
S.D.	0.068	0.007	0.024	0.032	0.001	575	---	3.20	291
7	5.168	3.0	1.720	7.069	4.980	2003	---	23.30	1713
8	5.130	3.0	1.710	7.069	5.000	1715	---	18.23	1881
9	5.407	3.0	1.800	7.069	4.950	1547	---	19.84	1559
Mean	5.235	3.0	1.740	7.069	4.970	1755	---	20.48	1717
S.D.	0.150	0.0	0.049	0.000	0.000	230	---	2.63	161

Appendix B1: Triaxial tests on solid coal (dia = 2 1/8 inch)
Group B2

Specimen #	Height H inches	Diameter W inches	H/W	X-Section Area sq. inches	Unit WT x 10 lbs/cu in	Confining Pressure σ_3	Peak Strength σ_p psi	Residual Strength σ_R psi	Modulus E x 10 psi	$\sigma_p - \sigma_3$	$\sigma_R - \sigma_3$
1	3.84	2.124	1.80	3.543	4.800	0	1930	0	18.01	1930	0
2	4.160	2.108	1.98	3.464	5.108	0	2130	0 -		2130	0
3	4.18	2.115	1.98	3.513	4.9	0	2152	0 -		2152	0
4	4.348	2.120	2.05	3.530	4.900	0	2396	0	20.97	2396	0
5	4.200	2.120	1.98	3.530	4.900	0	1750	0	23.87	1750	0
Mean	4.140	2.115	1.96	3.516	4.900	0	2072	0	20.95	2072	0
S.D.	0.184	0.009	0.09	0.031	0.100	0	244	0	2.93	244	0
1	4.355	2.115	20.60	3.513	5.200	1000	5158	3160	28.49	4158	2160
2	4.355	2.12	2.06	3.53	4.900	1000	5184	5065	26.54	4184	4065
Mean	4.355	2.117	2.06	3.521	5.050	1000	5170	4112	27.51	4171	3112
S.D.	0.000	0.003	0.00	0.012	0.210	0	18.4	1347	1.38	18	1347
1	4.023	2.111	1.91	3.499	5.320	2000	8180	6664	33.73	6180	4664
2	4.410	2.124	2.08	3.543	4.890	2000	5419	5292	23.75	3419	3292
3	4.240	2.125	1.99	3.547	4.880	2000	6495	6115	26.89	4495	4115
Mean	4.224	2.120	1.99	3.529	5.030	2000	6698	6023	28.12	4698	4023
S.D.	0.190	0.008	0.09	0.027	0.250	0	1391	690	5.1	1391	690
1	4.335	2.120	20.40	3.530	4.940	3000	7819	7631	23.56	4819	4631
2	4.365	2.115	2.06	3.513	5.170	3000	8454	7053	30.70	5454	4053
Mean	4.350	2.110	2.05	3.521	5.050	3000	8136	7342	27.13	5.36	4342
S.D.	0.020	0.003	0.14	0.012	0.160	0	449	488	5.04	449	488
1	4.225	2.116	1.99	3.516	4.840	4000	8174	7918	16.98	4.74	3918
2	4.867	2.102	1.93	3.470	4.950	4000	8870	7815	24.80	4870	3815
3	4.239	2.116	2.00	3.517	5.160	4000	7745	7267	27.12	3745	3267
Mean	4.176	2.111	1.97	3.501	4.980	4000	8263	7666	22.70	4263	3666
S.D.	0.094	0.008	0.04	0.027	0.160	0	568	349	5.19	568	349
1	3.850	2.116	1.82	3.517	4.810	6000	12982	12490	31.49	6982	6490
2	3.650	2.115	1.73	3.513	4.970	6000	11614	10316	28.28	5614	4316
Mean	3.750	2.116	1.77	3.515	4.890	6000	12298	11403	29.88	6298	5403
S.D.	0.140	0.001	0.06	0.002	0.113	0	967	1537	2.26	967	1537
1	4.400	2.11	2.08	3.463	4.98	7500	14086	12128	28.31	6586	4628
2	4.355	2.118	2.06	3.523	4.87	7500	13556	12602	30.71	5056	5102
Mean	4.377	2.114	2.07	3.493	4.92	7500	13821	12365	29.51	6321	4865
S.D.	0.	0.006	0.01	0.042	.077					575	3

Appendix B1: Triaxial tests on solid coal (dia = 2 1/8 inch)
Group B2

Specimen #	Height H inches	Diameter W inches	H/W	X-Section Area sq. inches	Unit WT x 10 lbs/cu in	Confining Pressure σ_3	Peak Strength σ_p psi	Residual Strength σ_R psi	Modulus E x 10 psi	$\sigma_p - \sigma 3$	$\sigma_r - \sigma 3$
1	3.887	2.104	1.85	3.477	4.940	10000	18947	18119	32.56	8947	8119
2	3.930	2.115	1.86	3.513	5.180	10000	15610	15371	30.98	5610	5371
Mean	3.908	2.109	1.86	3.495	5.060	10000	17278	16745	31.77	7278	6475
S.D.	0.030	0.007	0.01	0.026	0.169	0	2359	1943	1.11	2359	1943

Appendix B2: Triaxial tests on solid coal (3 inch dia.)
Group B3

Specimen #	Height H inches	Diameter W inches	H/W	X-Section Area sq. inches	Unit WT x 10 lbs/cu in	Confining Pressure $\sigma 3$	Peak Strength σ_p psi	Residual Strength σ_R psi	Modulus E x 10 psi	$\sigma_p - \sigma 3$	$\sigma_r - \sigma 3$
7	5.168	3.000	1.72	7.069	4.98	0	2003	0	23.38	2003	0
8	5.130	3.000	1.72	7.069	4.98	0	1715	0	18.23	1715	0
9	5.407	3.000	1.72	7.069	4.98	0	1547	0	19.84	1547	0
Mean	5.235	3.000	1.74	7.069	4.97	0	1755	0	20.48	1755	0
S.D.	0.150	0.000	0.49	0.000	0.002	---	238	---	2.63	230	---
1	5.620	3.000	1.87	7.092	4.93	2000	8798	5499	22.78	6798	3499
2	4.285	2.985	1.43	7.000	4.85	2000	5742	5622	---	3742	3622
3	4.590	2.998	1.53	7.022	4.77	2000	9467	5929	24.71	7467	3929
Mean	4.832	2.99	1.61	7.038	4.85	2000	8002	5683	23.74	6002	3683
S.D.	0.699	0.008	0.23	0.048	0.08	---	1985	221	1.36	1985	221
1	4.675	2.990	1.56	7.022	5.10	4000	11347	8937	35.24	7347	4937
2	4.250	2.998	1.42	7.022	4.90	4000	10236	9621	28.02	6236	5621
Mean	4.462	2.990	1.49	7.022	5.00	4000	10791	9279	31.63	6791	5279
S.D.	0.300	0.008	0.099	0.000	0.14	---	785	483	5.10	785	483
1	5.956	3.003	1.98	7.082	5.31	1000	2279	1880	16.23	1279	880

Appendix B3: Triaxial tests on solid coal (dia. = 2 1/8 inch) H = 2.375
Group B4

Specimen #	Height H inches	Diameter W inches	H/W	X-Section Area sq. inches	Unit WT x 10 lbs/cu in	Confining Pressure	Peak Strength psi	Residual Strength psi	Modulus E x 10 psi	p - 3	r - 3
1	2.275	2.120	1.07	3.529	4.92	0	2329	-	21.68	2329	-
2	2.257	2.120	1.06	3.529	4.97	0	1428	-	11.43	1428	-
3	2.205	2.116	1.04	3.516	4.81	0	2542	-	17.98	2542	-
Mean	2.246	2.118	1.06	3.524	4.900	0	2099	-	17.03	2099	-
S.D.	0.036	0.002	0.015	0.007	0.08	0	591	-	5.19	591	-
1	2.255	2.117	1.070	3.519	5.22	1000	5541	4774	24.09	4541	3774
2	2.220	2.122	1.050	3.536	4.90	1000	5289	4942	20.68	4289	3942
3	2.130	2.12	1.010	3.529	4.91	1000	5151	5015	18.26	4151	4015
Mean	2.200	2.119	1.040	3.528	5.01	1000	5380	4910	21.00	4380	3910
S.D.	0.065	0.002	0.030	0.008	0.18	0	210.0	123	2.93	210	123
1	2.160	2.117	1.020	3.519	5.00	2000	6564	6206	15.25	4564	4206
2	2.050	2.117	0.970	3.519	4.90	2000	6973	-	17.40	4973	-
3	2.110	2.124	0.930	3.543	4.90	2000	7680	7480	22.37	5688	5480
Mean	2.106	2.119	0.973	3.527	4.93	2000	7075	6843	18.34	5075	4843
S.D.	0.055	0.004	0.045	0.0138	0.058	0	569	900	3.65	568	900
1	2.285	2.125	1.075	3.549	4.90	4000	6649	6483	6.60	2649	2483
2	2.120	2.12	1.000	3.529	5.10	4000	9402	9317	23.26	5402	5317
3	2.120	2.12	1.000	3.529	5.00	4000	9946	9946	26.7	5946	5946
Mean	2.175	2.121	1.025	3.535	5.000	4000	8665	8542	18.85	4665	4582
S.D.	0.096	0.003	0.043	1.737	0.1	0	1767	1844	10.75	1767	1845
1	2.305	2.126	1.080	3.549	4.900	6000	11158	10684	18.83	5158	4684
2	2.20	2.122	1.070	3.536	5.100	6000	10961	10859	19.16	4961	4859
3	1.995	2.121	0.940	3.533	5.000	6000	11684	11548	24.14	5684	5548
Mean	2.193	2.123	1.030	3.539	5.000	6000	11267	11030	20.44	5267	5030
S.D.	0.172	0.003	0.070	0.008	0.100	0	373	456	3.25	373	456
1	2.110	2.113	0.998	3.526	4.830	8000	13749	13749	18.00	5749	5749
2	2.210	2.112	1.046	3.503	4.990	8000	14845	14845	19.48	6845	6845
3	2.010	2.128	0.944	3.539	5.050	8000	-	-	-	-	-
Mean	2.110	2.117	0.996	3.522	4.956	8000	13897	13897	18.70	5897	289
S.D.	0.100	0.0089	0.051	0.018	0.113	0	289	289	0.99	289	

Appendix C1: Triaxial tests - recaspected broken coal (35,000 psi H = 2.375 recapture pressure) D 0.84" H/D = 2.4

Specimen #	Height H inches	Diameter W inches	H/W	X-Section Area sq. inches	Unit WT x 10 lbs/cu in	Confining Pressure σ_3	Peak Strength σ_p psi	Residual Strength σ_R psi	Modulus E x 10 psi	$\sigma p - \sigma 3$
1	1.965	0.835	2.350	0.548	4.480	500	1971		1.510	1471
2	1.969	0.848	2.320	0.565	-	500 -		-	-	
3	2.010	0.850	2.370	0.567	4.220	500	2540		1.480	2040
4	1.977	0.845	2.340	0.561	4.270	500	2566		1.790	2066
Mean	1.986	0.844	2.340	0.560	4.320	500	2359		1.570	1859
S.D.	0.024	0.007	0.021	0.009	0.130	-	336		0.200	336
1	1.975	0.850	2.320	0.567	4.400	1000	4126		2.520	3126
2	1.970	0.85	2.330	0.567	4.300	1000	3597		4.130	2597
3	1.980	0.845	2.340	0.561	4.290	1000	4278		4.010	3278
Mean	1.977	0.848	2.330	0.565	4.330	1000	4000		3.550	3000
S.D.	0.003	0.003	0.010	0.004	0.061	-	357		0.890	357
1	1.905	0.830	2.390	0.541	4.440	2000	7200		5.540	5200
2	1.980	0.827	2.390	0.537	4.450	2000	7932		5.560	5932
3	2.040	0.845	2.410	0.561	4.220	2000	7165		5.420	5165
Mean	2.000	0.834	2.400	0.546	4.870	2000	7435		5.510	5435
S.D.	0.033	0.010	0.110	0.013	0.130	-	430		0.075	430
1	2.075	0.84	2.470	0.553	4.360	4000	10632		8.110	6632
2	1.990	0.845	2.360	0.560	4.300	4000	12957		9.090	8957
3	2.00	0.835	2.490	0.548	4.210	4000	13467		8.770	9467
Mean	2.050	0.840	2.440	0.554	4.290	4000	12320		8.650	8320
S.D.	0.046	0.005	0.070	0.006	0.750	-	1492		0.500	1492
1	2.093	0.833	2.490	0.545	4.310	6000	16183		11.860	10183
2	2.135	0.842	2.530	0.559	4.340	6000	16636		10.320	10636
3	2.095	0.838	2.520	0.541	4.310	6000	16303		10.460	10302
Mean	2.101	0.835	2.510	0.548	4.320	6000	16370		10.880	10370
S.D.	0.024	0.006	0.020	0.009	0.170	-	234		0.851	234
1	1.955	0.845	2.310	0.561	4.250	8000	18502		14.120	10502
2	2.015	0.835	2.410	548.000	4.370	8000	16533		10.360	8533
3	1.960	0.835	2.350	0.548	4.390	8000	18394		12.480	10394
Mean	1.977	0.838	2.360	0.552	4.340	8000	17810		12.320	9810
S.D.	0.033	0.006	0.050	0.008	0.750	-	1106		1.880	1106
1	2.002	0.830	2.410	0.541	4.450	0	47		0.138	47
2	2.010	0.830	2.420	0.541	4.400	0	24		0.074	24
3	2.000	0.834	2.400	0.546	4.420	0	39		0.106	39

Appendix C1: Triaxial tests - recompacted broken coal (35,000 psi) H = 2.375
recapture pressure) D 0.84" H/D = 2.4

Specimen #	Height H inches	Diameter W inches	H/W	X-Section Area sq. inches	Unit WT x 10 lbs/cu in	Confining Pressure σ_3	Peak Strength σ_p psi	Residual Strength σ_R psi	Modulus E x 10 psi	$\sigma p - \sigma 3$
4	2.195	0.835	2.630	0.548	4.060	0	192		0.239	192
5	2.085	0.835	2.490	0.548	4.210	0	151		0.193	151
6	2.060	0.835	2.470	0.548	4.300	0	211		0.217	211
Mean	2.058	0.833	2.470	0.545	4.300	0	110		0.159	110
S.D.	0.075	0.002	0.860	0.003	0.149	0	84		0.630	84

Appendix C2: Triaxial tests - recompacted broken coal H = 2.375
25,000 psi recompaction pressure) D 0.84" H/D = 2.4

Specimen #	Height H inches	Diameter W inches	H/W	X-Section Area sq. inches	Unit WT x 10 lbs/cu in	Confining Pressure σ_3	Peak Strength σ_p psi	Residual Strength σ_R psi	Modulus E x 10 psi
1	1.995	0.835	2.390	0.548	4.450	500	2530		2.450
2	1.985	0.842	2.360	0.548	4.390	500	2154		2.770
3	2.027	0.834	2.430	0.548	4.410	500	2857		2.510
Mean	2.002	0.837	2.390	0.548	4.420	500	2513		2.580
S.D.	0.220	0.004	0.004	0.000	0.030	-	352		0.170
1	2.015	0.832	2.420	0.544	4.480	0	43		0.104
2	1.985	0.830	2.390	0.541	4.400	0	31		0.091
3	1.970	0.830	2.370	0.541	4.400	0	30		0.089
4	2.105	0.835	2.620	0.548	4.090	0	54		0.147
5	2.195	0.835	2.630	0.548	4.160	0	57		0.131
6	2.199	0.835	2.630	0.548	4.050	0	71		0.133
Mean	2.090	0.833	2.510	0.545	4.250	0	47.8		0.116
S.D.	0.112	0.002	0.129	0.003	0.170	-	16		0.024
1	2.015	0.335	2.410	0.548	4.320	1000	4160		3.500
2	2.000	0.845	2.370	0.561	4.280	1000	4705		3.540
3	2.010	0.845	2.380	0.561	4.260	1000	3957		3.560
Mean	2.008	0.842	2.390	0.557	4.290	1000	4274		3.530
S.D.	0.008	0.006	0.021	0.008	0.031	-	387		0.030
1	1.995	0.845	2.360	0.561	4.260	2000	6845		7.720
2	1.950	0.838	2.350	0.541	4.32	2000	7098		7.090
3	1.985	0.838	2.390	0.541	4.420	2000	7208		6.150
4	1.985	0.836	2.390	0.541	4.650	2000	6987		5.940
Mean	1.970	0.834	2.370	0.546	4.410	2000	7034		6.990
S.D.	0.020	0.007	0.210	0.010	0.171	-	155		0.790
1	1.913	0.835	2.290	0.567	4.290	4000	12380		9.280
2	2.035	0.835	2.440	0.567	4.190	4000	12169		8.880
3	1.995	0.825	2.420	0.535	4.470	4000	12336		8.330
Mean	1.981	0.832	2.380	0.556	4.310	4000	12295		8.560
S.D.	0.062	0.006	0.010	0.018	0.141	-	111		0.633
1	2.010	0.845	2.380	0.561	4.250	6000	15935		9.670

Appendix C2: Triaxial tests - recompacted broken coal H = 2.375
25,000 psi recompaction pressure) D 0.84" H/D = 2.4

Specimen #	Height H inches	Diameter W inches	H/W	X-Section Area sq. inches	Unit WT x 10 lbs/cu in	Confining Pressure σ_3	Peak Strength σ_p psi	Residual Strength σ_R psi	Modulus E x 10 psi	$\sigma p - \sigma 3$
1	1.985	0.838	2.390	0.541	4.480	8000	18188	13.38		
2	1.988	0.845	2.350	0.561	4.290	8000	18716	12.61		
3	1.980	0.845	2.340	0.561	4.080	8000	peak -			
Mean	1.984	0.84	2.360	0.554	4.280	8000	18452	12.97		
S.D.	0.004	0.009	0.260	0.011	0.200 -		373	0.51		

Appendix C3: Triaxial tests on recompacted broken coal
35,000 psi recompaction pressure) D = 2.125 H/D = 2.2

Specimen #	Height H inches	Diameter W inches	H/W	X-Section Area sq. inches	Unit WT x 10 lbs/cu in	Confining Pressure σ_3	Peak Strength σ_p psi	Residual Strength σ_R psi	Modulus E x 10 psi	$\sigma_p - \sigma_3$
1	4.195	2.170	1.905	3.700	4.370	0	42		0.0570	
2	4.120	2.190	1.880	3.767	4.270	0	36		0.0524	
3	3.970	2.175	1.820	3.715	4.350	0	47		0.0569	
4	3.965	2.175	1.820	3.715	4.370	0	53		0.0580	
5	4.020	2.150	1.870	3.630	4.400	0	215		0.541	
6	4.105	2.170	1.930	3.690	4.240	0	121		0.357	
7	4.105	2.175	1.890	3.715	4.220	0	123		0.379	
8	4.195	2.165	1.940	3.681	4.280	0	175		0.427	
9	4.125	2.160	1.910	3.664	4.340	0	250		0.600	
10	4.167	2.160	1.930	3.664	4.460	0	89		0.303	
11	4.165	2.155	1.930	3.647	4.480	0	102		0.281	
Mean	4.105	2.167	1.890	3.690	4.340	0	114		0.283	
S.D.	0.083	0.011	0.040	0.038	0.085	-	73		0.200	
1	4.134	2.165	1.910	3.681	4.360	500	2085		3.980	
2	4.330	2.165	2.000	3.681	4.170	500	2656		4.100	
Mean	4.230	2.165	1.960	3.681	4.260	500	2770		4.040	
S.D.	0.140	0.000	0.060	0.000	0.134	-	162		0.085	
1	4.126	2.157	1.910	3.654	4.430	1000	4893		4.950	
2	4.035	2.150	1.870	3.657	4.420	1000	3918		4.050	
3	4.035	2.170	1.860	3.690	4.400	1000	4730		0.910	
Mean	4.065	2.161	1.880	3.667	4.42	1000	4523		6.230	
S.D.	0.052	0.007	0.026	0.024	0.015	-	512		2.310	
1	4.285	2.165	1.980	3.681	4.430	2000	7807		8.040	
2	4.291	2.175	1.970	3.715	4.210	2000	7720		8.970	
3	4.095	2.170	1.890	3.715	4.360	2000	6912		5.050	
Mean	4.223	2.170	1.950	3.704	4.330	2000	7479		7.350	
S.D.	0.111	0.005	0.050	0.019	0.112	-	493		2.050	
1	4.159	2.159	1.930	3.647	4.470	4000	12437		9.510	
2	4.199	2.121	1.980	3.701	4.340	4000	11024		8.060	
Mean	4.179	2.138	1.960	3.674	4.410	4000	11730		8.780	
S.D.	0.028	0.024	0.035	0.038	0.091	-	999		1.030	

Appendix C3: Triaxial tests on recompacted broken coal
35,000 psi recompaction pressure) D = 2 1/3 H/D = 2

Specimen #	Height H inches	Diameter W inches	H/W	X-Section Area sq. inches	Unit WT x 10 lbs/cu in	Confining Pressure σ_3	Peak Strength σ_p psi	Residual Strength σ_R psi	Modulus E x 10 psi	$\sigma_p - \sigma_3$
2	4.430	2.165	2.050	3.681	4.300	6000	14841		10.54	
3	4.325	2.163	2.000	3.674	4.400	6000	15514		10.22	
Mean	4.377	2.164	2.030	3.677	4.350	6000	15177		10.38	
S.D.	0.074	0.001	0.035	0.005	0.070	-	476		0.22	
1	4.327	2.160	2.000	3.664	4.350	8000	16441		12.65	
2	4.301	2.160	1.990	3.664	4.370	8000	18105		11.12	
3	4.215	2.160	1.950	3.664	4.460	8000	18105		11.60	
Mean	4.281	2.160	1.980	3.664	4.400	8000	17603		11.79	
S.D.	0.058	0	0.026	0	0.076	-	1006		0.83	

Appendix C4: Triaxial tests on recompacted broken coal
25,000 psi recompaction pressure) D = 2.125 H/D 2.2

Specimen #	Height H inches	Diameter W inches	H/W	X-Section Area sq. inches	Unit WT x 10 lbs/cu in	Confining Pressure σ_3	Peak Strength σ_p psi	Residual Strength σ_R psi	Modulus E x 10 psi	$\sigma_p - \sigma_3$
1	4.105	2.155	1.900	3.647	4.300	0	140		0.527	
2	4.102	2.160	1.900	3.664	4.280	0	119		0.419	
3	4.120	2.160	1.910	3.664	4.300	0	134		0.397	
5	4.170	2.165	1.930	3.681	4.440	0	122		0.341	
6	4.200	2.157	1.950	3.654	4.420	0	113		0.269	
Mean	4.139	2.159	1.920	3.662	4.350	0	126		0.391	
S.D.	0.043	0.004	0.025	0.013	0.075	0	11		0.096	
1	4.210	2.160	1.950	3.664	4.380	500	3226		3.89	
2	4.415	2.165	2.040	3.681	4.320	500	3031		3.80	
Mean	4.313	2.162	1.990	3.672	4.350	500	3128		3.85	
S.D.	0.145	0.003	0.068	0.012	0.042	-	137		0.06	
1	4.322	2.160	2.000	3.664	4.340	1000	4913.0		4.28	
2	4.395	2.160	2.030	3.664	4.340	1000	4290		3.77	
3	4.375	2.160	2.030	3.664	4.310	1000	4610		3.96	
Mean	4.364	2.160	2.020	3.664	4.330	1000	4604		4.000	
S.D.	0.038	0.000	0.017	0.000	0.017	-	311		0.256	
1	4.305	2.16	1.990	3.664	4.290	2000	8187		5.940	
3	4.155	2.166	1.920	3.684	4.350	2000	8436		5.830	
Mean	4.230	2.163	1.960	3.674	4.320	2000	8311		5.880	
S.D.	0.106	0.004	0.050	0.014	0.042	-	176		0.077	
1	4.467	2.163	2.070	3.674	4.320	4000	12452		7.810	
2	4.226	2.16	1.960	3.664	4.460	4000	12641		7.180	
Mean	4.346	2.161	2.010	3.669	4.390	4000	12546		7.500	
S.D.	0.170	0.002	0.077	0.007	0.098	-	134		0.445	
1	4.234	2.155	1.960	3.647	4.400	8000	17800		11.20	
2	4.166	2.165	1.920	3.681	4.310	8000	16560		10.03	
Mean	4.200	2.160	1.940	3.664	4.360	8000	17180		10.61	
S.D.	0.048	0.007	0.028	0.024	0.064	-	876		0.83	

Appendix D: Shear Box Test Results

Specimen #		#1			#2			#3	
Area - $m^3 x 10^{-3}$	3.48			3.83			3.59		
Normal force N	Shear Force N	Normal Stress k N/m^2	Shear Stress k N/m^2	Shear N	Normal Stress k N/m^2	Shear Stress k N/m^2	Shear Force N	Normal Stress k N/m^2	Shear Stress k N/m^2
200	41.6	57.5	11.9	30	52	7.8	47.6	56	13
400	116.6	115	33.5	185	157	48	-	-	-
600	145.8	172	41.9	355	261	93	212	167	59
800	210.5	229	60.5	555	417	145	-	-	-
1000	-	-	-	-	-	-	388	278	108
1600	484.2	459	139	755	587	197	650	445	181
2250	-	-	-	-	-	-	900	627	251
3250	1091.9	933	314	1210	848	316	1244	906	346
4250	-	-	-	1544	1109	403	1760	1184	490
5200	1681.1	1494	482	1762	1358	450	2000	1448	557

Specimen #		#4			#5			#6	
Area		3.87			2.60			4.14	
200	22.7	50	5.7	18.6	77	7	0	48	0
600	109	151	27	111	231	43	73	145	17
1000	225	253	57	231	384	89	123	241	29
1600	435	403	109	431	615	166	300	386	73
2250	553	567	139	625	865	240	442	543	107
3250	835	819	210	925	1250	356	679	785	165
4250	1122	1070	282	1261	1634	484	894	1026	216
5200	1319	1309	332	1400	2000	538	1150	1256	278

Specimen #		#7			#8	
Area		3.29			4.35	
200	50	61	15	84	46	19
600	170	182	52	211	137	48
1000	269	303	82	412	230	95
1600	512	486	155	675	368	155
2250	762	683	232	969	517	223
3250	1102	988	335	1412	747	325
4250	1331	1292	405	1709	977	393
5200	1587	1580	982	1950	1195	448

Appendix E: Uniaxial tests on coal plates ($H/W < 1$)

Specimen #	Height inches	Depth inch	Width W inch	$\frac{H}{W}$	Area sq. inch	Unit Weight lbs/cu in x 10^{-3}	Peak Uniaxial Strength psi	Residual Strength psi	Modulus E x 10^4psi psi
1	1.30	9.0	8.95	.145	80.6	5.07	6458	?	14.7
2	1.32	9.0	9.0	.147	81.0	4.95	7080	997	16.2
3	1.27	9.0	9.0	.141	81.2	-	674	1108	14.7
4	1.31	4.53	2.75	.48	12.5	5.06	2417	681	16.1
5	1.26	4.35	2.80	.45	12.8	5.11	1555	787	14.0
6	1.30	4.37	4.34	.30	19.0	5.25	3796	1282 ?	19.3
7	1.38	4.54	4.40	.31	20.0	4.98	2937	690 ?	16.8